EARTHQUAKE EARLY WARNING APPLICATIONS USING DOWNHOLE ARRAYS IN ISTANBUL

by

Uçkan Mertcan ARSLAN

B.S., Civil Engineering, İzmir Institute of Technology, 2016

Submitted to the Kandilli Observatory and Earthquake Research Institute
in partial fulfilment of the requirements for the degree of
Master of Science

Graduate Program in Earthquake Engineering
Boğaziçi University

2019

ACKNOWLEDGEMENTS

I would like to express my sincere thanks to my supervisors Prof. Ali PINAR and Prof. Seyyit Ümit DİKMEN for their invaluable guidance and pieces of advices, endless patience, infinite encouragement and their excellent lectures throughout this study.

I would like to express my special thanks to all my lecturers in Boğaziçi University, Department of Earthquake Engineering and İzmir Institute of Technology, Department of Civil Engineering for their precious assistance, theoretical and practical knowledge and passion.

On the other hand, many thanks to my friends for being there for me when I needed and sharing great experiences.

Finally, I would like to express my sincerest thanks to my parents Haydar Mesut & Arife ARSLAN for their endless support, encouragement, help, patience and trust throughout my education and my life. I would like to thank my little sister Başak for being with us.

ABSTRACT

EARTHQUAKE EARLY WARNING APPLICATIONS USING DOWNHOLE ARRAYS IN ISTANBUL

The Kocaeli (Mw 7.5) and Düzce (Mw 7.2) earthquakes that occurred in 1999 revealed the fact that the earthquakes in Marmara Region should be considered especially in terms of the damage that may result in Istanbul. An Emergency Response and Early Warning System was established to reduce possible losses after a damaging earthquake in Istanbul and to produce Rapid Loss Maps to assist rescue teams with emergency response.

The main element of the Earthquake Early Warning is the rapid and reliable estimation of the magnitude of the earthquake. In order to calculate the magnitude of the earthquake, it is necessary to determine whether the earthquake fracture will continue or not. This is generally understood from the characteristics of the initial movement (P waves). For this purpose, the characteristics of P waves have been determined by using the τc - Pd method and the waveforms of earthquakes recorded by the vertical component acceleration sensors located on the bottom of the wells and on the surface. Most of the downhole array data is from ATK station. The surface records used are from the early warning stations operated by KOERI and the strong motion network operated by AFAD. As a result, two models have been developed to predict the magnitude of an impending large earthquake and the peak ground velocity (PGV) amplitudes associated with it. A verification process of the models has been applied to predict the moment magnitude of September 26, 2019 Mw=5.7 offshore Silivri earthquake. The models developed from the ATK downhole array predicted the size of the earthquake as Mw=5.8 within 7 seconds of the origin time which in turn yield about 15 seconds early warning time for most of the Istanbul Metropolitan area. The models developed using waveforms recorded at surface have predicted the size of the earthquake as Mw=6.1 which is comparable to the Mw=6.0 prediction of Wu and Kanamori (2005) model. The size and amplitude of the prediction models obtained in this study have been considerably improved compared to the models published a decade ago.

ÖZET

İSTANBUL'DA KUYU İÇİ KAYITLAR KULLANILARAK DEPREM ERKEN UYARI UYGULAMALARI

1999 yılında meydana gelen Kocaeli (M_w 7.5) ve Düzce (M_w 7.2) depremleri, Marmara Bölgesi'nde meydana gelmesi olası depremin özellikle İstanbul'da yaratacağı hasara karşı hazırlıklı olunması gerçeğini ortaya çıkarmıştır. İstanbul'da olabilecek hasar yapıcı bir deprem sonrasında olası kayıpların azaltılması ve acil müdahale ile kurtarma ekiplerine yardımcı olacak Kayıp Haritalarının hızlıca üretmek amacıyla, Acil Müdahale ve Erken Uyarı Sistemi kurulmuştur.

Deprem Erken Uyarısının ana unsuru deprem büyüklüğünün hızlı ve güvenilir bir şekilde tahmin edilmesidir. Deprem büyüklüğünü hesaplamak için, deprem kırığının devam edip etmeyeceğini belirlemek gerekir. Bu genellikle ilk hareketin özelliklerinden anlaşılır (P dalgaları). Bu amaçla, P dalgalarının karakteristikleri τ_c - Pd metodu ve kuyuların en alt noktasında ve yüzeyinde yer alan dikey bileşen ivme sensörleri tarafından kaydedilen deprem dalga formları kullanılarak belirlenmiştir. Kuyu dizi verilerinin çoğu ATK istasyonundandır. Kullanılan yüzey kayıtları, KOERI tarafından işletilen erken uyarı istasyonlarından ve AFAD tarafından işletilen kuvvetli yer hareketi ağındandır. Sonuç olarak, yaklaşmakta olan büyük bir depremin büyüklüğünü ve bununla ilişkili maksimum yer hızı (PGV) genliklerini tahmin etmek için iki model geliştirilmiştir. 26 Eylül 2019 Mw=5.7 açık deniz Silivri depreminin moment büyüklüğünü tahmin etmek için modellerin bir doğrulama işlemi uygulanmıştır. ATK downhole dizisinden geliştirilen modeller, deprem büyüklüğünün başlangıç anından itibare 7 saniye içinde Mw=5.8 olarak tahmin edildi ve bu da İstanbul Büyükşehir bölgesinin çoğu için yaklaşık 15 saniye erken uyarı süresi verdi. Yüzeyde kaydedilen dalga formları kullanılarak geliştirilen modeller, Wu ve Kanamori (2005) modelinin Mw=6.0 öngörüsü ile karşılaştırılabilir olan deprem boyutunu Mw=6.1 olarak tahmin etti. Bu çalışmada elde edilen tahmin modellerinin büyüklüğü ve genliği, on yıl önce yayınlanan modellere kıyasla oldukça geliştirilmiştir.

TABLE OF CONTENTS

LIST OF FIGURES

LIST OF TABLES

LIST OF SYMBOLS

A	: Constants obtained by the least squares method
a	: Constants of the devices
B	: Constants obtained by the least squares method
b	: Constants of the devices
c	: Constants of the devices
M_b	: Body-wave magnitude
M_{est}	: Estimated magnitude
M_L	: Local magnitude
M_s	: Surface-wave magnitude
M_w	: Moment magnitude
P_d	: The largest value obtained from the displacement record in a time window
P_{max}	: Largest amplitude value read in 3-second P wave
T_i^p	: The dominant period
t_i	: Time at i
T_{pmax}	: Maximum dominant period
t_w	: Time window
x_i	: Recorded velocity
X_i	: Anti-aliased (smoothed) the square of the velocity record
$u(t)$	: Vertical component displacement record
$\dot{u}(t)$	: Vertical component velocity record
$\hat{u}(f)$	: The frequency spectrum of $u(t)$
τ_c	: The period of the initial part of the P wave
$\langle f^2 \rangle$	: The weighted average of $\lvert\hat{u}(f)\rvert^2$ and f^2
Δt	: The lag time

LIST OF ACRONYMS / ABBREVIATIONS

AFAD	: Disaster and Emergency Management Presidency
ANSS	: Advanced National Seismic System
ATK	: Atakoy Downhole
BCAV	: Bracketed Cumulative Average Velocity
BSSA	: Bulletin of the Seismological Society of America
BUKOERI	: Boğaziçi University, Kandilli Observatory and Earthquake Research Institute
CAV	: Cumulative Absolute Velocity
CDMG	: California Department of Conservation, Division of Mines and Geology
CIRES	: Seismic Recording and Instrumentation Centre
CISN	: California Integrated Seismic Network
CUBE	: Caltech and USGS Broadcast of Earthquakes
EEW	: Earthquake Early Warning
ElarmS	: Earthquake Alarm System
EPRI	: Institute for electrical energy research
EQAS	: Earthquake Quick Alarm System
FREQL	: Fast Response Equipment against Quake
FTH	: Fatih Downhole
GFZ	: German Research Center for Geosciences
JMA	: Japan Meteorology Agency
JR	: Japan Railway
KOERI	: Kandilli Observatory Earthquake Research Institute
LTA	: Long term average
NIED	: National Research Institute for Earth Science and Disaster Prevention
PGA	: Peak Ground Acceleration
PGD	: Peak Ground Displacement
PGV	: Peak Ground Velocity
REDI	: Rapid Earthquake Data Integration
RTRI	: Railway Technical Research Institute
SAS	: Seismic Alert System

SASMEX	: Seismic Alert System of Mexico
SASO	: Oaxaca Seismic Alert System
STA	: Short term average
TREIRS	: Taiwan Rapid Earthquake Information Release System
TSMIP	: Taiwan Strong Motion Instrumentation Program
TUBITAK	: The Scientific and Technological Research Council of Turkey
UREDAS	: Urgent Earthquake Detection and Alarm System
USGS	: United States Geological Survey
VSN	: Virtual Sub-Network
ZYT	: Zeytinburnu Downhole

1. INTRODUCTION

Earthquake phenomenon is among the most damaging events caused by the Earth itself. With the progress of urbanization around the world, earthquakes are becoming a serious threat to urban areas near subduction zones or major active faults. The earthquake preparation and production process are extremely complex, and observations cover a relatively short period compared to large earthquake cycles (Satrioano et al. 2010). For these reasons, a reliable earthquake prediction is not currently available (Kanamori, 2003; 2008). The validity of the estimates is desirable in order to protect large urban areas from damage and loss.

Therefore, a new approach to mitigating seismic risk has emerged in the last two decades due to advances in digital seismology and communication. This new paradigm is based on the concept of real-time earthquake information systems in which computer-assisted seismic stations with integrated fast telemetry and automatic processing are installed to provide fast and reliable information on earthquake parameters and to develop support and emergency response on expected ground motion. This process is known as an earthquake early warning system and is now becoming a viable and promising approach to mitigate losses caused by major earthquakes (Kanamori et al. 1997; Allen et al. 2009; Satriano et al. 2010).

Early warning, interruption of the high voltage lines by the automatic transmission of the warning signal to the relevant institutions by detecting an earthquake that may cause damage at the locations closest to its source, stopping the activities that may cause danger in critical chemical production plants, nuclear power plants and refineries, subway, It makes it possible to stop public transportation vehicles such as high-speed trains and commuter trains, to stop the elevators in skyscrapers and shopping centres at the floor level and to open all the doors, to operate the necessary generators and to take many similar important measures (Goltz, 2002; Harben, 1991).

The transmission or information of emergency response information is provided by the rapid collection and analysis of the necessary data during and immediately after a devastating earthquake from a network of strong ground motion recorders (accelerometers) located in densely populated areas of a city. The aim of emergency response is to send the damage distribution map to the relevant administrative and first response institutions as quickly as possible. Thus, these institutions will be informed about earthquake damage. Although it is seen as a post-earthquake study, the information that will constitute the infrastructure for the damage distribution map is obtained in real time during the earthquake. The delay is entirely due to the time spent waiting for the end of the earthquake and preparing the map. For example, in the Istanbul Earthquake Emergency Response System, the process of producing the damage distribution map and transmitting it to the related units is completed within approximately 5 minutes (Erdik et al., 2003).

Since the primary and secondary seismic waves generated during an earthquake propagate at different velocities, they reach the earthquake recording stations in certain sequences. The P wave travelling with propagation velocities between 5.0-7.4 km / sec arrives first and then S wave travelling with 3.0-4.0 km / sec arrives (Clark, 1971). The time difference of P and S waves arriving at a station also increases as the distance from the earthquake's epicentre increases. This increase is to save time in terms of early warning. However, the fact that the data communication speed with the radio frequency between the earthquake stations and the main data centre is very high (300.000 km / sec) has an important place in the EEW system (Saita and Nakamura, 2003). The EEW system will warn a few seconds to tens of seconds before the devastating S wave of a major earthquake arrives and will help to minimize the possible damage to an area during and after the earthquake. In addition, some EEW systems installed for engineering purposes (Erdik et al., 2003) produce an earthquake alarm by checking whether the amplitude of the incoming seismic wave exceeds a certain threshold level without attempting to detect the P wave. Depending on the eccentric location of seismic devices and possible earthquakes, it allows the excitation of a structure, plant area from a few seconds to tens of seconds before and the automation systems deemed necessary.

In general, an EEW warning system requires seismic stations, computer and software required for the data processing centre, device-equipment for continuous data

communication between the data centre and the stations, and the necessary apparatus for transmitting the warning signal.

All EEW systems must first detect a damaging earthquake and then emit a useful alarm signal (Allen et al., 2009). The first example implemented in the sense of EEW system is the system consisting of seismographs with mechanical alarms which were commissioned in 1960s by JR (Japan Railway) to slow down and stop high speed trains (Ashiya, 2004). In later years, UREDAS (Urgent Earthquake Detection and Alarm System), presented by Nakamura (1988) and used by the Japanese Railways, has become the most scientifically recognized example. Today, many countries have established and are trying to install the EEW system. Main countries having EEW systems and focusing on EEW methods are Japan, Mexico, Taiwan, The United States and Turkey.

In Japan, which is one of the countries most affected by the earthquakes, especially with the development of Japanese Railways high speed train systems, attention has been paid to the use of warning devices and EEW system. Beginning with the UrEDAS devices developed by Nakamura (1988), and in later years with its advanced derivatives, Compact UrEDAS, FREQL (Fast Response Equipment against Quake Load), and finally EQAS (Earthquake Quick Alarm System) with the EEW network (Ashiya, 2004). In general, it is known that these systems that produce alarms by detecting the earthquake in place by making use of a small number of stations give numerous successful results (Nakamura, 2008).

In southern California (USA), the presence of a large number of faults and effective earthquake formation do not allow the use of a simple EEW system. For this reason, it is tried to detect the formation of the source in the shortest time, in seconds and to generate the correct alarm. Numerous and frequently placed seismic devices (broadband and accelerometer) by utilizing the first few seconds of the earthquake, magnitude determination studies have been made (Allen and Kanamori, 2003; Lockman and Allen, 2005; Olson and Allen, 2005).

Istanbul, Marmara Region in particular is among the greatest economic power and the city has a population of Turkey. The region is under the control of the North Anatolian Fault

in terms of tectonic and earthquake activity and exhibits a large number of small but few major earthquake activities (Ambraseys and Finkel, 1991; Gürbüz et al., 2000). In the light of statistical data, the probability of an earthquake with a magnitude of 7.0 was determined to be 2%, especially in Istanbul (Erdik et al., 2004). For this reason, earthquake phenomenon is gaining more importance for Istanbul and Marmara Region.

Because of this importance, the aim of this study is to develop an earthquake early warning algorithm and to determine the appropriateness of τ_c - P_d approach for Istanbul and Marmara Region. During the thesis study, strong ground measurements made at the bottom of the wells and on the surface are correlated with the size of the earthquakes and the associated PGV values to establish τ_c - P_d relations to be used for earthquake early warning (EEW).

2. LITERATURE REVIEW

The increase in urbanization along with the developing industrialization and the fact that a significant part of the growing cities take place in the regions with high earthquake hazard suggests that the loss of life and property after an earthquake can be experienced in larger sizes. Especially the losses caused by earthquakes in the densely populated areas in the last 20 years increase these concerns. The 1995 Kobe (Mw = 6.7) earthquake that occurred in Japan, the 1994 Northridge (Mw = 6.8) earthquake that occurred in the State of California, USA,1999 Chi-Chi (Mw = 7.6) earthquake occurred in Taiwan, 2004 Sumatra earthquake, occurred in Indonesia (Mw = 9.2) and April 2005 (Mw = 8.6) earthquakes are a few examples. The ever-evolving electronic technology in every field allows the immediate monitoring and evaluation of earthquake ground motion observations with the industrialization.

Together with these developments, scientists have determined the location of the earthquake near the source of the earthquake and directed to the automatic generation and transmission of earthquake warning and alarm information. As a result, this orientation makes it possible to take important measures during and after the earthquake by alerting the cities and regions to be exposed to the earthquake, stopping the necessary activities or putting them into operation.

For this purpose, similar systems were founded in Japan, Mexico, Taiwan, United States and Turkey (Figure 2-1).

From the countries focusing on the EEW system; Japan, Mexico, Taiwan and the United States are located in the vicinity of the Circle-Pacific, a highly active seismic zone, the Fire Circle seismic belt (Figure 2-2). Although the systems established in the countries mentioned above differ in terms of their infrastructures and applied algorithms, they serve essentially the same purpose.

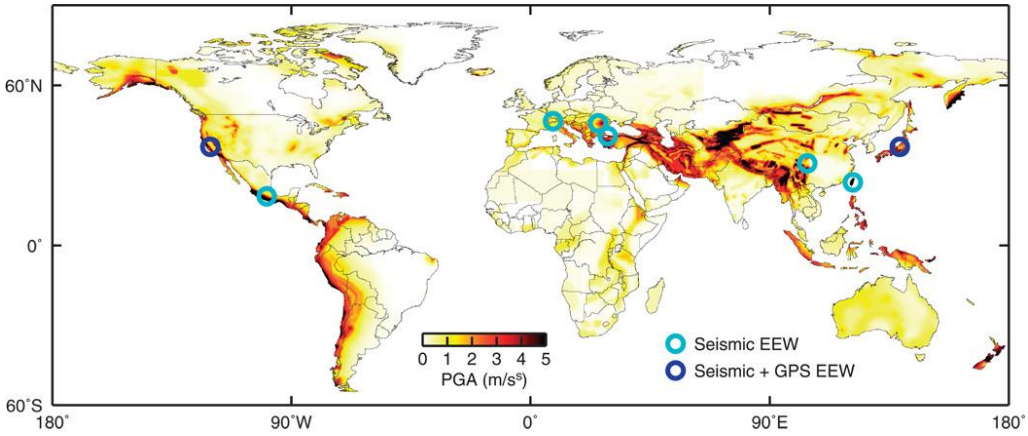

Figure 2.1. Countries Having EEW Systems (Minson et al., 2015).

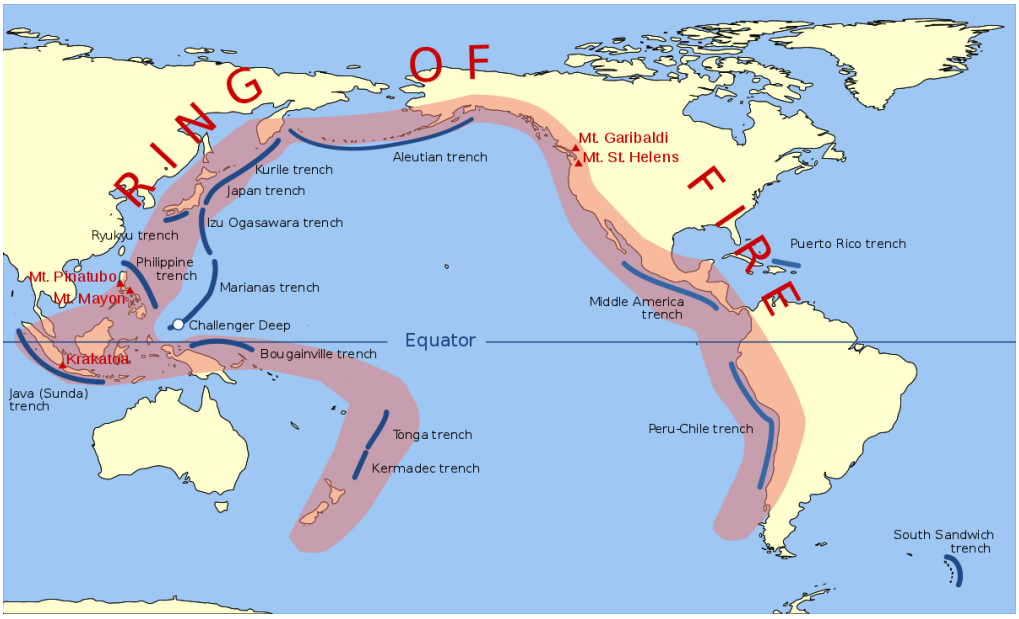

Figure 2.2. Pacific Fire Circle (https://en.wikipedia.org/wiki/Ring_of_Fire).

The following sections describe the structure and status of the systems in the countries where EEW systems are installed.

2.1 Japan

The installation of alarm-enabled seismographs initiated by Japanese Railways dates back to the 1960s. In 1964, for the trains called Shinkansen (bullet train), 20 km along the

line were put on seismographs with mechanical alarm features and threshold level 40 gals. With the establishment of the Tohoku high-speed train system in the 1970s, it was aimed to stop the trains according to the size of the earthquake by putting seismographs on the Pacific Ocean coast for this fast train. In 1985, the prototype UrEDAS was established. This system uses the P wave of the earthquake and makes an alarm in about 3 seconds by estimating epicenter and magnitude. This system, which can cover 20 km area, is followed by Compact UrEDAS which is capable of giving warning in 200 km area in 1998. This new type of device has an S wave alarm function in addition to UrEDAS. Figure 2-3 shows UrEDAS and Compact UrEDAS used in Japanese Railways. The method developed by Nakamura (1988) is used to determine the magnitude of the P wave and the eccentricity is determined by the magnitude-amplitude relationship. In addition, the new generation of classical UrEDAS and Compact UrEDAS; FREQL is considerably reduced. This new device, which includes all functions of UrEDAS and Compact UrEDAS, has the property of giving earthquake parameters 1-2 seconds after the determination of P wave (Nakamura et al., 2006). Since 2005, FREQL has been used by the Tokyo fire department against backdrops during the demolition-construction-construction works after the main shock (Nakamura, 2008). However, EQAS, which calculates the rapid size and eccentric distance, was commissioned on the railways after 2000 (Ashiya, 2004).

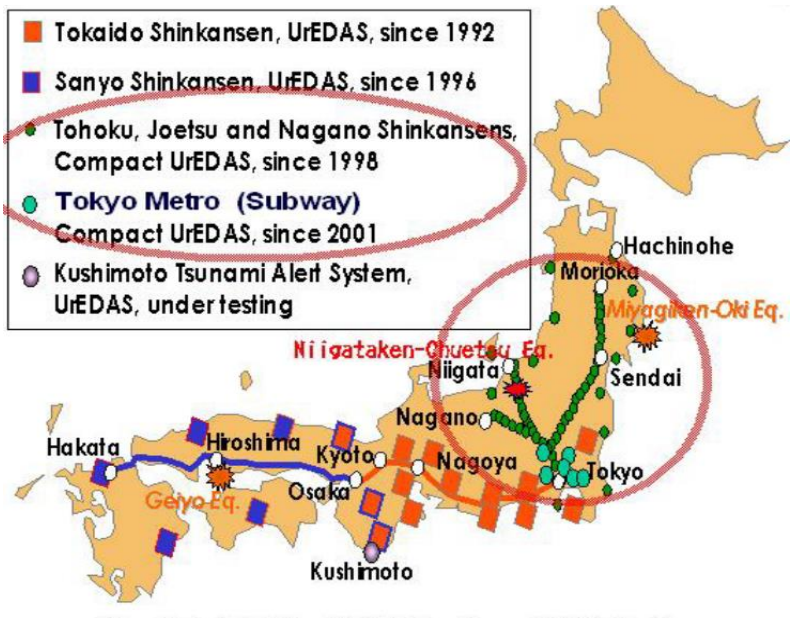

Figure 2.3. Uredas and Compact Uredas Devices Distributon (http://www.sdr.co.jp/eng_page/papers/EEWcaltechCompactPresen.pdf).

The development of a national earthquake warning system has been the result of the Kobe earthquake in 1995 (Allen et al., 2009). After this earthquake, a large number of permanent seismic networks were established (Okada et al., 2004). 800 accelerometers are used by NIED (National Research Institute for Earth Science and Disaster Prevention) and 200 accelerometers are used by JMA. 20-25 km of device is provided throughout the country (Allen et al., 2009). In this co-operating system, if any station has recorded a ground movement above 100 cm/s^2, the warning is triggered by exceeding the threshold level. The network approach is also applied in the system.

According to this approach, the characterization of the source is based on the detection of P waves in one or more stations. The location is first determined. Using the single station P wave detection and the inclination at the beginning of the earthquake, the external distance is determined (Ashiya, 2004; Odaka et al., 2003). The earthquake zone is determined by triggering the P wave by one or more stations. The location of the ground motion is triggered by a larger number of stations. The magnitude estimation is made using the P wave amplitude-scale of magnitude. The size calculation is constantly updated with the amplitude increase in the vector sum of the three component waveforms observed (Allen et al., 2009; Kamigaichi, 2004). In addition to the station threshold level, the first warning is given if the magnitude or maximum seismic intensity value calculated during a possible earthquake exceeds the magnitude and intensity threshold levels (anyone). In Japan, threshold level values were taken as 6 for size and 5+ for scale of JMA ranging from 0 to VII (Kamigaichi, 2004). According to the developed Mercalli Magnitude scale, if a value of VII or above is obtained, it is broadcast by the JMA to the public via television and radio channels (Allen et al., 2009).

2.2 Mexico

The Michoacán earthquake (Glass, 1989) on 19 September 1985 (Ms = 8.1) was instrumental in the establishment of the EEW system for the city of Mexico. The system, which was started to be installed in 1989, was completed and commissioned in August 1991. It is of great importance since it is the first EEW system which can make a warning to the public in the world. All studies have been carried out with the support of the governorship

of Mexico City. A total of 12 accelerometers were placed along the coast of Guerrero, about 300km, on average 25 km (Figure 2-4) (Espinosa-Aranda et al., 1995). Iglesias et al. (2007), although the system has been removed to 15 stations, 12 accelerometer stations are used today (Suarez et al., 2009). This system, which is the best example of the frontal detection method, can give a warning time to the city of Mexico about 60 seconds before a possible earthquake (Espinosa-Aranda et al., 1992; Iglesias et al., 2007). SAS (Sistema de Alerta Sísmica = Seismic Alert System) is called the system automatically detect P and S waves. Wave detection is made with threshold level and STA / LTA (short term average / long term average) approach. Then according to the magnitude and the size of the value obtained from the local radio channel is restricted to the alarm between 5.0 and 6.0, for M_b 6.0 alarm alert is made to the public (Espinosa-Aranda et al., 1992). The SAS system, which recorded 2000 earthquakes ranging in magnitude from 3.0 to 7.3 up to now, has issued a warning for the public / public warning for 13 earthquakes following the triggering of the P wave, and a warning signal for 53 earthquakes (Espinosa-Aranda and et al., 2009; Suarez et al., 2009). The best outcome in terms of EEW time was in the 7.3 Copala earthquake, which occurred on September 14, 1995, with a warning time of 72 seconds (Espinosa-Aranda et al., 2003). On June 15, 1999, after an earthquake of 6.7 that hit the city of Oaxaca, the Department of Civil Defence of Oaxaca requested the design and installation of an EEW system for Oaxaca from the CIRES (Centro de Instrumentacion y Registro Sismico A.C = Seismic Recording and Instrumentation Centre).

In 2003, the so-called SASO (Systema de Alerta Sismica de Oaxaca = Oaxaca Seismic Alert System) was completed. Until now, three warning signs have been issued by SASO and 5 preventive warning signals have been issued for medium sized earthquakes. The distribution of the seismic stations used together with SAS stations in Oaxaca EEW System is given in Figure 2-5. Two EEW systems have been integrated into each other and the agreement of two cities has been made by the Governorate of the two cities to call SASMEX (Seismic Alert System of Mexico) (Espinosa-Aranda et al., 2009).

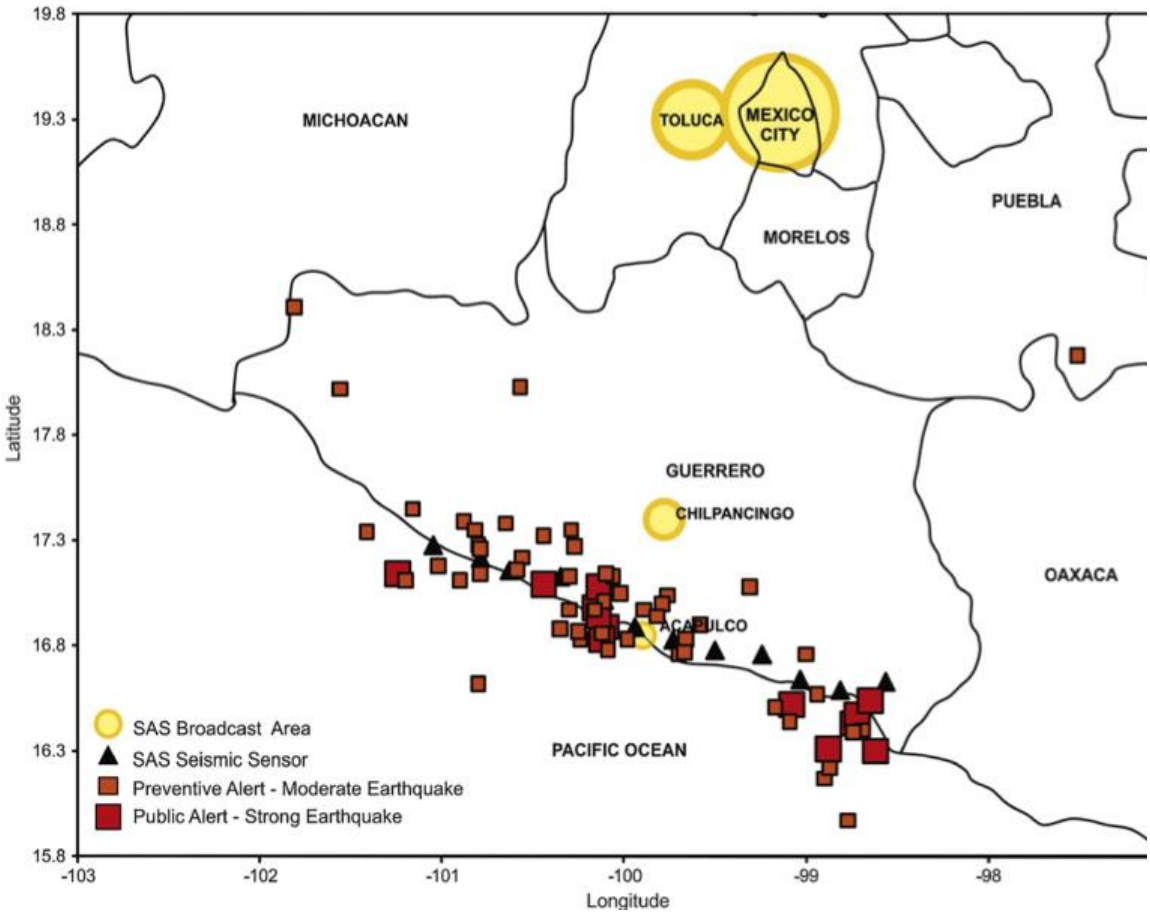

Figure 2.4. Mexico City and EEW Sensors (Espinosa-Aranda, 2009).

Figure 2.5. Oaxaca City and EEW Sensors (Espinosa-Aranda, 2009).

2.3 Taiwan

Taiwan is located to the west of the Ring of Fire zone, one of the highly active seismic zones and because of this location, Taiwan very often exposed to major earthquakes. On November 15, 1986, M_L = 6.8 (Mw = 7.8) earthquake occurred in Hualien District, east of Taiwan, caused great damage due to the ground amplifications 120 km from the epicentre in the capital, Taipei (Hsaio et al. 2009; Wu et al., 1999). After the earthquake in Taiwan in particular, the studies on earthquakes started to be focused. Taiwan Central Meteorological Bureau (CWB) started to work on the installation of seismic devices in the scope of Taiwan Strong Motion Instrumentation Program called TSMIP in 1992, in order to create a data bank that will include high quality earthquake records that will help seismology and earthquake engineering works. (Liu et al., 1999).

Approximately, 650 modern digital accelerometers have been installed throughout the country within the program (Wu et al., 2002). As a result of the researches and studies conducted by CWB, RTE system which is called as TREIRS (Taiwan Rapid Earthquake Information Release System) which is used for rapid reporting of earthquake was established on March 3, 1996 (Wu et al., 2003a). The map of focus, magnitude information and intensity of earthquakes larger than magnitude 4.0 is provided within 1 minute (Teng et al., 1997; Wu et al., 2004). This system consists of 82 seismic networks in real time, including accelerometer stations (Wu et al., 2002, 2004). The number of stations increased to 86 in 2005 (Wu and Kanamori, 2005a) and in 2009 to 109 (Hsaio et al., 2009). Station distributions of seismic networks are given in Figure 2-6.

Another important thought that emerged from the earthquake of November 15, 1986, which gave weight to earthquake studies in Taiwan, was the idea of establishing an earthquake early warning system in Hualien region. With the help of a system that forecast the earthquake within 30 seconds to be established saves tens of seconds for the city of Taipei for pre-earthquake preparations. A prototype network was created for the Taipei EEW System in the Hualien District, which included 16 accelerometers. This system, called the sub-network approach, was tested in 1998-1999 and it was determined that there could be a warning time of about 15 seconds (Wu et al., 2004).

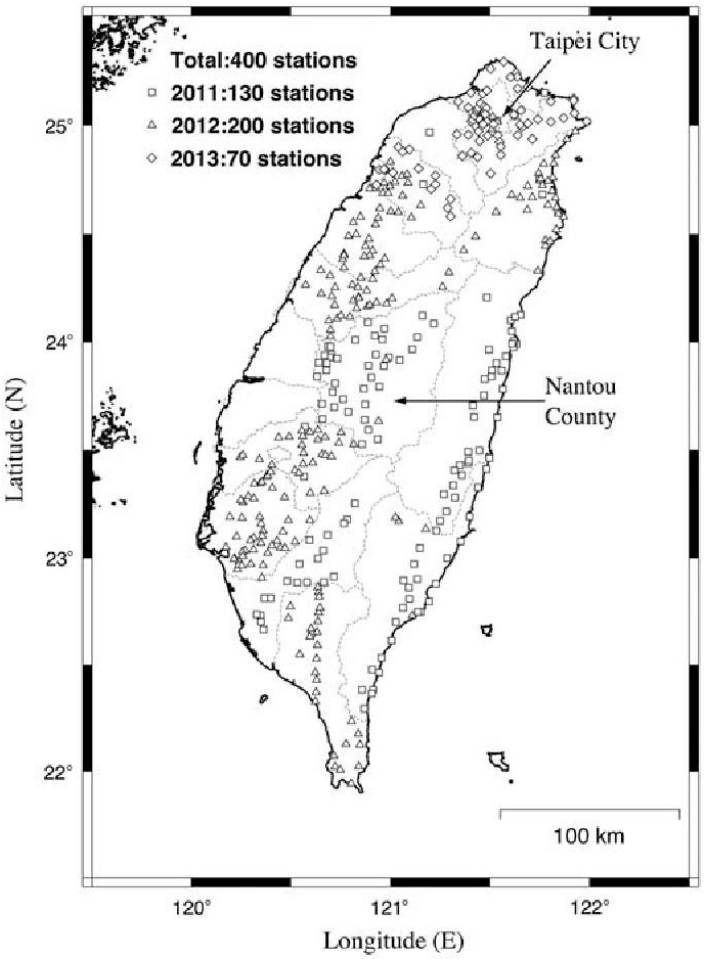

Figure 2.6. Seismic Sensors located in Taiwan (Wu et al., 2013).

As a result, the installation of the Taiwan EEW System found in 2001 (Allen et al., 2009). The system operated by CWB uses the earthquake stations of TREIRS installed within an area of 100x300 km^2. The use of the so-called VSN (Virtual Sub-Network) method, which was developed from the sub-network for the EEW system, was adopted (Hsaio et al., 2009; Wu and Teng, 2002). VSN is an automatically running, event-dependent and time-varying system. According to VSN method; When the RTD system is triggered, the stations at a distance of 60 km away from the first station are excluded from the calculation. In other words, only seismic stations within the 60 km distance to the eccentric zone are involved in the calculation of epicenter and magnitude (Wu et al., 2004). After the detection of earthquakes in the Hualien region, which is located in the suburban zone in eastern Taiwan, it is revealed that it is possible to make a warning approximately 20 seconds

before earthquake about 70 km away from all the settlement areas, especially to the city of Taipei, which is 120 km away (Allen et al., 2009; Wu and Kanamori, 2005a; Wu, 2007).

2.4 United States of America

The major earthquakes on the eastern Pacific ridge of the Pacific Fire Circle zone have affected the west coast of the United States, especially California, the largest province. The information obtained from the past to the present shows this effect clearly (CGS, 2007).

Studies aimed at reducing the disaster damages in the US for the last 50 years include both long-term risk assessment and assessment studies as well as post-earthquake information. Although the studies on reducing long-term earthquake risks and losses have been mostly used for structural regulations, they have been made with risk maps (Allen and Kanamori, 2003).

After the earthquake, information activities were provided within different programs. The most important ones are;

- ANSS (Advanced National Seismic System) conducted throughout the country by USGS (United States Geological Survey) (Benz et al., 2001)
- REDI (Rapid Earthquake Data Integration) offered by the University of Berkeley and USGS for the central and northern regions of the State of California (Gee et al., 1996)
- CUBE (Caltech and USGS Broadcast of Earthquakes), conducted by Caltech (California Technical University) and USGS (Kanamori et al., 1991)
- TriNet is founded by Caltech, USGS and CDMG (California Department of Conservation, Division of Mines and Geology) (Hauksson et al., 2001).

TriNet, which is part of CISN (California Integrated Seismic Network) provides rapid post event notification in Southern California State and includes approximately 150 wideband and accelerometers, deployed within 20 km. The locations of the TriNet devices that are placed given in Figure 2-7.

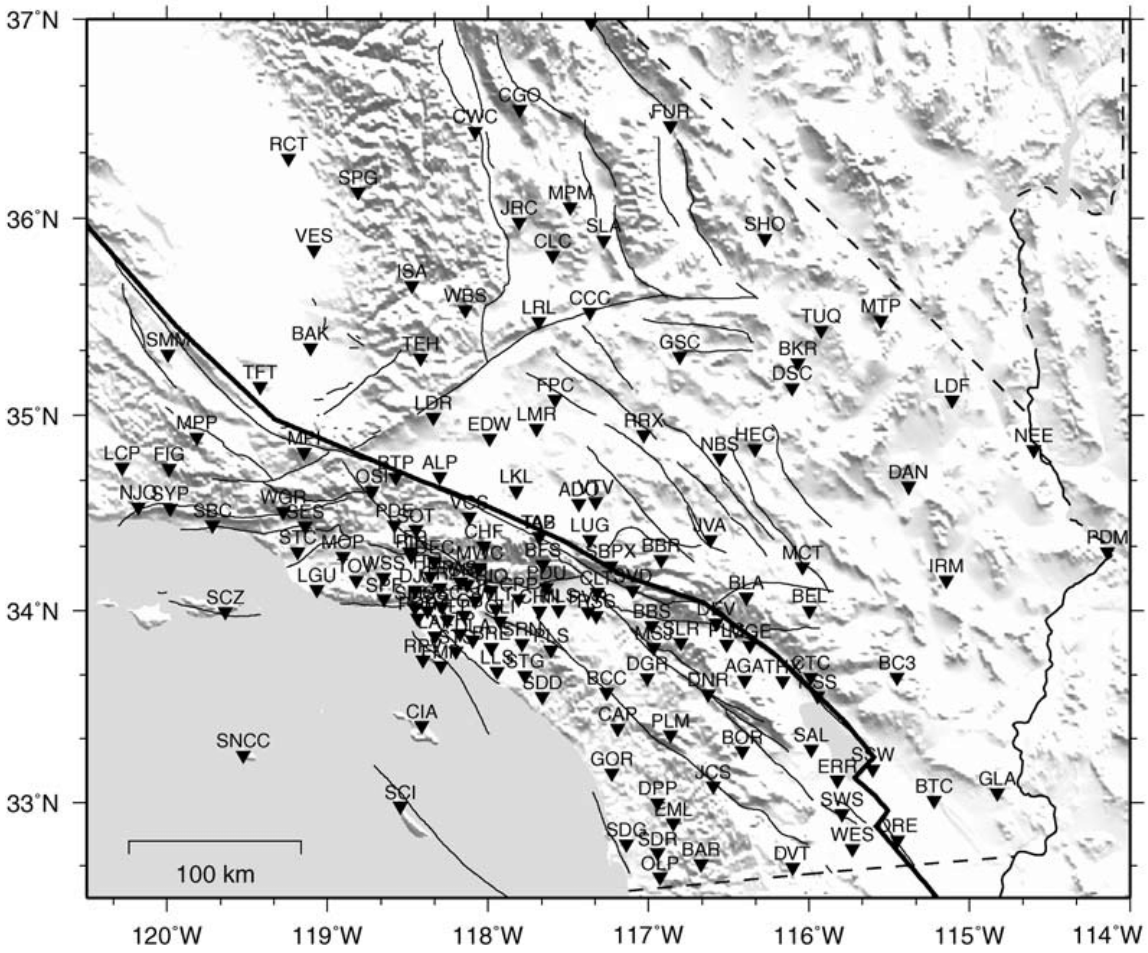

Figure 2.7. Locations of TriNet Stations in California (Tan et al. 2010).

Information or information is carried out over the Internet in a few minutes following the earthquake by the CUBE pager system. The greatest acceleration values observed during the earthquake are used to produce the Shake Maps (USGS, 2000; Wald et al., 1999), 3-5 minutes after the earthquake (Allen and Kanamori, 2003).

Although there are studies on the EEW system and methods of earthquake in the US, there is no warning system for public warning. Work has been carried out especially for Southern California and the State of Northern California in order to increase EEW time and thus to ensure system and method reliability. The ElarmS (Earthquake Alarm System) for the State of Southern California uses TriNet stations. The ElarmS system makes the epicenter determination in 1-2 seconds by triggering 2 or 3 stations. While determining the magnitude, as in the UrEDAS warning system used in Japan, the first few seconds of the

earthquake (<4 sec) is extracted from the frequency content of the frequency-dominant period relationship is used (Allen, 2004, 2007; Allen and Kanamori, 2003; Lockman and Allen, 2005). This system is very similar to the UrEDAS methodology, the main difference is that it uses a network. Allen (2009) states that the warning period for California using regional seismic networks can be approximately 1 minute. Two examples that this period would be possible are given. It was stated that this warning period could be possible during a break from the northern end of the San Andreas Fault, starting from the Salmon Trough and heading towards the city of Los Angeles, which might be towards the San Francisco Bay (Allen, 2009). In the state of California, although the necessary legislation has been prepared for the use of early warning signals, especially in high-speed trains, it is pending, but active work to be carried out after the legalization of legislation will be the first in EEW (Allen et al., 2009).

2.5 Turkey

Historical earthquakes indicate that the Marmara Region is exposed to large seismic activities and potentially has a seismic risk. Two major earthquakes in particular, the 17 August 1999 Kocaeli (Mw = 7.5) and 12 November 1999 Düzce (Mw = 7.2) earthquakes have positively triggered the preparations for a possible major earthquake that will affect Istanbul and its environment in the future. It has been decided to establish "Istanbul Earthquake Emergency Response and Early Warning System" by the Cabinet of the Republic of Turkey. Boğaziçi University, Kandilli Observatory and Earthquake Research Institute established by the project "EEW" within the scope of 10 strong ground motion stations were established (Erdik et al., 2003). The project is carried out by the Department of Earthquake Engineering.

The locations of these stations have been decided as Adalar, Tuzla, Yalova, Gebze and Marmara Ereğlisi etc. and they are specified by taking into consideration the logistic criteria such as station security, data transmission security and proximity to the fault line (Figure 2-8). By means of radio-link from stations (BOTAS, SINANOBA and YAKUPLU stations were transferred to satellite in 2008), the data in real time and in real time is automatically evaluated at the headquarters.

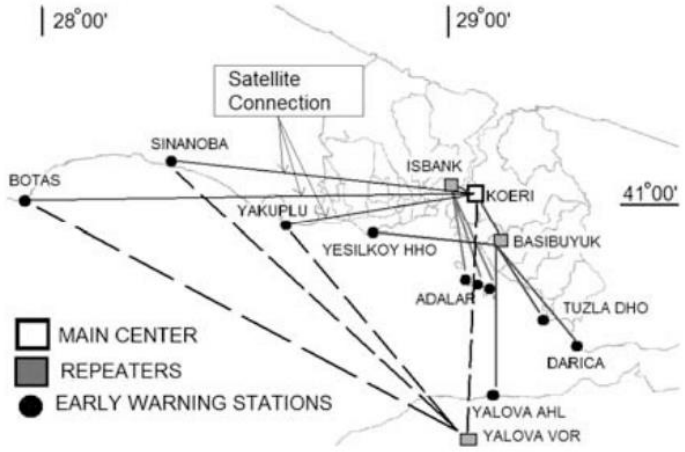

Figure 2.8. İstanbul EEW Station Locations (Erdik et al. 2003).

This system, which worked until December 2012, was changed to Emergency Response and Early Warning System with the contributions of Istanbul Governorship and Synthesis Ground and Structural Engineering. A new seismic network consisting of 120 emergency responders and 10 early warning stations was re-established by adding 20 new devices to the system. The main purpose of this seismic network is to produce Quick Loss Maps (http://www.ewistanbul.com/Icerik.aspx) to help mitigate potential losses after a damaging earthquake in Istanbul and help emergency responders and rescue teams. Strong ground motion generates the data from the earthquake network using ELER program and creates rapid shake maps and damage distribution maps after a damaging earthquake. Data transmitted from the earthquake stations to the main data centre in KOERI via GSM or fiber-optic cable are automatically evaluated at the main centre.

It is checked by the system that the threshold levels are exceeded by at least 3 stations in a 10 second (adjustable) time window continuously. After exceeding the level value, the decision is made, and the alarm is automatically generated by the software. The maximum acceleration value Peak Ground Acceleration (PGA) or Cumulative Absolute Velocity (CAV) threshold levels are used to trigger the earthquake. The current system is already operated based on the acceleration threshold level. Depending on the earthquake source parameters and the coordinates of the location to be affected, the warning signal related to an earthquake that may cause damage can be given no more than 8 seconds (Erdik et al., 2003).

3. EARTHQUAKE EARLY WARNING METHODS

In all EEW systems, it is necessary to first detect the earthquake, and then transfer a useful warning signal to the users in a healthy way.

The quicker the earthquake detection is; the more time it will be earned for the alert. The distance between the epicentre and the area to be alerted allows the earthquake EEW system to make accurate decisions, and the area to be alerted provides sufficient time to implement pre-planned measures. For example, in the EEW system established in Mexico, the source is about 300-350 km from the city of Mexico, providing enough time for a healthy EEW message. This type is called; Front Detection, (Allen and Kanamori, 2003; Wu and Kanamori, 2005a). Earthquake EEW systems of Mexico, Taiwan and Istanbul are examples of this approach.

On the other hand, in regions with cities that have been exposed to constant ground vibrations such as the State of California or USA, and which have been deployed on active faults, faster decision-making and estimation approaches are required for the determination of the earthquake. This is made possible only by the use of many and frequently deployed stations. For example, in Japan, the epicentre of the major earthquakes is mostly deep-rooted, while the United States is a shallow source in California. In these regions, where various and different types of earthquake recorders (wideband and accelerometer) are operated, the approaches to calculate the position and magnitude determination in a short time by the first few seconds of the potential earthquake of P are called "On-site Detection" (Kanamori, 2005).

Briefly, the approaches that are called depending on the distance between the region to be stimulated and the earthquake source point are grouped in two groups. Although studies in both groups include different methods, they are used for earthquake triggering, location and size determination.

The Istanbul Earthquake EW System does not benefit from the difference between the arrival times of the P and S waves generated by a possible earthquake for the earthquake triggering and generation of the warning signal. The system generates alarms by automatically determining the earthquake with the principle of exceeding the PGA and CAV threshold levels. This type of approach is considered to be an approximation in order to gain more time possible by reducing the calculation time due to being very close to the fault. Therefore, it is called, Direct Engineering (Alcik et al., 2006). However, methods in other systems should be considered as seismological approaches because they try to give location and size by taking advantage of the first few seconds of the P wave and the S wave.

EW systems operated in Mexico and Romania perform their functions without the need for algorithm innovation due to the fixed time earned from fixed distances. On the contrary, Japan, Taiwan and the USA systems in Southern California are constantly looking for new developments to increase EW time. Therefore, they are now leading the way for early warning. In the following subsections, B-Delta (B-Δ) method, which is the main structure of EQAS which is used by RTRI (Railway Technical Research Institute) which gives great importance to EW in Japan, τ_c and P_d used in Taiwan and T_{pmax} method tested in California are seismological methods, detailed information and developments about CAV used in Istanbul Earthquake Early Warning System are presented under engineering methods.

3.1 Seismological Methods

In this chapter; The theoretical parts of B-Δ, τ_c - P_d and T_{pmax} methods used in Japan, Taiwan and South California are mentioned.

3.1.1. B-Delta Method

In Japan, UrEDAS has been used as a classic in the sense of EEW system in fast trains for a long time (Ashiya 2004; Nakamura, 2004). Recent studies on real-time seismology have led to the increase of national earthquake stations in Japan by both JMA and some

government departments. It is stated that this increase allows the development of the EQAS system by the Technical Research Institute of Railways (Ashiya, 2004). The EQAS system algorithm is the B-Delta method (Ashiya et al., 2003).

Although the EQAS was first described by Ashiya (2004), the first detailed information about the B-Delta method was found in a new method of estimating epicentral distance and a single seismic record by Odaka et al. (2003) and published as an article in Bulletin of the Seismological Society of America (BSSA). However, no relevant information has been found in the literature after 2004.

Odaka et al. (2003), using the first 3 seconds of the earthquake, $y(t)$ function to fit the earthquake waveform is given in equation 3.1;

$$y(t) = Bt * e^{-At} \tag{3.1}$$

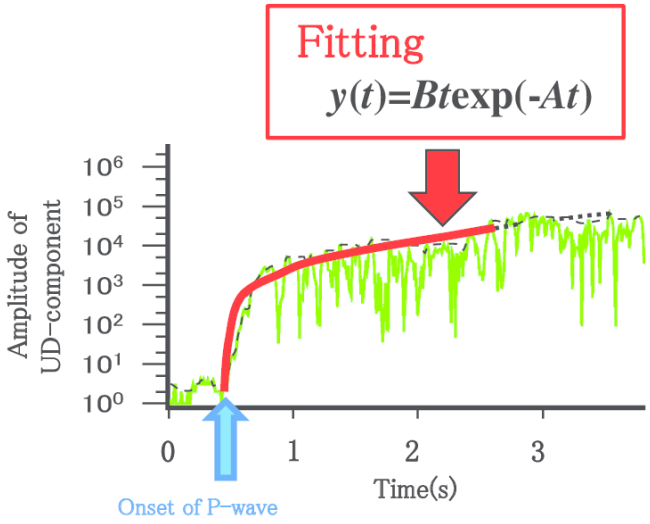

Figure 3.1. Graphical Represenation of the Method (Yamamoto et al. 2012).

The use of A and B constants obtained by the least squares method means that the coming earthquake is close or distant, small or large. The graphical representation of this method is given in Figure 3-1. The offered function $y(t) = Bt * e^{-At}$; t is the time in

seconds, the parameter *A* is the time change of the amplitude and the *B* parameter is related to the slope of the initial part of the P waveform (Kamigaichi, 2004).

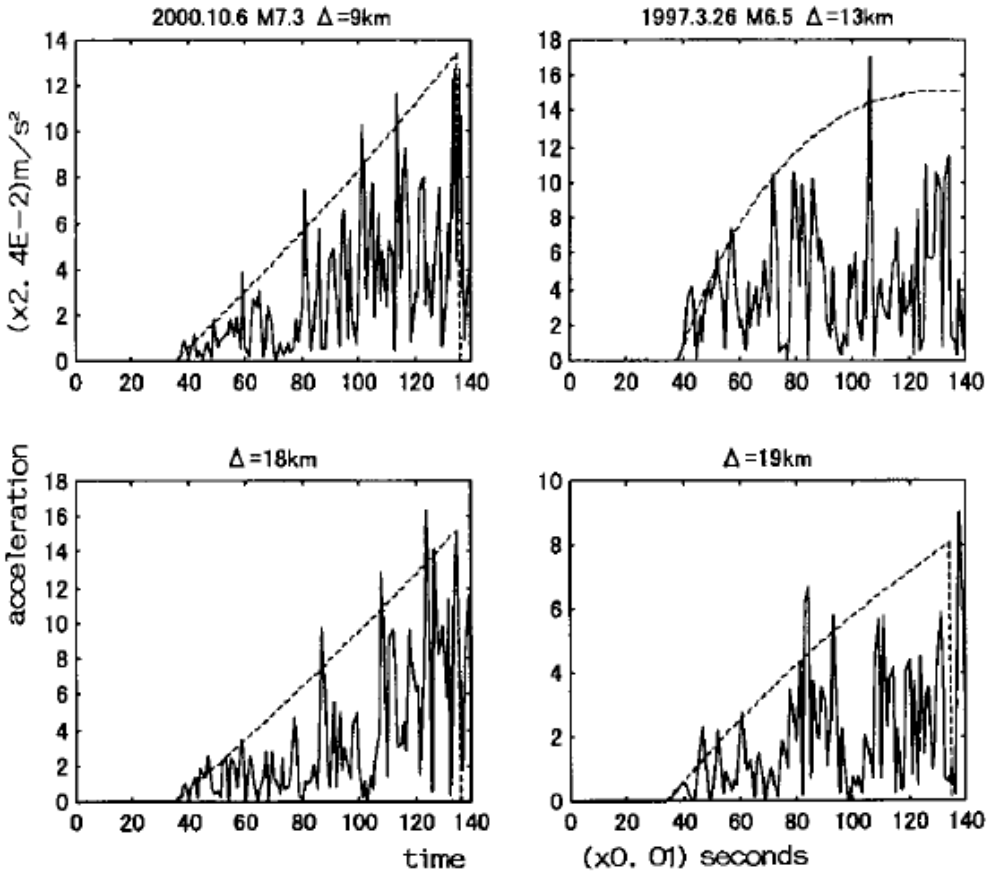

Figure 3.2. Behaviour of the starting parts of the function according to different dimensions (M) and epicentral distances (Δ) (Odaka et al., 2003).

The slope of the starting part of the P wave form is steep or soft, and it is related to the close or distal origin of the earthquake (Figure 3-2). A value of positive (+) or negative (-) causes the function graph to go up or down, indicating that the earthquake is small or large. Figure 3-3 shows how the function curve changes at different distances for different earthquakes.

Odaka et al. (2003), a total of 186 acceleration records of 10 earthquakes from the Kyoshin Network, whose magnitudes ranged from 3,9 to 7,3. All operations are performed on the vertical component. When the mean of the vertical components is taken and the orientations (trend) are cleared, the starting moment of the earthquake is automatically

selected as the point at which the noise levels exceed five times the standard deviation value. From this point on, there is the largest point of the data that has the absolute value over a specified time window (example: $t_w = 3\,sec$). These points are interpolated up to the number of data. The smallest squares method is applied to the interpolated data with the function $y(t) = Bt * e^{-At}$. Consequently, parameters A and B are calculated. The relation between B values and Δ is shown in Figure 3-4.

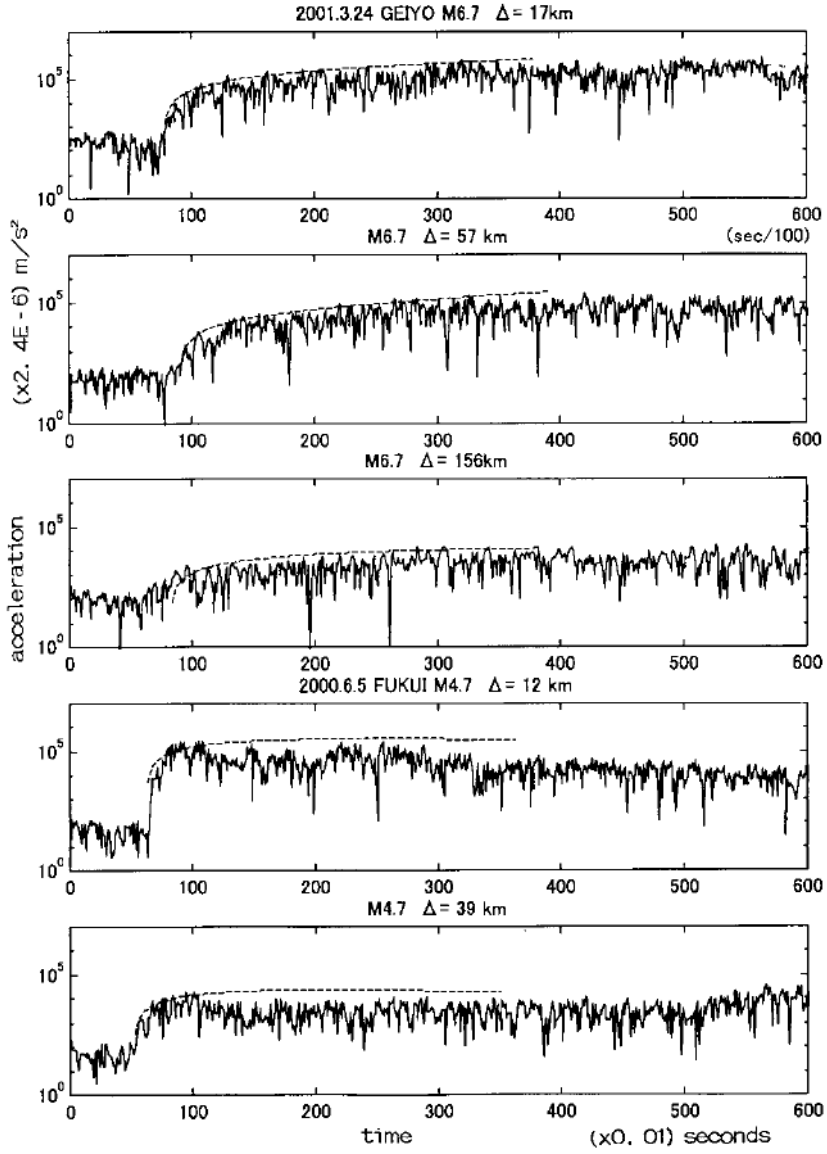

Figure 3.3. Logarithmic waveforms typical for large and small earthquakes (Odaka et al., 2003).

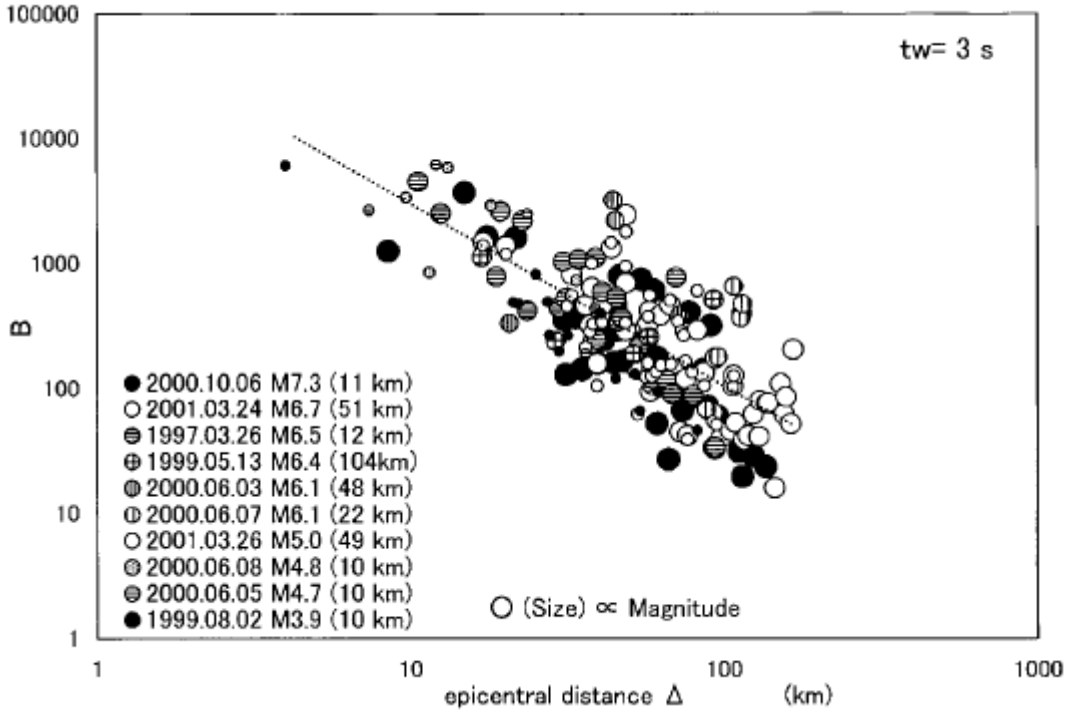

Figure 3.4. Relationship Between B values and epicentral distance Δ for of various magnitudes (Odaka et al., 2003).

It is possible to determine the approximate eccentricity with the B value obtained by using the first 3 second data from the moment of the start of the P wave of the single station vertical component acceleration record during an earthquake.

The rapid size estimation is made by using equation 3.2, after the size formula presented by Grecksch and Kumpel (1997) is adapted to the installed system.

$$M_{est} = a \log P_{max} + b \log B + c \qquad (3.2)$$

Here; M, the estimated magnitude calculated from the equation, a, b and c is the constants of the devices, P_{max} gives the largest amplitude value read in 3-second P wave. Size B is obtained after a very short period of time is determined. However, it is stated that there is no study related to A coefficients and it has been left to further dates (Odaka et al., 2003).

3.1.2. Tau-P-Max Method

In the United States, the studies aimed at reducing the disaster damages in the United States include long-term (50-year) period risk identification and post-earthquake information activities. In 2003, a third approach was presented by Allen and Kanamori (2003). In this approach, the feasibility of the short-term risk warning system for Southern California (Harben, 1991) and the ElarmS system, which uses the infrastructure of TriNet, can be used to deliver the EEW message from a few seconds to a few seconds ago (Allen, 2004, 2007; Allen and Kanamori, 2003).

Elarms begins to detect the initial time, location and magnitude of an earthquake in the first moment of the P wave. Then, the expected ground movement determines the environmental distribution of peak value using damping relationships. As a result, EW time is estimated from the time curves that occur with the S wave travel. However, studies have focused more on the magnitude prediction. It is reported that the size of the P wave is estimated using the frequency content and this method is similar to the method used by Nakamura (Allen and Kanamori, 2003). The difference between them can be summarized as follows; using a network, the filter applied and the process-control period.

Allen and Kanamori (2003) in their study, they used 53 California earthquakes with a magnitude ranging from 3.0 to 7.3. Two criteria were observed in the selection of these earthquakes; (1) the earthquake was recorded by two or more broadband seismographs, (2) The External distance is 100 km below the stations to be stowed. Control periods are continuously calculated using the vertical components of speed sensors using the following recursive relationship for each station (Allen, 2007; Allen and Kanamori, 2003; Lockman and Allen, 2005; Olson and Allen, 2005).

$$T_i^p = 2\pi \sqrt{\frac{X_i}{D_i}} \tag{3.3}$$

$$X_i = \alpha\, X_{i-1} + x_i^2 \tag{3.4}$$

$$D_i = \alpha\, D_{i-1} + (dx/dt)_i^2 \tag{3.5}$$

Here; at the moment the dominant period of T_i^p any i, x_i-recorded speed record, X_i anti-aliased (smoothed) the square of the speed record, the speed record is softened via the square of the derivative of α smoothing coefficient of 0.999 (Allen, 2004; Allen and Kanamori, 2003, Lokman and Allen, 2005). $\alpha = 0.99$ for 100 samples/sec, $\alpha = 0.95$ for 20 samples/sec by Allen (2007) and Olson and Allen (2005).

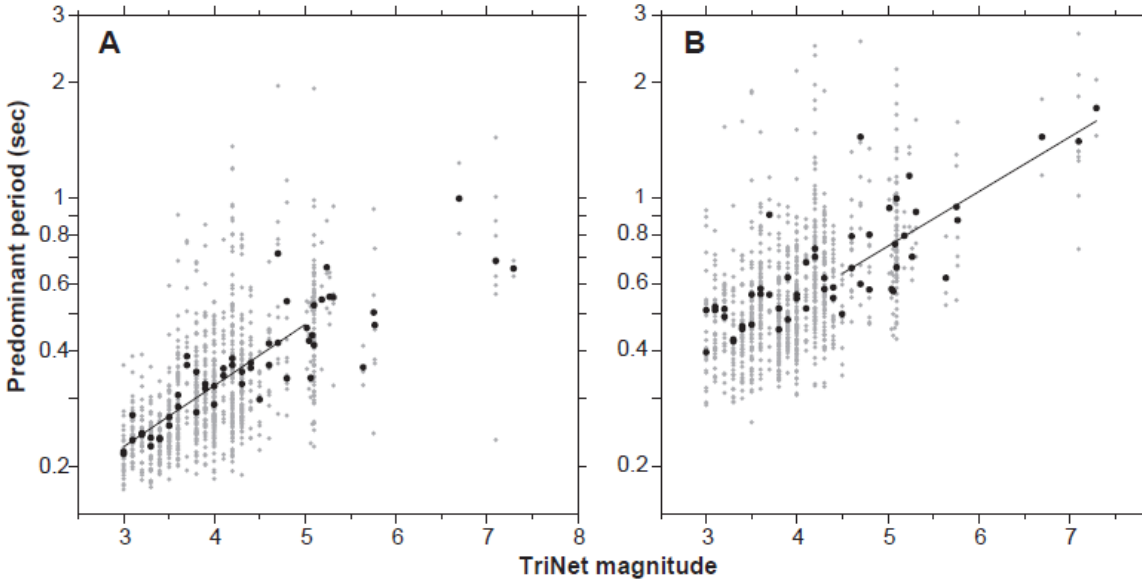

Figure 3.5. Predominant Period and Magnitude (Allen ve Kanamori, 2003).

In the study conducted by Allen and Kanamori (2003), two separate linear relationships between T_{max}^p and Magnitude were presented (Figure 3-5). These relationships were removed separately as a result of off-line studies. The light-coloured points given in Figure 3-5 give the period values for each station and the black points give the period averages for each earthquake. First, small for earthquakes (3.0≤m≤5.0) vertical component broadband speed records were filtered with 10 Hz low-pass filter. In small earthquakes, it is stated that the appropriate results were obtained with the use of 1-2 seconds of data window length. The resulting linear relationship is given in the following equation 3.6 (Allen, 2004, Allen and Kanamori, 2003).

$$m_l = 6.3\, log\left(T_{max}^p\right) + 7.1 \tag{3.6}$$

The velocity data for earthquakes whose magnitude is M>4.5, is filtered with a 3 Hz low-pass filter and with the help of the equations 3.3, 3.4 and 3.5, dominant periods are obtained. It is stated that the best result in terms of time estimation is obtained in the first 4 seconds of data, and the linear relationship obtained is given in the following equation 3.7 (Allen, 2004, Allen and Kanamori, 2003).

$$m_h = 7.0\, log\left(T_{max}^{p}\right) + 5.9 \tag{3.7}$$

The importance of the T_{max}^{p} method can be summarized briefly as follows:

- First, it was announced in the literature by Allen and Kanamori (2003) in the Journal of Science in 2003. Using the existing installed TriNet stations in California Nakamura's method has been tried to be adapted. The general difference of the system called alarms is that it uses a network from Uredas.
- Two years later, Lockman and Allen (2005), Allen and Kanamori's 2003 studies examined the scattering of single stations in dominant periods, and found that the distance-P amplitude-TP relationship was a striking study in order to achieve regional damping and to seek answers to the question of one station station possible in California. They used the first 4 seconds of the P wave in their studies.
- The same year Olson and Allen (2005), in addition to the Earthquake Data used by Allen and Kanamori in 2003, used Japan, Taiwan and Alaska data to recalculate the magnitude of M (M>6,0) by looking at the first 4 seconds of P wave.
- Two years later, Wurman and the other. (2007) reported that the elarms system calibrated 43 earthquakes ranging from 3.0 to 7.1 in size. As a result of the calibration of the ElarmS system, which is determined by using peak amplitude and greatest dominant period, they detected the initial magnitude value error in the first seconds as 0.72 units.
- Another study in 2007 was conducted by Lockman and Allen (2007) on the relationship between magnitude-period scaling for Japan and the North Pacific region. The study results were compared with the study results of Allen and Kanamori (2003) for California in 2003. They conclude that the increase in reliability in magnitude estimation can be achieved with the increase in the number of stations

that give rise to judge period observations. This number is subtracted from 1 station to 4 station and it is indicated that more clearly results are obtained. As a result, the average absolute value for Southern California is 0.5 units of the size error.

3.1.3. τ_c-P_d Method

It was found out that it was possible to warn the city of Taipei about 20 seconds ago, especially 120 km away from the city of Taipei, with the determination of earthquakes in Hualien region in eastern Taiwan (Allen el al., 2009; Hsaio et al., 2009; Wu and Kanamori, 2005a; Wu, 2007). However, since the earthquake of magnitude 7.6 occurred in 1999 occurred in the central parts of Taiwan away from Hualien region, a different network was sought. CWB has been looking for a solution optimized between the virtual subnet concept and reliable size detection and EEW. After 2000-2001, the VSPN method is used to calculate the stations 60 km away from the first programmed station (Wu et al., 2009). In other words, the inclusion of seismic stations within a distance of 60 km in close proximity to the outer dome in the calculation of epicentre and magnitude causes the system to not provide warning in this area (figure 3-6).

The Chi-Chi earthquake on September 20, 1999 (Chang et al, 2000.). A possible earthquake in central Taiwan, equivalent to its location, will give the city of Taipei a warning time of more than 20 seconds, 145 km away. On the other hand, the EEW durations to be expected throughout the country are given in figure 3-6. The Black star in figure represents the outer crust of The Chi-Chi earthquake. For this reason, a different approach is needed to provide EEW in areas near the source. In 2005, Kanamori (2005), Nakamura (1988) and Allen and Kanamori (2003) introduced a new parameter (τ_c) with the approach it developed by taking advantage of. τ_c uses the first 3 seconds of the earthquake to reflect the magnitude of that earthquake (Kanamori, 2005).

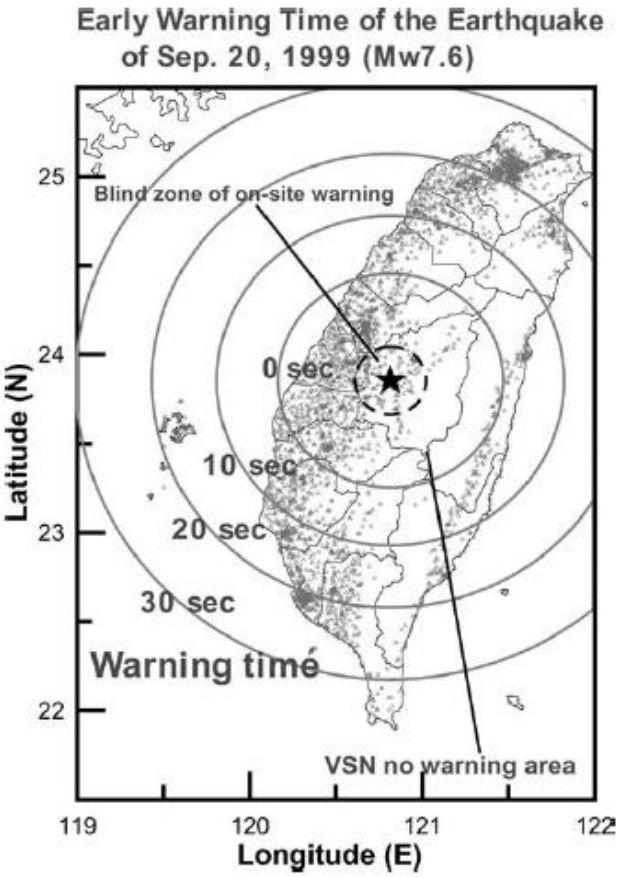

Figure 3.6. Expected VSN-based EWS early warnin times (Wu and Kanamori, 2005a).

In general, when the shear movement stops or continues, it is reflected in the initial movement period of the earthquake. Small and large tremors produce short and long periods of initial movements, respectively. In this context, it is very important to define the average period instead of the period of the first movement during the first movement. Also, the method of Nakamura is also used in the average period (Kanamori, 2005). Wu and Kanamori (2005a) have performed the following procedure modified by the method used by Nakamura. $u(t)$ vertical component displacement record, $\dot{u}(t)$ vertical component velocity record is calculated as follows:

$$r = \frac{\int_0^{t_0} \dot{u}^2(t)dt}{\int_0^{t_0} u^2(t)dt} \tag{3.8}$$

Here, the integral (0, 0) t is taken from the beginning moment of the P wave between t_0 time. t_0 is set to 3 seconds. Using the Parseval theorem,

$$r = \frac{4\pi^2 \int_0^\infty f^2 |\hat{u}(f)|^2 df}{\int_0^\infty |\hat{u}(f)|^2 df} = 4\pi^2 \langle f^2 \rangle \tag{3.9}$$

Where $\hat{u}(f)$ is the frequency spectrum of $u(t)$ and $\langle f^2 \rangle$ is the weighted average of $|\hat{u}(f)|^2$ and f^2.

$$\tau_c = \frac{1}{\sqrt{\langle f^2 \rangle}} = \frac{2\pi}{\sqrt{r}} \tag{3.10}$$

Thus, τ_c is used as a parameter representing the period of the initial part of the P wave (Kanamori, 2005; Wu and Kanamori, 2005a; Wu and Kanamori, 2008A). Waveforms were used by Wu and Kanamori (2005a), resulting in the kinematic source model (figure 3-7) of Sato and Hirasawa (1973), to show that τ_c is a good measure of the magnitude of the earthquake. Here, waveforms within the first 3 seconds of the onset of the earthquake, M_w>6.5 earthquakes are similar to waveforms. Figure 3-8 shows the size of τ_c values calculated by displacement waveforms. In this way, τ_c is saturated after M_w>6.5. This kinematic source model, the first three of the initial record of an earthquake using 6.5 seconds, it shows that earthquakes less than 6.5 can be predicted easily (Wu and Kanamori, 2005a).

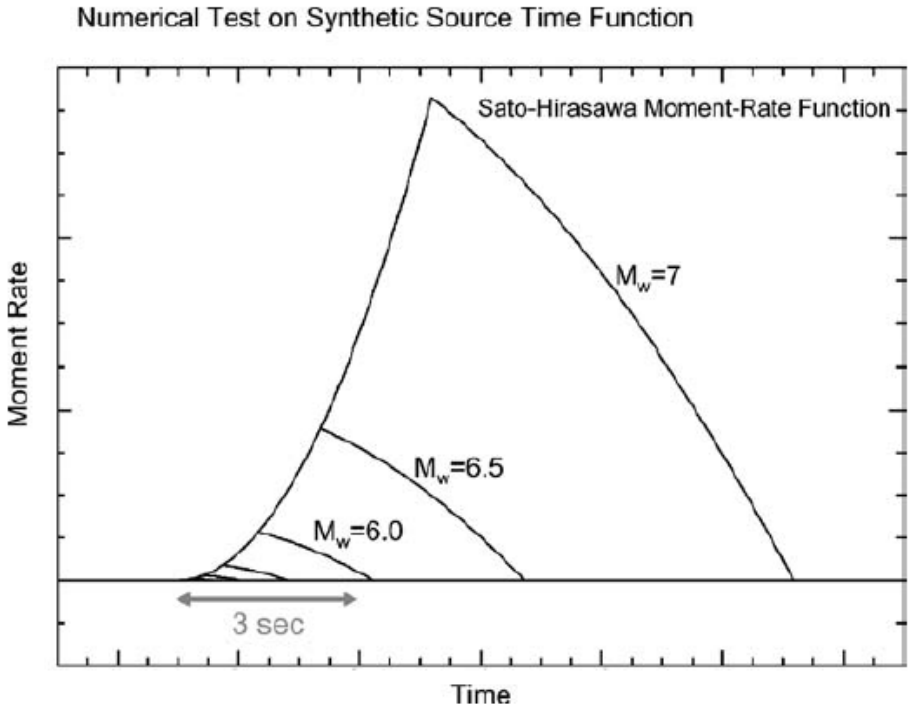

Figure 3.7. Displacement waveforms computed for the kinematic source model of Sato&Hirasawa, 1973 (Wu and Kanamori, 2005a).

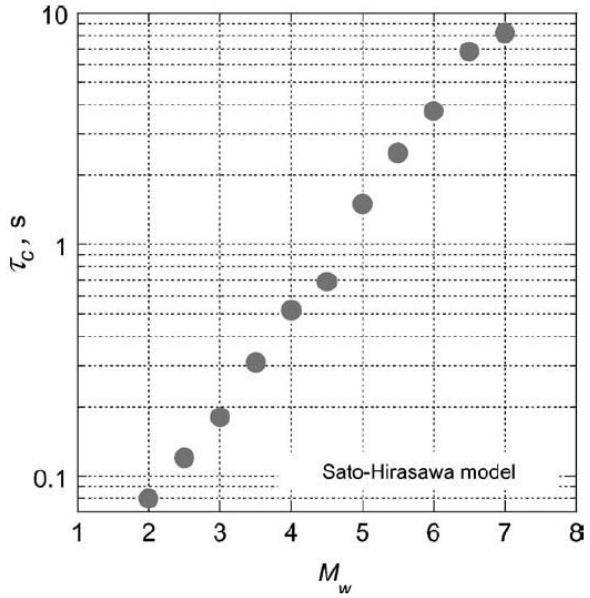

Figure 3.8. τ_c in seconds computed for the displacement waveforms of the Sato&Hirasawa, 1973 (Wu and Kanamori, 2005a).

If a longer value of t_0 is taken, it is stated that larger earthquakes can be predicted but not suitable for EEW purpose and not practical. However, the results obtained from synthetic data, 2,8≤m≤8,0 ranging from 23 earthquakes 131 records using the solution obtained, MW>7,0 earthquake without a saturation sign of τ_c increased was determined. In the first three seconds, a relationship can be used for larger earthquakes (Kanamori, 2005).

The first of two important objectives of the earthquake EEW is to estimate the magnitude of the S wave at any site by taking advantage of the start of the P wave, and the second is to determine the magnitude of the S wave at any site. The power of the shock is practically represented by the maximum acceleration (PGA), the maximum speed (PGV) and the maximum displacement (PGD) obtained from the three components. Speed by taking the Integral of the acceleration record, once again the Integral is repeated, the displacement record is obtained.

Using the Pd parameter obtained from the largest amplitude of the vertical displacement recorded from the beginning of the P wave (Wu and Kanamori, 2008a). They stated that PGV can be estimated to be recorded at that location. The Pd is the largest value obtained from the displacement record in a time window (t_0 =3 sec). In addition, they indicate that the above parameter should be used for rapid and reliable size determination (Wu and Kanamori, 2008a).

In τc and Pd Method, Data-Processing vertical component acceleration records are started by marking phase transitions. In order to obtain the speed and displacement signals for each record, the vertical component acceleration registers are taken twice in succession. This data is filtered by the single-way butterfly filter, which has a cutting frequency of 0.075 Hz, to eliminate the low-frequency drift resulting from the integral process. From the initial moment of P wave detected, the integral is taken between t_0 time window (3 seconds). The R ratio is calculated using the resulting displacement and velocity data in equation 3.8. with the substitution of r in equation 3.10 τ_c values are obtained.

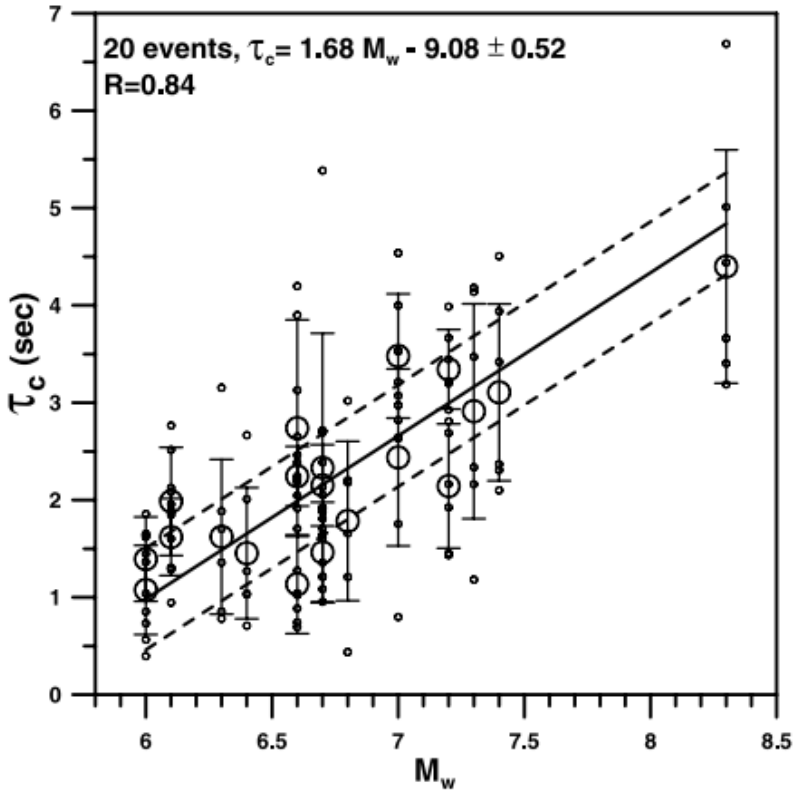

Figure 3.9. Relation between τ_c and moment magnitude, M_w (Wu and Kanamori, 2008b).

Wu and Kanamori (2005a, 2005b, 2008b), and Wu et. Al. (2006, 2007) studies were carried out to determine parameters (τ_c and P_d) in Southern California, Taiwan and Japan. Figure 3.9 shows a good linear relationship between τ_c and M_w. The straight line shows the straight line with the smallest squares and the straight lines show the standard deviation. Symbols are displayed by taking the average in order of registration. It is remarkable that the τ_c values of potentially damaging, destructive earthquakes are greater than 1 second (τ_c >1 sec). As a result of the linear relationship, the size estimate is given in the following equation.

$$M_w = 3.373 \log\tau_c + 5.787 \pm 0.412 \qquad (3.11)$$

Figure 3-10 shows the linear relationship between P_d and PGV using a total of 780 records of 54 earthquakes selected from three regions, whose outer centre distance is less than 30 km. The straight line shows the straight line with the smallest square method, and

the cut lines show the standard deviation (Wu and Kanamori, 2008a). As a result of previous studies, if PD>0,5 cm, PGV value in that area exceeded 20 cm/sec as damaging level (Wu and Kanamori, 2008a). For the estimation of PGV, the equation 3.12, which is derived from the result of the linear relationship between PD and PGV, is as follows:

$$\log(\mathrm{PGV}) = 0.903\log(\mathrm{P_d}) + 1.609 \pm 0.309 \qquad (3.12)$$

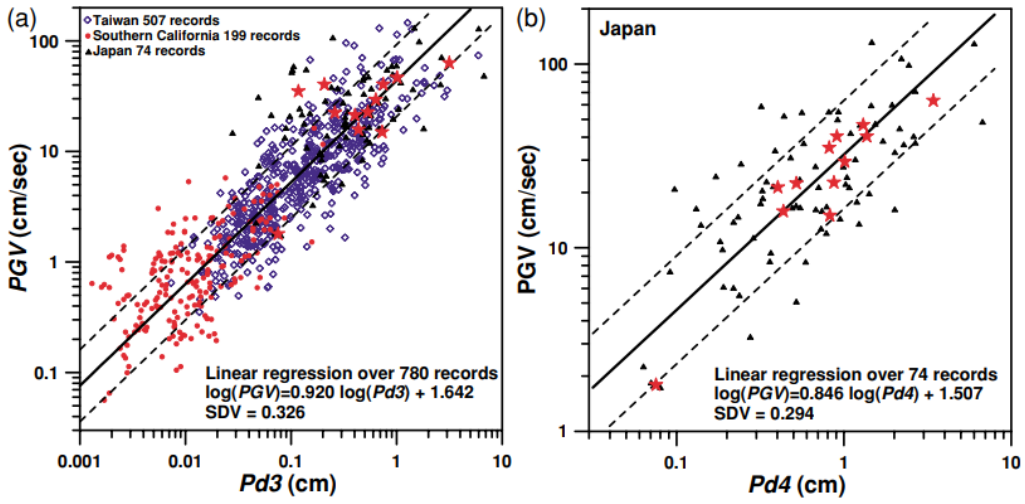

Figure 3.10.(a). Relationship between peak initial three-second displacement amplitude and peak ground velocity(PGV) (b) Rlationship between peak initial four-second displacement amplitude anad PGV.

In summary, when τ_c >1 sec and P_d>0.5 cm, it is assumed that the level of an earthquake, which is usually greater than 6.0 magnitude, is very high in that area. The result is considered and used as two basic parameters for τ_c and P_d earthquake EEW approach (Shieh et al., 2008; Wu and Kanamori, 2005a, 2005b, 2008a, 2008b; Wu et al., 2007).

We can briefly summarize the basic developments regarding τ_c-P_d method as follows:

- In 2005, Wu and Kanamori (2005a) tried to improve the methods of Allen and Kanamori in 2003 by Nakamura's work in 1988. The first 3 seconds of the P wave are used to present the TC parameter, which is a new parameter.

- Earthquake Early Warning parameters a study was carried out to determine τ_c and P_d values for Southern California (Wu et al., 2007). In this study, the first 3 seconds of P wave were taken. A relationship between τ_c - size and τ_c - size for Southern California, and for Southern California and Taiwan, they have also identified a relationship between P_d-PGV. It is stated that the increase in station frequency and number of stations will strengthen early warning detection.
- The study conducted by Wu and Kanamori (2008a) in 2008 was also on TC and Pd. In this study, they used data from Japan, Taiwan and Southern California. In light of these data, if the P_d value exceeds 0.5 cm, it is stated that the PGV value in the field exceeds the damaging level (approximation -20 cm/sec). In addition, at least 4 stations were calculated with the mean τ_c error resulting from the size ± 0.4 unit was given.

3.2 Engineering Methods

An example of earthquake EEW systems with engineering parameters is the Istanbul earthquake warning system, which is run by Boğaziçi University Kandilli Observatory and Earthquake Research Institute. In this system, the amplitude of the incoming seismic wave exceeds a specified threshold level is checked and the earthquake is decided, and alarm is generated. PGA and CAV values are used as threshold level (Alcik et al., 2006; Erdik et al., 2003).

3.2.1. PGA

PGA is an earthquake accelerometer and is used as an input in earthquake engineering. The Richter magnitude scale of earthquakes as the total size is 48 and not just on supply for a geographical area taken as a measure that would shake from an earthquake. The unit is g or m/s2.

Filter must be applied to avoid unwanted sudden noise peaks from high frequency harmonics. The ground acceleration value filtered by a band-pass filter is a simple and useful

trigger parameter. As one axis can be used, three components (X, Y, Z) are used (Razinkov, 2009).

In order to avoid problems in close and distant earthquakes, it is more logical to use three components depending on the work area. PGA is defined as follows;

$$\mathrm{PGA} = \max|\mathrm{a(t)}| \tag{3.13}$$

$$|\mathrm{a(t)}| = \sqrt{\mathrm{a_x^2(t) + a_y^2(t) + a_z^2(t)}} \tag{3.14}$$

Here, t Time, a acceleration record, x, y, z specifies the direction of the three components.

3.2.2. CAV

CAV is not a parameter that can cause error, such as the maximum acceleration value. This algorithm appears to be an easier parameter to specify a system requirement to alert for nuclear power plants in the eastern part of the United States. The EPRI (Institute for electrical energy research) was sponsored by the study conducted in 1988 and CAV was defined as follows:

$$\mathrm{CAV} = \int_0^{\mathrm{t_{max}}} |\mathrm{a(t)}|\mathrm{dt} = \sum_0^{\mathrm{t_{max}}} |\mathrm{a(t)}|\mathrm{dt} \tag{3.15}$$

Here; t_{max} earthquake recording time, a Acceleration recording and t Time. In the 1988 study, the damaging, damaging threshold level of nuclear power plants by EPRI was given as 0.300 g*sec (EPRI, 1988). The parameter CAV (EPRI, 1988; EPRI, 1991; Lee and Lee, 2001), which is usually used in the EEW system for nuclear power plants, is used and tested in conjunction with PGA (Erdik et al., 2003).

The CAV is more sensitive to low-frequency movements, which are generally considered destructive than high-frequency movements. This explains the high harmony between CAV and seismic magnitude (EPRI, 1991).

3.2.3. BCAV

In order to reduce the impact of long-term earthquakes with low acceleration values on the CAV, a modification was made in 1991. As a result of this study, CAV was presented as $BCAV$ (Bracketed Cumulative Average Velocity) in a new expression (EPRI, 1991). After this date, in the literature, when it is called CAV, it is actually mentioned about $BCAV$. The $BCAV$ presented is introduced in the following format.

$$\mathrm{BCAV} = \sum \int_{t_i}^{t_i+\Delta t} |a(t)|dt \tag{3.16}$$

Here, the lag time Δt, t_i any time, t time, a acceleration values. After PGA exceeds the threshold level of 0.025 mg (Max $|a(t)|$>0.025g), the CAV starts to be calculated. As a result of the studies, the new CAV value was 0.166 g*sec (EPRI, 1991). The threshold level of CAV is 0.33 g*sec-0.50 g*sec (Lee and Lee, 2001; Lee and others, 2006).

4. CASE STUDY: ISTANBUL – MARMARA REGION

4.1.Importance of The Area

Turkey is located on the ALP-Himalaya earthquake zone, one of the active earthquake zones in the world. It is known that 92% of our country is in earthquake zones, 95% of our population is in earthquake danger, 98% of large industrial centres and 93% of our dams are in earthquake zones. In the last 58 years, about 60.000 people have died from earthquakes, more than 100.000 people have been injured and nearly 400.000 buildings have been destroyed or severely damaged (Earthquake Research Department, 2009).

One of these earthquake regions is the Marmara region. The Marmara region is bounded by approximately 26°-31° East longitudes and 40°-41°north latitudes. The tectonic and earthquake activity of this region is known to be under the control of the Western arms of KAF and the southwest Anatolia trench zone in the South (Barka and Kadinsky-Cade, 1988; Barka, 1991). In addition, the region exhibits numerous small earthquakes that show that young tectonic movements are intensifying (Üçer, 1990); (2000) and occasional large earthquakes (Ambraseys and Finkel, 1991; Ambraseys and Jackson, 2000; Kalafat et al., 2007). Statistical data indicate that a historical and current destructive earthquake has occurred every hundred years in the Marmara region (Koçyigit, 2006). The Marmara region covers an important area of the first and second earthquake regions, with a surface area of 67.000 km2, with a total of 11 cities, including Istanbul, Kocaeli and Bursa, which are the most industrial and commercial centres of Turkey. Two recent earthquakes in the Marmara region, 17 August 1999 Kocaeli (Mw=7.5) and 12 November 1999 (Mw = 7.2) Düzce, undoubtedly were the disasters of the century. After these earthquakes, more than 18,000 of our citizens have died, more than 48,000 have been injured at various levels, 375,000 buildings have been damaged at various rates and our economy has lost around 15 billion US dollars (Ünal, 2002). The probability of a 7-magnitude earthquake in Istanbul is 1/50. Although this possibility seems small, there are three cities that share this situation in the World; Istanbul, Tokyo and San Francisco (Erdik et al., 2004). For this reason, the

earthquake phenomenon is a little more important every day for both Istanbul and Marmara region.

4.2.Tectonic Structure of the Area

The young tectonic period in Turkey began 11 million years ago when the Arabian Peninsula hit Anatolia. After this collision, first East, then all Anatolia was thickened and after this thickening reached a level where the continental crust could not be met, Anatolia started to move towards the west. The movement of Anatolia to the west occurred along the North Anatolian with the right side and East Anatolian faults with the left side (Figure 4.1). In Figure 4.1, the inner triangular lines show active training zones, inner triangular lines show active reverse faults, and straight lines show normal faults. The fact that KAF became a right-lateral fault corresponds to about 5 million years ago (Tüysüz, 2010).

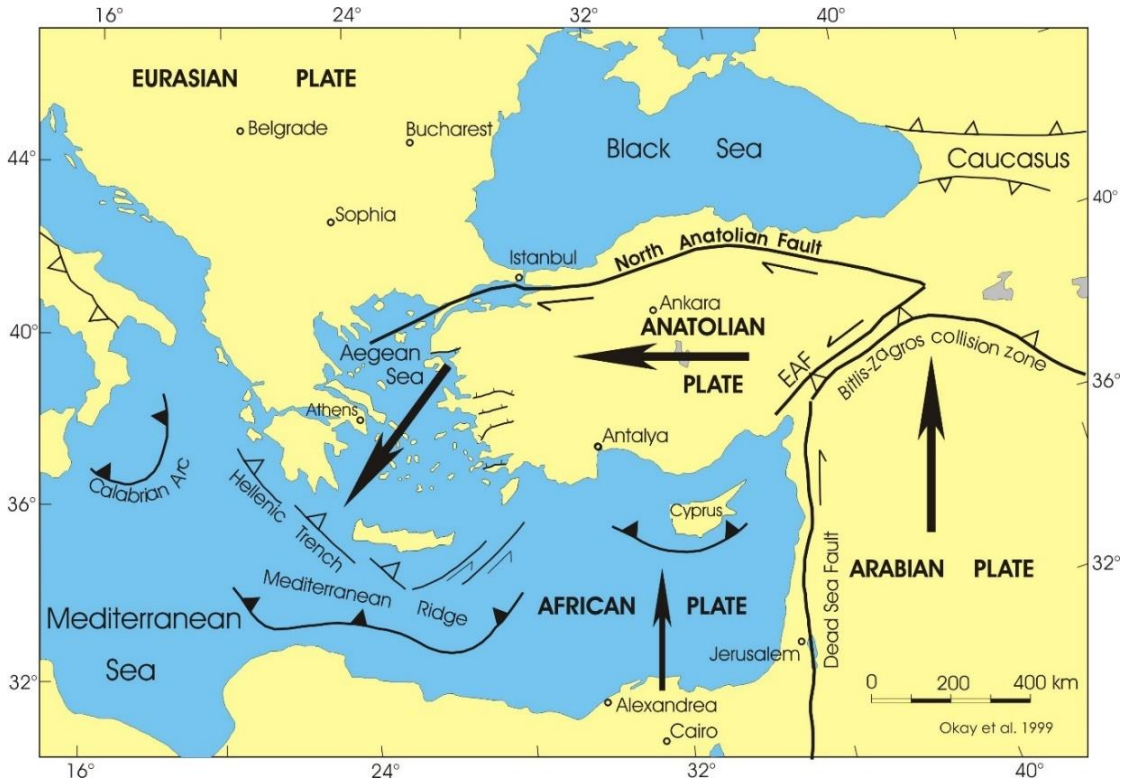

Figure 4.1. Tectonic Map of East Mediterranean (Okay et al. 1999).

The Marmara Sea, which is approximately 240 km long, 70 km wide and an area of 11,500 km2, is the only inland sea within the borders of Turkey, is a young Inland Sea from a geological point of view. The Marmara Sea is located on two important branches of Kaf. The northern arm of these enters the Marmara Sea from the Gulf of Izmit in the East and extends from the sea to the North Aegean. The second column passes south of Iznik Lake and enters Gemlik Bay, following approximately the southern coast of Marmara Sea and extends to Kapidağ Peninsula, where it runs out of the sea and continues to the Aegean Sea from inside the Biga Peninsula. In the basins of the sea, the north half of the depth of 1,200 meters in the South is separated from the shallow continental shelf area by an apparent Westernized slope of 100 meters. In the deep section of the north, there are three deep basins separated by thresholds. These are Tekirdağ, central Marmara and Çınarcık basin from West to East. These basins, filled with thick sediments, are still being filled (Okay et al., 2000) with a depth of 600 to 800 meters from each other is divided by horizontal-southwest ridges (Tüysüz, 2010).

Barka and Kadinsky-Cade (1988) suggested that the Marmara Sea was opened as a series of basins (figure 4.2). Figure 4.2 shows the discrete lines 20. the surface cracks of earthquakes in the century, yellow areas between 1700 and 2100 fracture between the fault segments and the affected areas show. The original map, which belongs to Barka (1997), was modified and taken from Gürbüz et al. (2000). However, recent studies indicate that no traces of the strike slip structure were observed and that the tectonic structure of today was not strike slip structure (Imren et al, 2003).

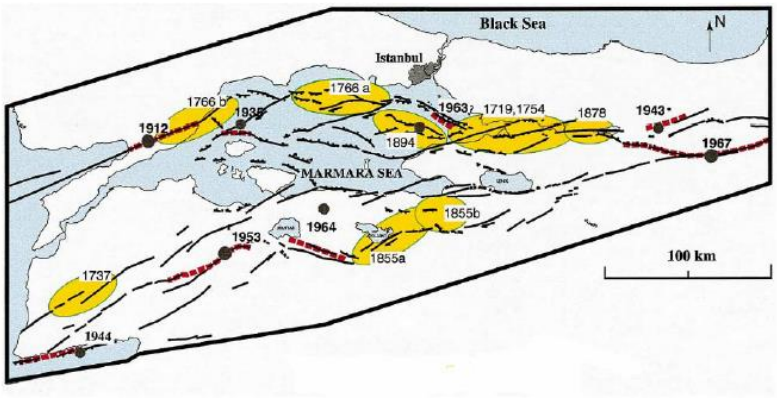

Figure 4.2. Marmara Region Earthquake History (Gürbüz et al. 2000).

Recently, Le Pichon et al. (2001) interpreted Kaf's geometry in the Marmara Sea in the light of the data obtained by the “Le Suroit” ship. According to this research based on bathymetry and seismic reflection profiles, the structure of the Marmara Sea is shown in figure 4.3. According to these maps, the main arm of Kaf entering the Marmara Sea from the east of Izmit Bay enters the Çınarcık Basin at the exit of the Gulf and this hole is traced to the South and west of the islands in a way bordering from the North. The fault extending between Çınarcık - Yalova to the south of Çınarcık Basin, which can be clearly traced to the aftershocks of the August 17 earthquake, cannot be seen on this map because of the fact that it has not been studied in shallow waters. After the south of the islands, the main fault branch turns and gains the east-west slope. This turnout area off Yeşilköy is characterized by North-South trapping faults. This indicates that the rotation of the fault creates a jamming effect here. The Çınarcık Basin is limited to the Middle Marmara rise in the West. The main fault, which continues to the north of this elevation, passes through the Kumburgaz Basin and enters the central Marmara Basin in the West. This basin is filled with soft, water-filled sediments that are not sealed inside, and the fault cannot be observed as well as the other sections, and it is observed in the form of a large number of small faults. The trace of the main fault in the Western Marmara rise, which constitutes the western border of the Central Marmara Basin, is very evident. The fault which cuts the ridge sharply enters the Tekirdag Basin to the West. The main fault passing to the south of the basin then goes ashore from the south of the Ganos mountains to the Gulf of Saros (Tüysüz, 2010).

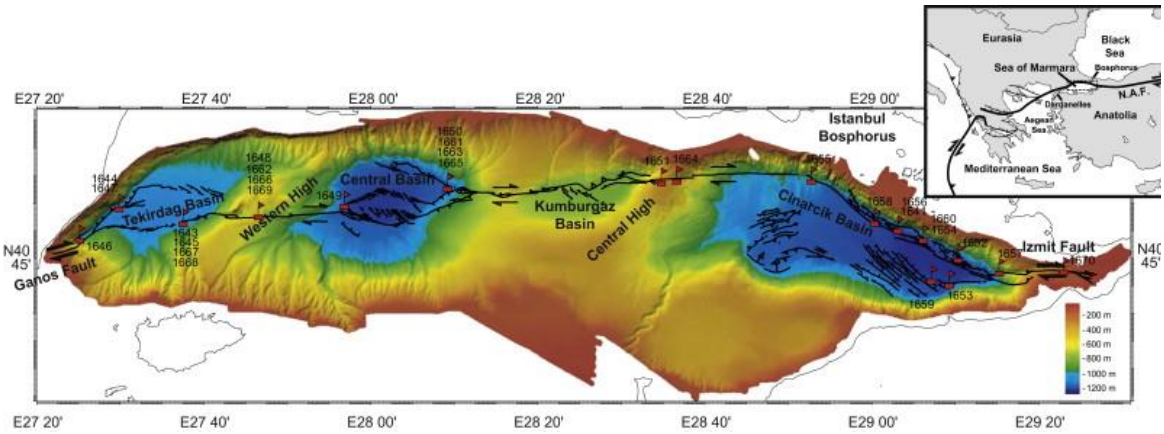

Figure 4.3. Structure of Marmara Sea (Burnard et al., 2012).

These faults have been reported to be major earthquakes in the past (Ambraseys and Jackson, 2000). When we look at the distribution of these earthquakes in Figure 4.4, an intensive earthquake activity is clearly observed in and around the Marmara Sea. In the North Marmara Sea, in the Gulf of Izmit and Saros, in the west of Kapıdağ peninsula, in the Çınarcık Basin, in the Gulf of Gemlik and in the east of Bursa earthquakes are observed. In summary, the eastern-western extent of the earthquake activity in Marmara is quite evident. The fact that the seismicity here is quite well aligned with the historical seismicity pattern given in Figure 4.2 can give information about the reliability of the historical earthquake database.

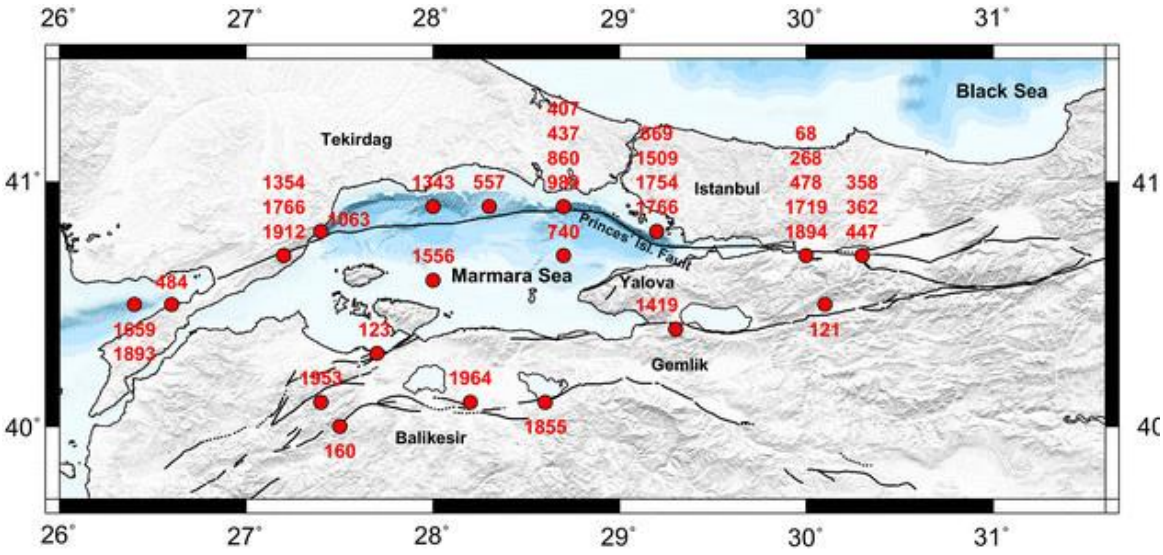

Figure 4.4. Past Important Earthquakes Occurred in Marmara (Ambraseys, 2002).

4.3.Downholes Operated in Istanbul

KOERI operates three seismic downhole arrays on theWest side of Istanbul (Figure 4.5 and 4.6). They are namely Atakoy (ATK), Fatih (FTH) and Zeytinburnu (ZYT) seismic downhole arrays, named after their districts. ATK and FTH arrays are located approximately 2 km inland from the shore of the Marmara Sea, while the ZYT is only about 400 m inland. The longest linear distance between the two arrays is about 9 km between ATK and FTH. At this point, it should be noted that all three downhole arrays are immediately North of the present seismic gap where the location of the impending earthquake expected.

All instrumentation used in the downhole arrays are Kinemetrics make. The sensors in the downholes are HypoSensor type and the surface sensors are EpiSensor type. All are triaxial force balance accelerometers. The recordings are continuously made at a rate of 200 Hz. The data recorded by all the sensors in the arrays are transferred to the Kandilli Observatory Earthquake Research Institute of Boğaziçi University on real time basis through internet connection.

Figure 4.5. Locations of the Downhole Arrays Operated by KOERI.

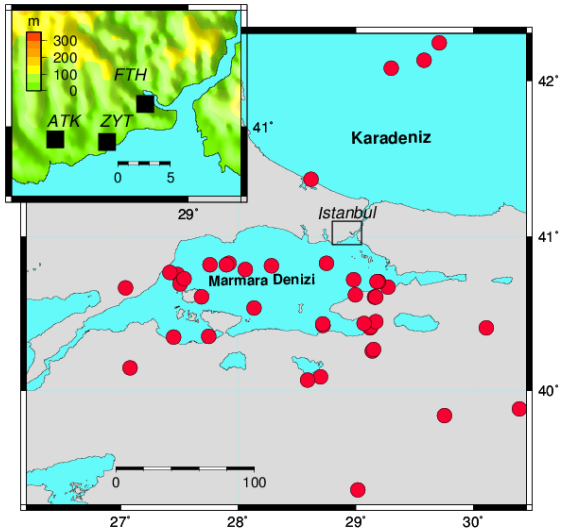

Figure 4.6. *Ataköy, Zeytinburnu and Fatih Wells Distribution (Dikmen and Tanırcan, 2017).*

4.3.1. Atakoy Downhole Array (ATK)

Atakoy downhole array was deployed in 2005 as part of a research project of KOERI together with German Research Center for Geosciences (GFZ). The array is located in a residential neighborhood in the West side of Istanbul at about 15 km from the Historic Peninsula.

The ATK array has instrumentation at the ground surface and at 25, 50,70 and 140m depths. The downholes are placed in the corners of a 3.0x3.0 m^2 area inplane. The surface instrument is located in the center of this square area. The array is at about 15.0m above the sea level.

4.3.2. Fatih Downhole Array (FTH)

The Fatih Downhole Array is located within the Fatih Mosque Complex in the Historic Peninsula of Istanbul. The array was deployed through are search project funded by the Scientific and Technological Research Council of Turkey (TUBITAK) and Bogazici University. The array was deployed in 2010 and consists of 3 downholes. The array has instrumentation at 23,60 and 136m depths as well as one on the ground surface. The array is at about 68.0m above the sea level.

4.3.3. Zeytinburnu Downhole Array (ZYT)

The Zeytinburnu Downhole Array is located within premises of the Zeytinburnu Municipality's complex. The financial support for the array was provided through are search project funded by The Scientific and Technological Research Council of Turkey (TUBITAK) and Bogazici University. The array was deployed in 2010 and consists of 3 downholes. The sensors are placed at the ground surface and at 30,57 and 288m depths. The top of the array is at about 22.0m above the sea level.

4.4.TauC-Pd Analysis

The two attributes, τ_c and the peak value of the filtered displacements (Pd), which are widely used in on-site earthquake early warning applications are determined from the initial part of the P waves using different time window lengths of 1,2,3 and 4 seconds as described in Wu and Kanamori (2005). The different time window lengths have been utilized to investigate whether better prediction models of PGV and magnitude are obtained. However, it is a well-known fact that too long time window duration compromises the ability for early warning. Here, the aim is to construct τ_c - M and PGV - P_d relationships using downhole arrays operated in Istanbul and compare them with the models derived from the AFAD surface data.

Bandpass filtering using corner frequencies of 0.075 and 25 Hz is applied to get rid of long period and high frequency noise. In order to detect the P wave arrival, STA (Short Term Average) / LTA (Long Term Average) ratio is used. The average amplitudes estimated from the short and long time windows define the STA and LTA values. In the analysis, STA is taken as 0.5 and LTA is taken as 5.0 seconds. The triggering threshold value is specified as 4 used to issue an earthquake alarm. After P-wave arrival is detected the τ_c and P_d parameters are estimated.

In the first stage, AFAD data were used to establish τ_c - M and PGV - P_d relationships based on 65 record files belonging to 46 earthquakes whose magnitudes vary in the range of 3.8 and 7.6 as described in the τ_c - P_d method. Details of the data obtained from AFAD are given in Table 4.1. For the selection criteria, a minimum peak acceleration value in the vertical component is taken as 30 mg and the maximum epicentral distance from is limited to 150 km. The acceleration waveforms satisfying these two criteria are included in the database to establish the τ_c - P_d prediction models.

Table 4.1. AFAD Earthquake Data.

Date	M	Location	Lat.	Long.
Feb. 14, 1996	4,2	Kemah	39.61 N	19.23 E
Jan. 22, 1997	5,0	Hatay	36.21 N	35.98 E
July 04, 1998	5,0	Adana	36.81 N	35.24 E
Aug. 17, 1999	7,6	Gölcük – Kocaeli	40.77 N	30.00 E
Sept. 13, 1999	5,8	İzmit – Kocaeli	40.73 N	30.01 E
Nov. 11, 1999	5,6	Düzce	40.74 N	30.24 E
Nov. 12, 1999	6,6	Düzce	40.80 N	31.18 E
Aug. 23, 2000	5,2	Akyazı	40.78 N	31.18 E
Oct. 14, 2000	4,7	Denizli	37.89 N	29.03 E
Dec. 02, 2001	4.5	Van	38.51 N	43.24 E
Apr. 03, 2002	4,4	Isparta	37.73 N	30.31 E
Dec. 14, 2002	5,1	Osmaniye	37.46 N	36.18 E
May 01, 2003	6,3	Bingöl	39.01 N	40.46 E
July 23, 2003	5,3	Buldan – Denizli	38.06 N	28.88 E
July 26, 2003	5,4	Buldan – Denizli	38.05 N	28.90 E
Sept. 23, 2003	4,2	Amasya	40.60 N	35.87 E
Feb. 08, 2006	4,3	Sakarya	40.73 N	30.40 E
Oct. 24, 2006	5,0	Gemlik – Bursa	40.44 N	29.07 E
Aug. 26, 2007	5,3	Karlıova – Bingöl	39.24 N	41.12 E
Oct. 29, 2007	5,0	Denizli	37.07 N	29.31 E
Dec. 27, 2007	5,2	Bala - Ankara	39.46 N	33.08 E
Feb. 17, 2009	4,8	Simav - Kütahya	39.15 N	29.04 E
Mar. 08, 2010	5,8	Kovancılar – Elazığ	38.77 N	40.03 E
Sept. 17, 2010	4,7	Gerger – Adıyaman	38.12 N	38.92 E
Nov. 11, 2010	4,7	Kuşadası	37.87 N	27.33 E
Jan. 20, 2011	4,1	Gölcük – Kocaeli	40.71 N	29.76 E
Feb. 05, 2011	4,0	Denizli	37.91 N	29.06 E
May 19, 2011	5,9	Simav – Kütahya	38.13 N	29.08 E
May 20, 2011	4,3	Simav – Kütahya	39.11 N	29.08 E

May 24, 2011	4,2	Simav – Kütahya	39.07 N	29.03 E
May 28, 2011	4,7	Simav – Kütahya	39.12 N	29.04 E
June 27, 2011	5,0	Simav – Kütahya	39.12 N	29.02 E
June 29, 2011	4,4	Adana	37,39 N	35.86 E
Oct. 23, 2011	4,0	Van	39.02 N	42.24 E
Nov. 09, 2011	5,7	Van	38.43 N	43.28 E
Dec. 04, 2011	4,8	Van	38.48 N	43.29 E
Jan. 21, 2012	4,1	Pasinler – Erzurum	39.91 N	41.69 E
Apr. 04, 2012	4,7	Gaziantep	36.95 N	35.86 E
May 03, 2012	5,2	Hisarcık – Kütahya	39.12 N	29.11 E
June 10, 2012	6,1	Fethiye – Muğla	36.36 N	28.93 E
July 22, 2012	4,8	Andırın – Kahramanmaraş	37.75 N	36.37 E
Sept. 19, 2012	5,0	Kahramanmaraş	37.28 N	37.14 E
July 30, 2013	5,3	Gökçeada – Çanakkale	40.30 N	25.79 E
Aug. 17, 2013	4,5	Gemlik – Bursa	40.41 N	29.11 E

In the τ_c - P_d algorithms it is considered that τ_c reflects the rupture duration or the size of the earthquakes. The larger the τ_c value the larger is the magnitude. That is to say, small and large tremors produce short and long periods of initial movements, respectively. Therefore, τ_c is used as a parameter representing the period of the initial part of the P wave.

The relationship between M and τ_c values obtained using the procedure given in section 3.1.3 and equations 3.8, 3.9 and 3.10 is given in figure 4.7. Here, τ_c values obtained from the vertical component acceleration recordings are shown in small circles. The red line shows the regression results obtained using the least squares method.

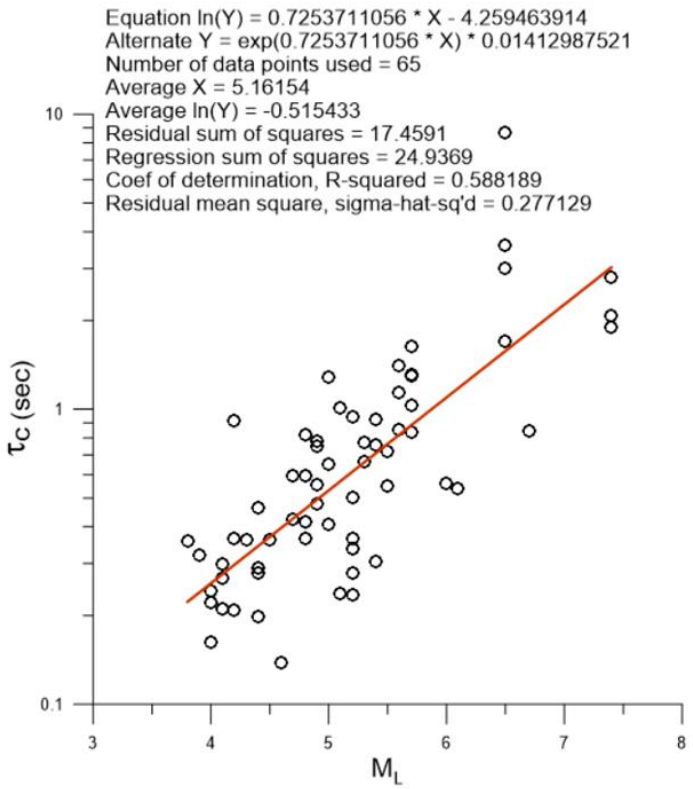

Figure 4.7. τ_c - M_L relation derived from AFAD earthquake records.

From Figure 4.7, the following relations are derived;

$$\log\tau_c = 0.72537\, M_w - 4.25946 \tag{4.1}$$

$$M_w = 1.3786 \log\tau_c + 5.87212 \tag{4.2}$$

showing the relationship between period and magnitude.

When we look at the relationship between τ_c and M in Figure 4.7, the scattering of τ_c is considerably high. Similarly, Wu et al. (2007) reported that large scattering may be encountered in earthquakes with magnitudes <5.5. However, the average τ_c values are also higher than those obtained in other studies, especially small earthquakes (Wu and Kanamori, 2005b). The first reason for large scattering is the low signal / noise ratio, which results in small amplitudes in the first three seconds of the earthquake (Wu et al., 2007). Likewise, data with small amplitudes in terms of early warning are often left out of interest.

Using the same database, a relation between P_d and PGV has been established as well. The P_d parameter reflects the largest amplitude of the vertical displacement observed in the initial portion of P waves, while PGV is estimated from the velocity records derived as integration of the acceleration records. The P_d value is the largest amplitude in the displacement records recorded in a time window (t_0 =3 sec) after the P-wave onset.

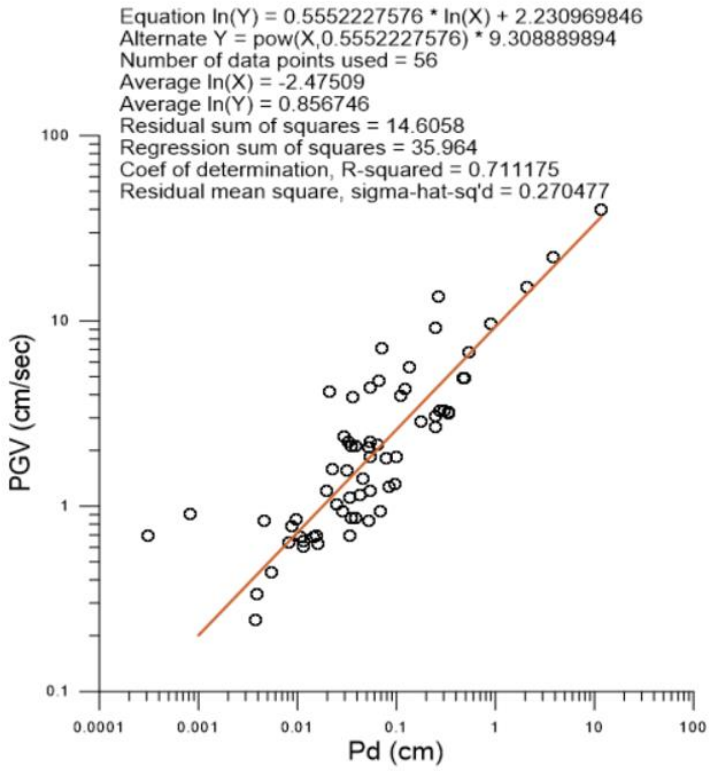

Figure 4.8. P_d - PGV Relation for AFAD Earthquake Records.

The relationship between P_d and PGV is given in figure 4.8. Here, P_d and PGV values obtained from the vertical component acceleration recordings are shown as small circles. The red line shows the line that is fit by the least squares method.

From Figure 4.8, the following relations;

$$\log PGV = 0.55522 \log P_d + 2.23097 \tag{4.3}$$

$$\log P_d = 1.801 \log PGV - 4.0182 \tag{4.4}$$

have been created between P_d and PGV.

In the second stage, using the acceleration records obtained from the downhole arrays operated by the Kandilli Observatory Earthquake Research Institute (KOERI) of Boğaziçi University in İstanbul, the model parameters (τ_c and P_d) have been estimated. The performance of the prediction models derived from the downhole arrays are compared with the derived equations from AFAD data stated in the first stage. Details of the data obtained from downhole arrays are given in Table 4.2. The records are shown in Appendix.

Table 4.2. Downhole Earthquake Data.

Date	M	Location	Lat.	Long.
May 24, 2014	6,9	Gökçeada	43.30 N	25.46 E
Nov. 27, 2013	4,7	Marmara Sea (Tekirdağ)	40.85 N	27.92 E
Feb. 5, 2014	3,8	Blacksea (İstanbul)	41.37 N	28.62 E
Nov. 24, 2013	4,8	Bünüş - Bolu	40.78 N	31.88 E
Jul. 3, 2014	4,5	Kuş gölü - Balıkesir	40.21 N	27.93 E
Apr. 29, 2015	4,0	Blacksea	42.08 N	29.30 E
May 11,2015	3,9	Gemlik - Bursa	40.42 N	29.13 E
Jun 7,2016	4,6	Gürsu - Bursa	40.26 N	29.14 E
Jun 7,2016	3,5	Gürsu - Bursa	40.27 N	29.15 E
Jun 25,2016	4,5	Marmara Sea (Yalova)	40.71 N	29.19 E
Jul,17,2016	4,0	Marmara Sea (Yalova)	40.71 N	29.18 E
Jan. 30, 2016	3,5	Marmara Sea	40.79 N	29.06 E
Mar 27, 2016	3,7	Marmara Sea	40.82 N	27.90 E
Mar 28,2016	3,7	Marmara Sea	40.73 N	27.54 E
Dec 15,2015	4,0	Blacksea	42.24 N	29.71 E
Dec 05,2015	3,7	Marmara Sea (Gemlik)	40.44 N	29.07 E
Nov.16,2015	4,2	Marmara Sea (Avcılar)	40.83 N	28.75 E
Oct. 28, 2015	4,5	Marmara Sea	40.82 N	27.76 E
Oct. 16, 2015	3,5	Gemlik - Bursa	40.45 N	29.17 E
Nov. 27, 2013	4,2	Marmara Sea	40.83 N	27.92 E

Sept. 24, 2019	4,7	Silivri	40.88 N	28.21 E
Sept. 26, 2019	3,7	Silivri	40.83 N	28.23 E
Sept. 26, 2019	5,8	Silivri	40.88 N	28.21 E
Sept. 26, 2019	3,9	Silivri	40.85 N	28.21 E
Sept. 26, 2019	3,5	Silivri	40.84 N	28.23 E
Sept. 26, 2019	3,9	Marmara Sea	40.85 N	28.28 E
Sept. 26, 2019	4,3	Silivri	40.87 N	28.25 E
Sept. 27, 2019	3,6	Marmara Sea	40.84 N	28.24 E
Sept. 28, 2019	3,8	Silivri	40.87 N	28.23 E

The relationship between M and τ_c values has been obtained using the procedure given in section 3.1.3 and equations 3.8, 3.9 and 3.10. The analysis is made for downhole array records dated between the years 2013 – 2019 including the September 26, 2019 Silivri earthquake sequence. In the analysis, 1, 2, 3 and 4 second time windows are used, and the graphs are given in the figures 4.9 - 4.12 for τ_c and M_L relation. Here, τ_c values obtained from the vertical component acceleration recordings are shown by small plus characters.

The relationship between P_d and PGV values obtained using the largest value obtained from the displacement record in the 1,2,3 and 4 seconds time windows are given in figures 4.13- 4.16. Here, P_d and PGV values obtained from the vertical component acceleration recordings are shown by plus characters.

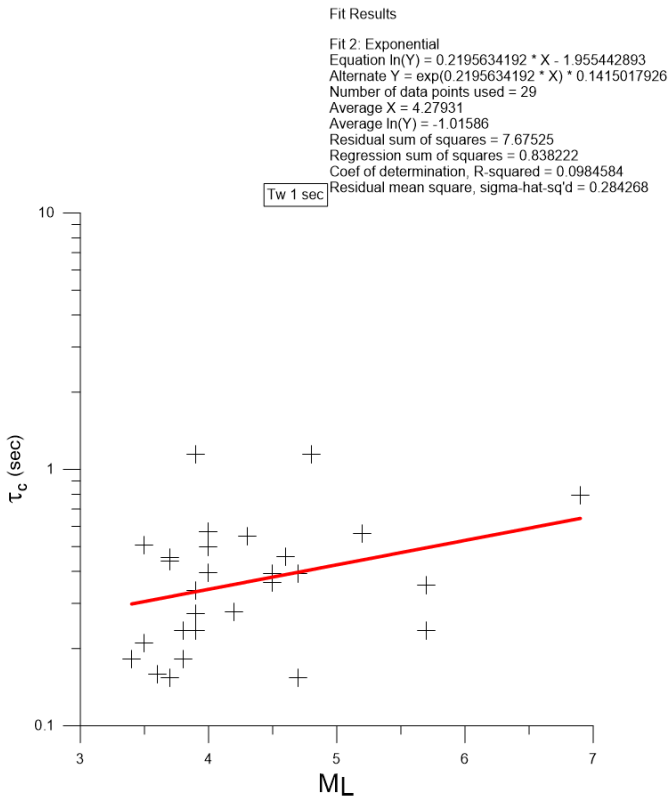

Figure 4.9. τ_c - M_L Relation for 2013 – 2019 Downhole Earthquake Records For 1-Second Time Window Length.

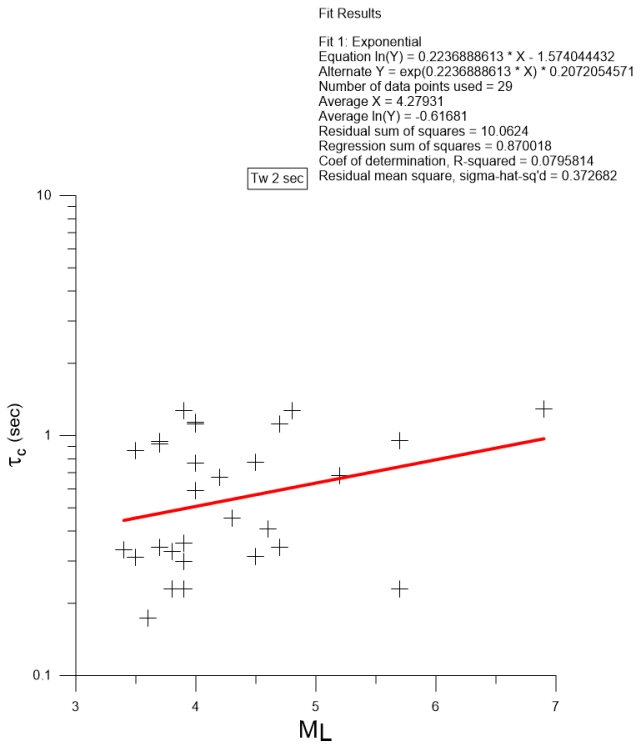

Figure 4.10. τ_c - M_L Relation for 2013 – 2019 Downhole Earthquake Records For 2-Second Time Window Length.

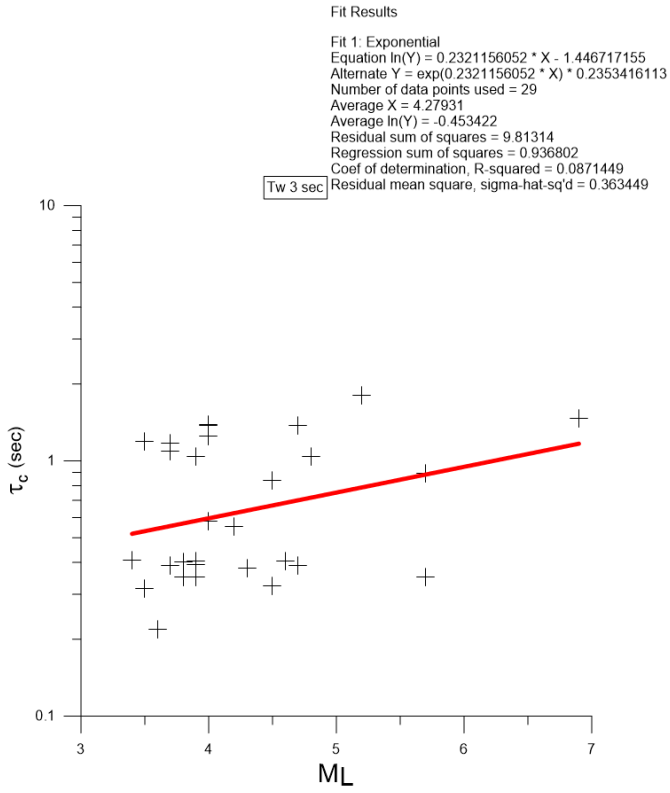

Figure 4.11. τ_c - M_L Relation for 2013 – 2019 Downhole Earthquake Records For 3-Second Time Window Length.

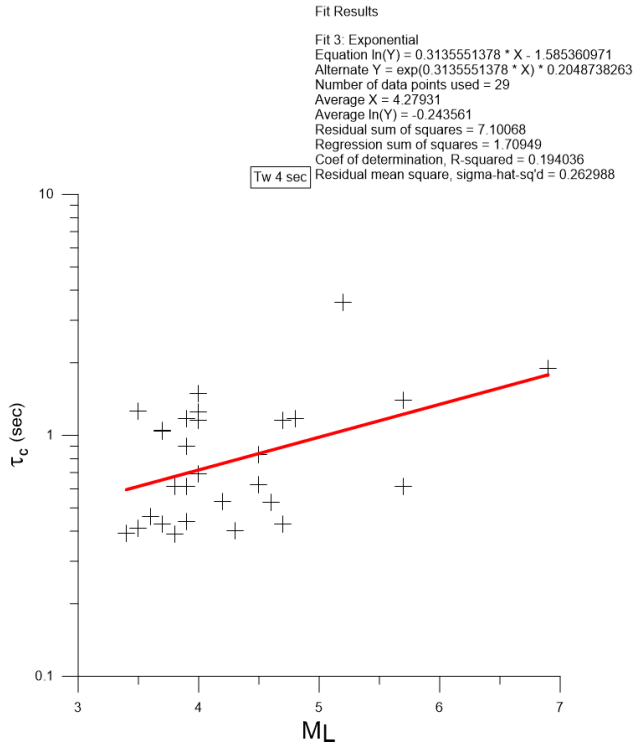

Figure 4.12. τ_c - M_L Relation for 2013 – 2019 Downhole Earthquake Records For 4-Second Time Window Length.

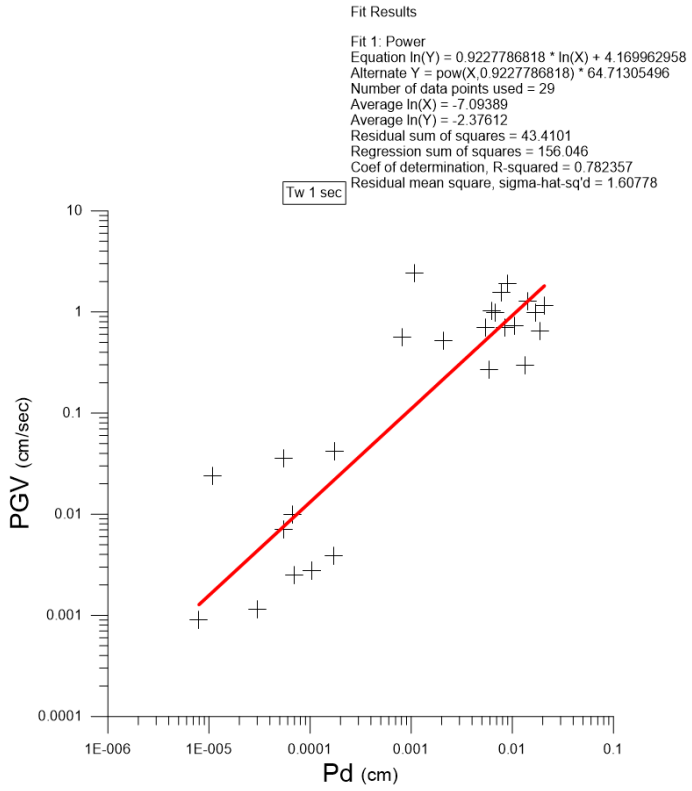

Figure 4.13. P_d - PGV Relation for 2013 – 2019 Downhole Earthquake Records For 1-Second Time Window Length.

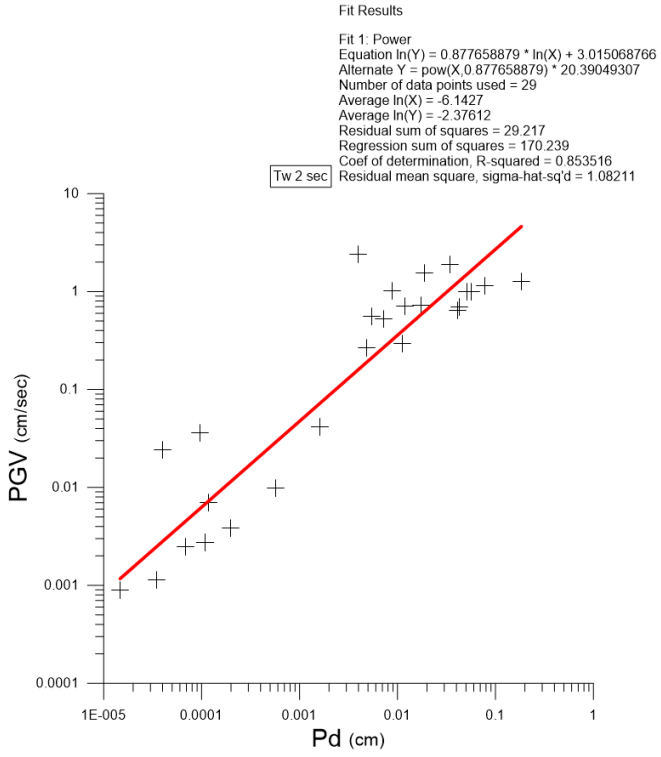

Figure 4.14. P_d - PGV Relation for 2013 – 2019 Downhole Earthquake Records For 2-Second Time Window Length.

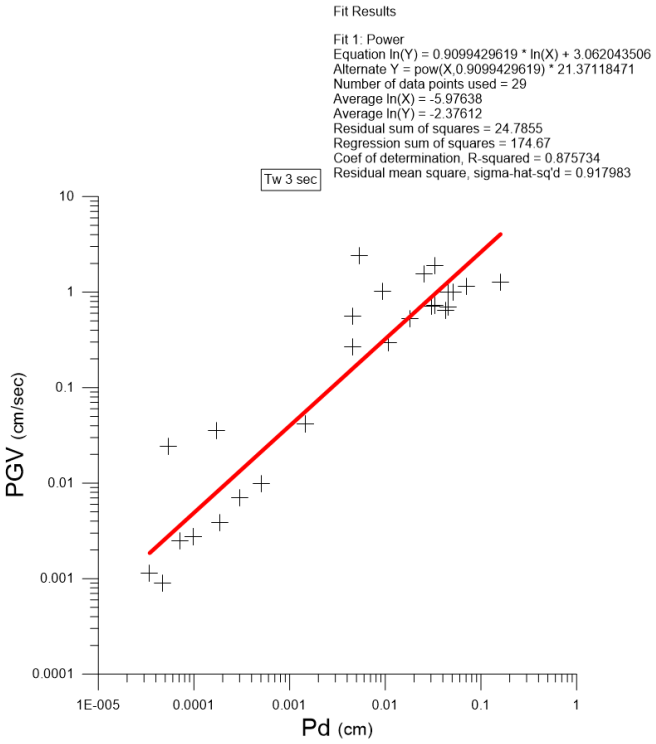

Figure 4.15. P_d - PGV Relation for 2013 – 2019 Downhole Earthquake Records For 3-Second Time Window Length.

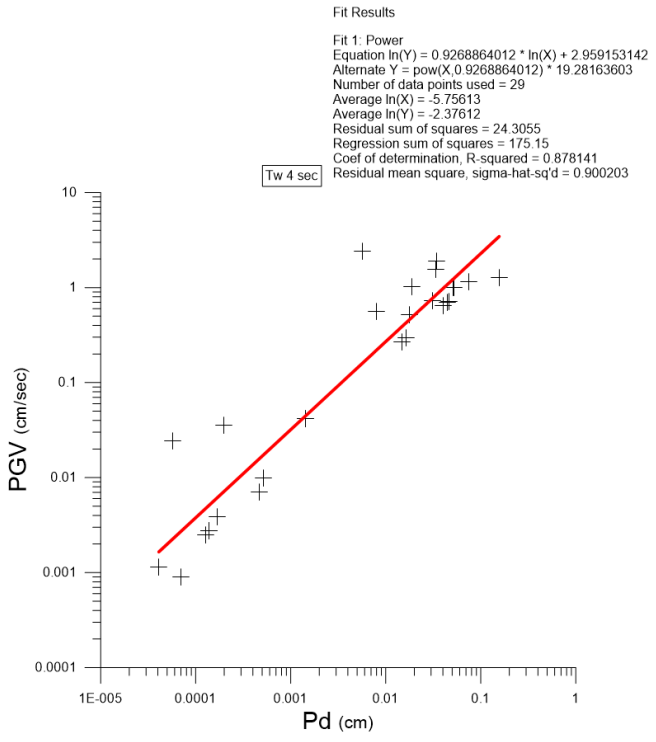

Figure 4.16. P_d - PGV Relation for 2013 – 2019 Downhole Earthquake Records For 4-Second Time Window Length.

Furthermore, similar analysis has been carried out for downhole array records that belong to Silivri Earthquake sequence. In the analysis, 1, 2, 3 and 4 second time windows are used, and the graphs are given in the figures 4.17 - 4.20 for τ_c and M_L relation. The relationship between P_d and PGV values obtained using the largest value obtained from the displacement record in the 1,2,3 and 4 seconds time windows are given in Figures 4.21- 4.24. Here, τ_c, P_d and PGV values obtained from the vertical component acceleration recordings are shown by small plus characters.

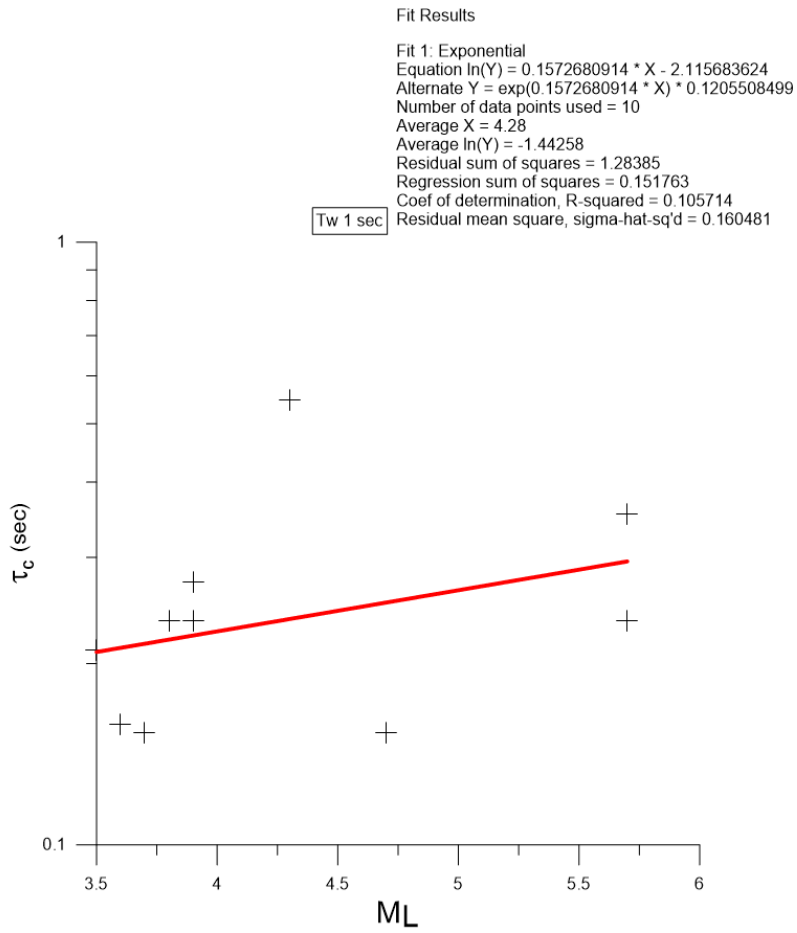

Figure 4.17. τ_c - M_L Relation for 2019 Silivri Earthquakes Downhole Earthquake Records For 1-Second Time Window Length.

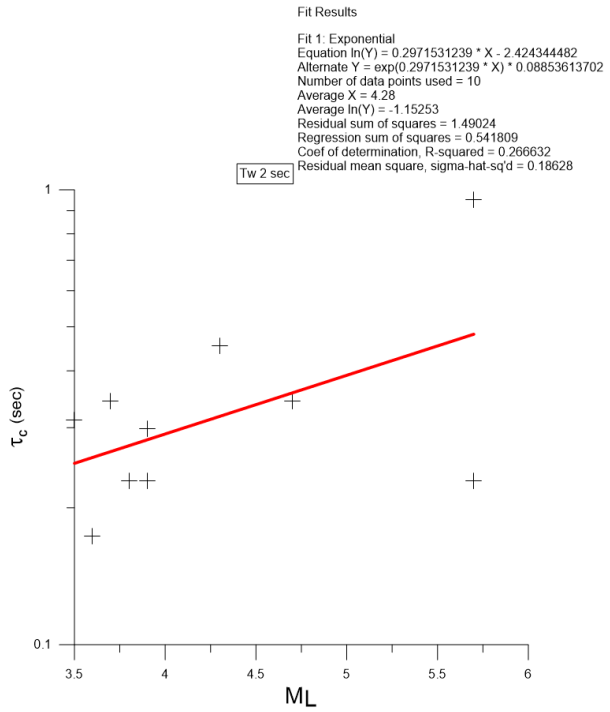

Figure 4.18. τ_c - M_L Relation for 2019 Silivri Earthquakes Downhole Earthquake Records For 2-Second Time Window Length.

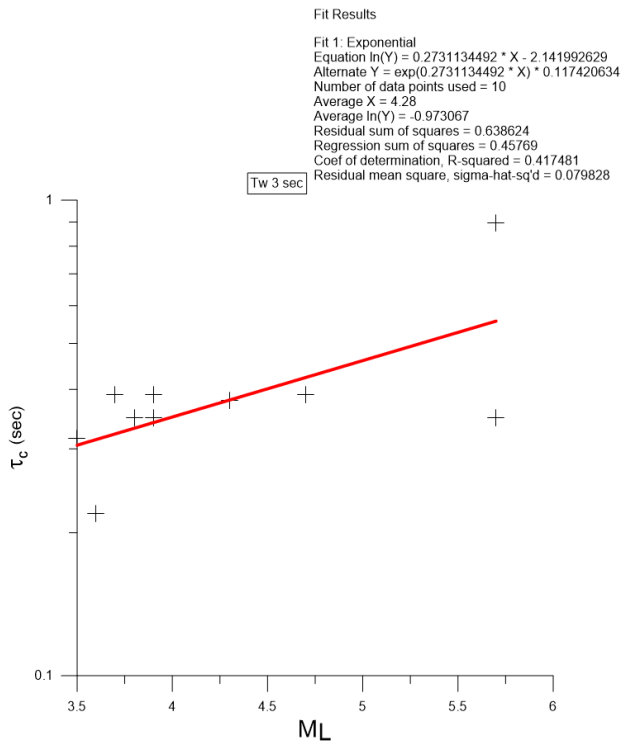

Figure 4.19. τ_c - M_L Relation for 2019 Silivri Earthquakes Downhole Earthquake Records For 3-Second Time Window Length.

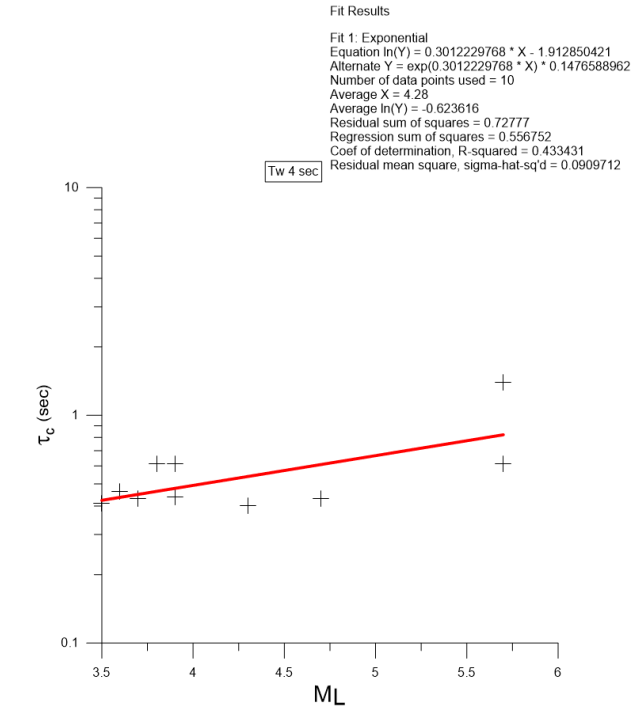

Figure 4.20. τ_c - M_L Relation for 2019 Silivri Earthquakes Downhole Earthquake Records For 4-Second Time Window Length.

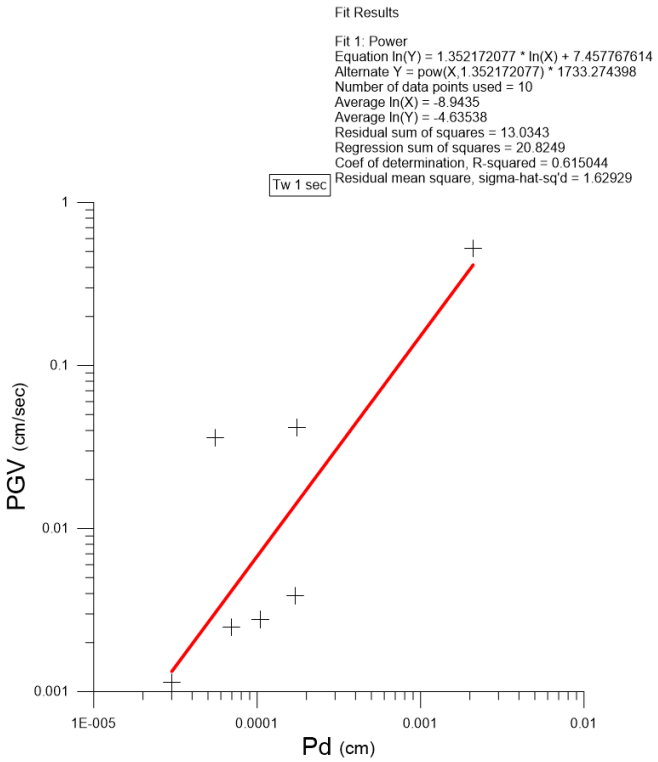

Figure 4.21. P_d - PGV Relation for 2019 Silivri Earthquakes Downhole Earthquake Records For 1-Second Time Window Length.

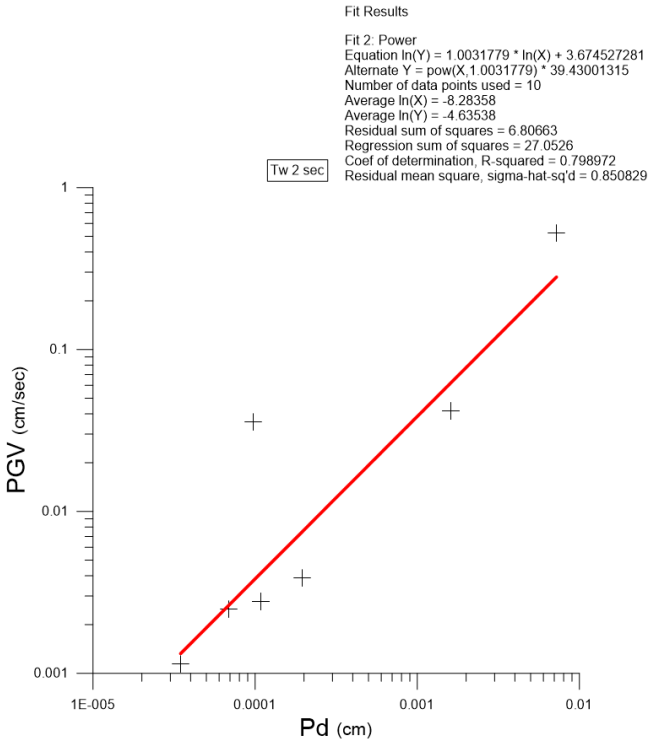

Figure 4.22. P_d - PGV Relation for 2019 Silivri Earthquakes Downhole Earthquake Records For 2-Second Time Window Length.

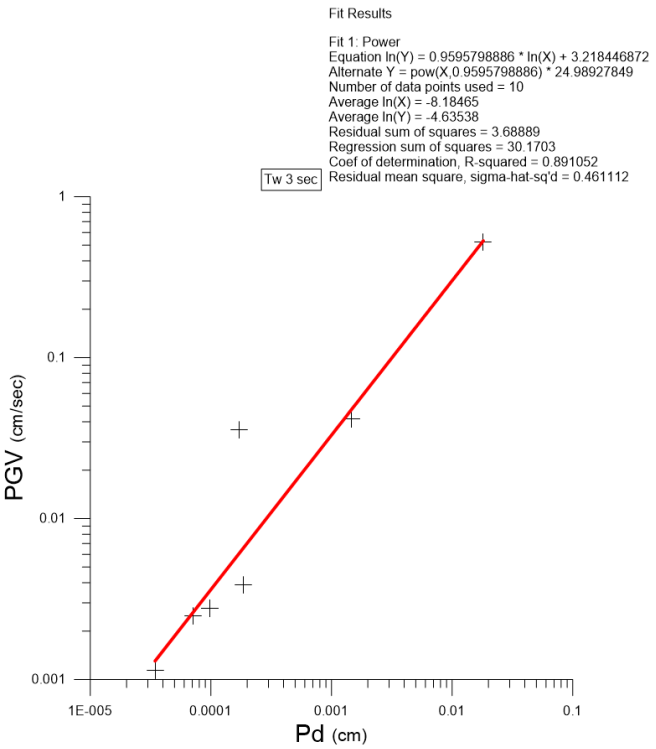

Figure 4.23. P_d - PGV Relation for 2019 Silivri Earthquakes Downhole Earthquake Records For 3-Second Time Window Length.

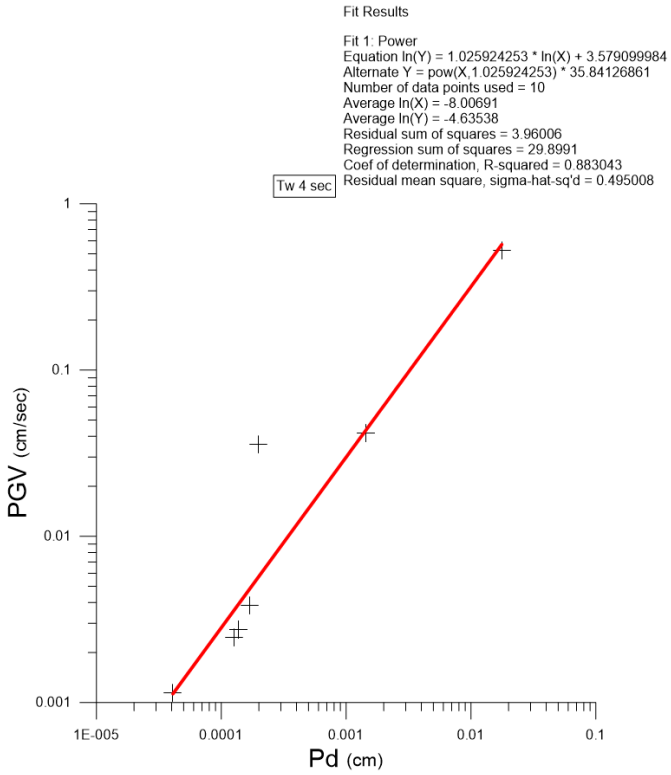

Figure 4.24. P_d - PGV Relation for 2019 Silivri Earthquakes Downhole Earthquake Records For 4-Second Time Window Length.

Derived relations are compared in Figures 4.25 and Figure 4.26. Here, values obtained from the vertical component acceleration data from downhole recordings are shown in pluses. The red line represents the regression fit line for downhole records. Figure 4.25 demonstrates large scattering in the data. However, figure 4. 26 indicates that estimation of PGV from P_d using downhole arrays tends to be more stable according to derived relation. Long-period noise effects could be the causative for the points placed far from the lines. However, P_d is well correlated with PGV in general.

From Figure 4.25, the following correlations;

$$\log\tau_c = 0.23212\ M_w - 1.44671 \tag{4.5}$$

$$M_w = 4.30812\ \log\tau_c + 6.2326 \tag{4.6}$$

were created for the relationship between period and magnitude.

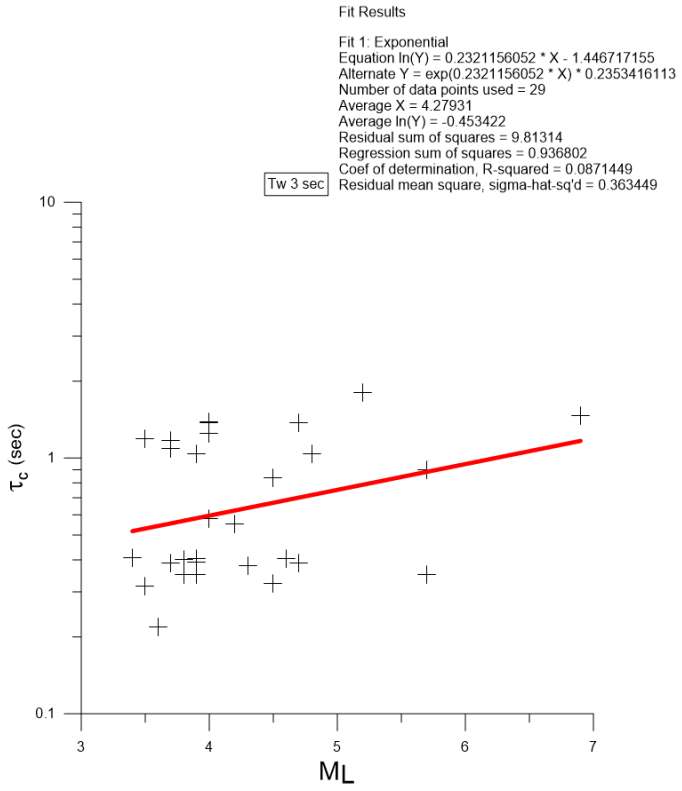

Figure 4.25. Comparison of τ_c - M_L Relations.

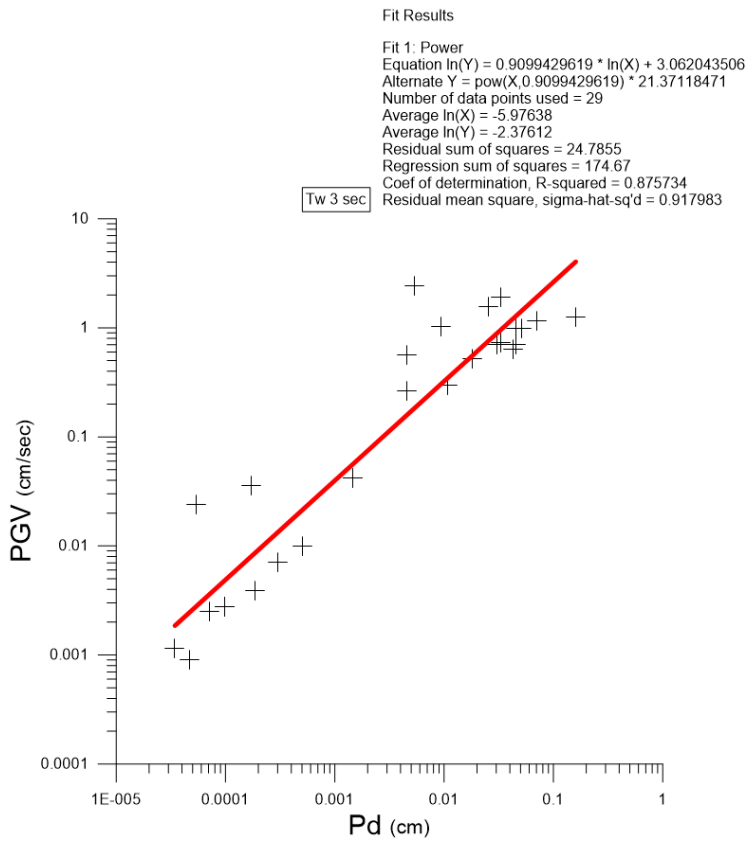

Figure 4.26. Comparison of P_d - PGV Relations.

From Figure 4.26, the following correlations;

$$\log PGV = 0.90994 \log P_d + 3.06204 \quad (4.7)$$

were created from the relationship between P_d and PGV.

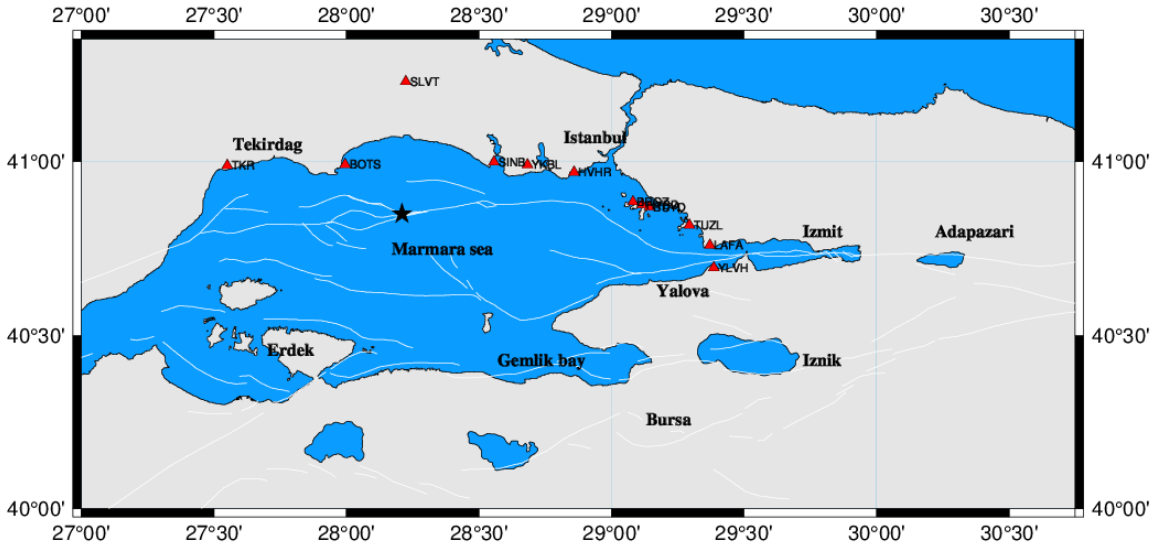

Figure 4.27. The star indicates the location of the 2019 offshore Silivri earthquake recorded at the strong motion early warning stations.

The BOTS EEW station located 25 km to the NW of the epicentre acquired the acceleration data that is used for verification of the models derived in the previous sections. From this BOTS vertical component record, τ_c and P_d are calculated as 1.1676 seconds and 0.03489 cm/s, respectively. The Wu & Kanamori's relation applied using the τ_c and P_d values of BOTS predicted the magnitude of the earthquake as Mw=6.0 and PGV as 2.0 cm/s. On the other hand, τ_c and P_d values derived from the ATK downhole are 0.8963 seconds and 0.01813 cm/s, respectively. Here, the magnitude is predicted as 5.7 and PGV as 0.556 cm/s using equations 4.6 and 4.7 for downholes. The predicted values are comparable to the magnitude reported by the national and international seismological agencies and the PGV values of the earthquake (Mw=5.7, PGV=0.61 cm/s). One may notice that the downhole array prediction model performs better and the prediction is much closer than Wu & Kanamori's relation.

In addition, the epicentre is about 75 km away from İstanbul Metropolitan area. This means that the S waves will travel that distance in 21 seconds considering a shear wave velocity of 3.5km/s. The epicentre distance to the BOTS station is about 25 km which corresponds to about 4 sec travel time from the source to the station. Along with the time to acquire 3 second P wave data one may notice that 7 second lapse time passed since the origin of the earthquake. That is to say, for the case of Silivri earthquake recorded at BOTS station 7 seconds since the origin of the earthquake is sufficient to issue an EEW alarm for the impending moderate size earthquake approaching Istanbul area. Considering the travel time duration (21 second) of the S-waves to Istanbul and the 7 seconds necessary to issue an alarm results in an early warning time of 14 seconds.

It is observed that changing the ratio of STA/LTA affects the given alarm. Increasing the ratio too much can cause missing events. On the other hand, decreasing the same ratio may result in false alarms. In the study, when the ratio is decreased to 3, 1 out of 30 records from downhole data has created a false alarm. Similarly, when the ratio is increased to 6, 1 out of 30 records from downhole data has created a missing alarm. Figure 4.28 and 4.29 shows us the analysis results of false and missing alarms.

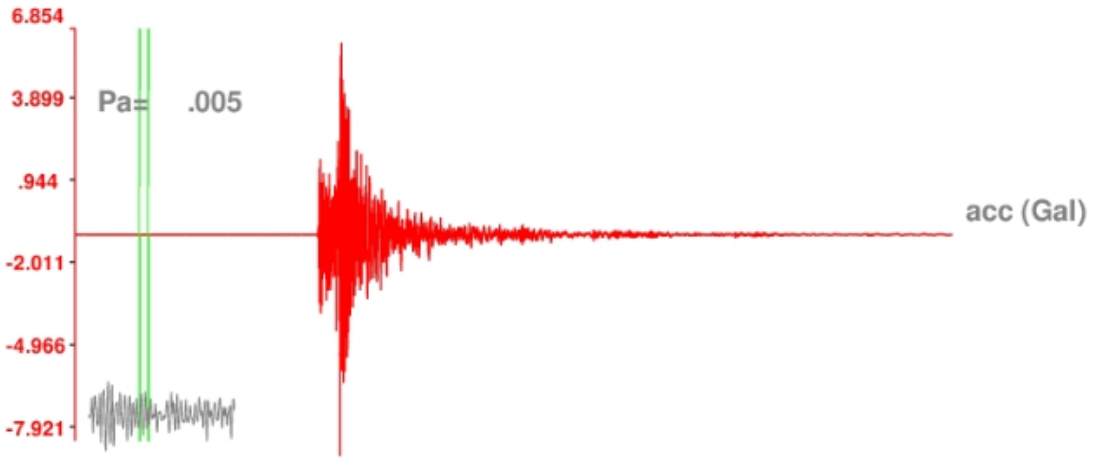

Figure 4.28. False Alarm.

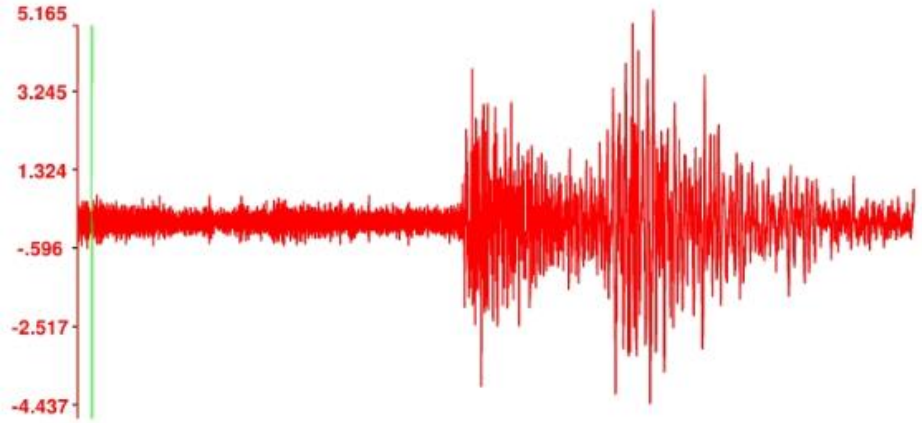

Figure 4.29. Missing Alarm.

In the final stage, earthquake triggering is compared. An earthquake alarm is hypothetically created using STA/LTA ratio using the accelerometers in these downholes. Firstly, 3-second time window is kept constant and effect of the number of stations on the early warning alarm is compared. Figure 4.30 shows a case for an alarm issue when all three sensors are necessary to trigger the system and Figure 4.31 shows having an alarm if only one sensor are needed to create a warning alarm signal.

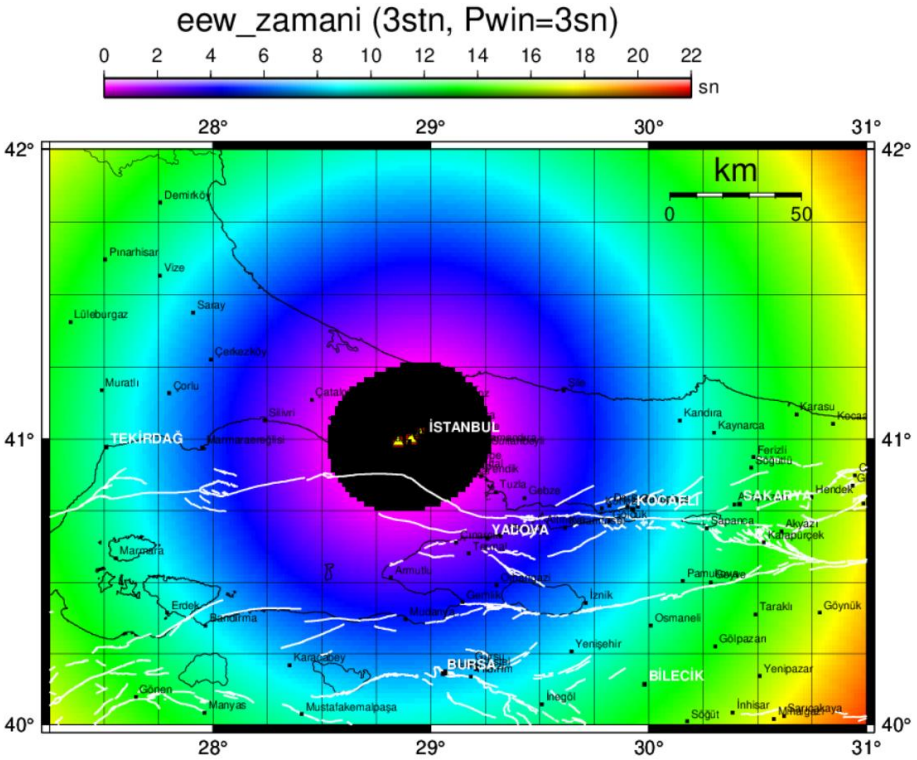

Figure 4.30. EEW Time For 3 Stations and 3-second Time Window.

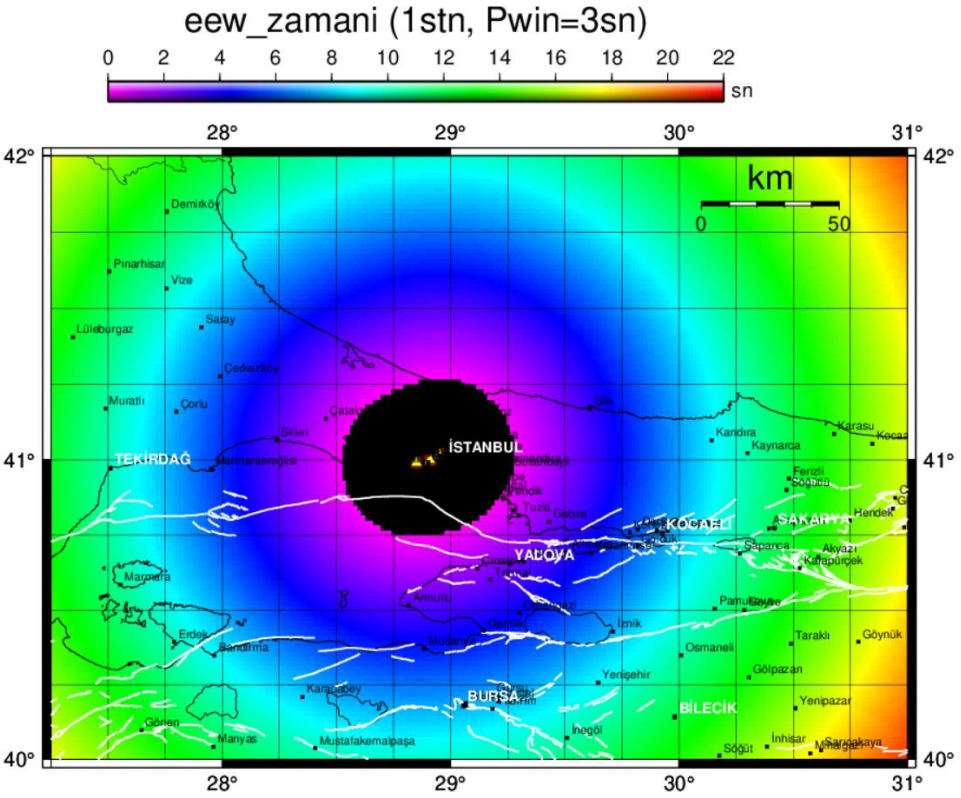

Figure 4.31. EEW Time For 1 Station and 3-second Time Window.

As a second step, 1-second time window is kept constant and effect of the number of stations on the early warning alarm is compared. Figure 4.32 shows having the alarm how early if all three sensors are necessary to trigger the system and Figure 4.33 shows having the alarm how early if only one sensor are needed to create warning alarm.

Yellow points and white lines represent downhole sensors and fault lines, respectively in figures 4.30, 4.31. 4.32 and 4.33. If an earthquake occurs in the black zones, no alarm will be created from these three downholes. If an earthquake occurs outside the black regions, KOERI will receive an alarm before the earthquake. Pink colour represents the alarm 0-2 seconds before the S wave arrival. Similarly, purple, dark blue, light blue and green indicates 2-4, 4-7, 7-10 and 10-14 seconds before S wave arrival.

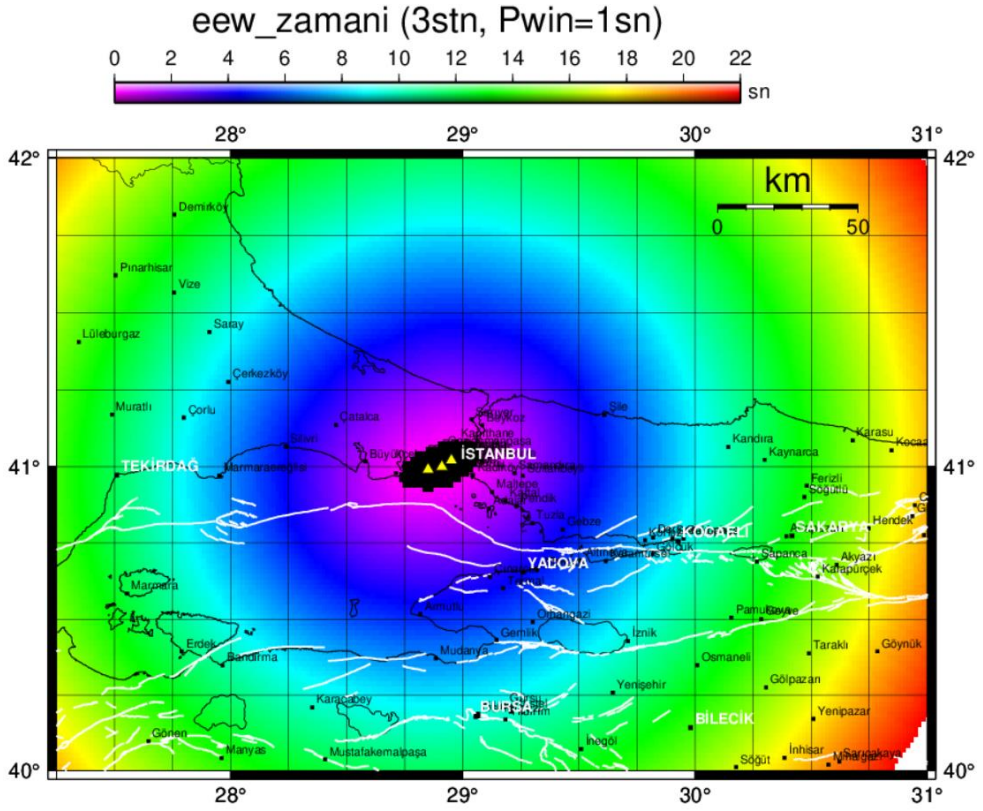

Figure 4.32. EEW Time For 3 Stations and 1-second Time Window.

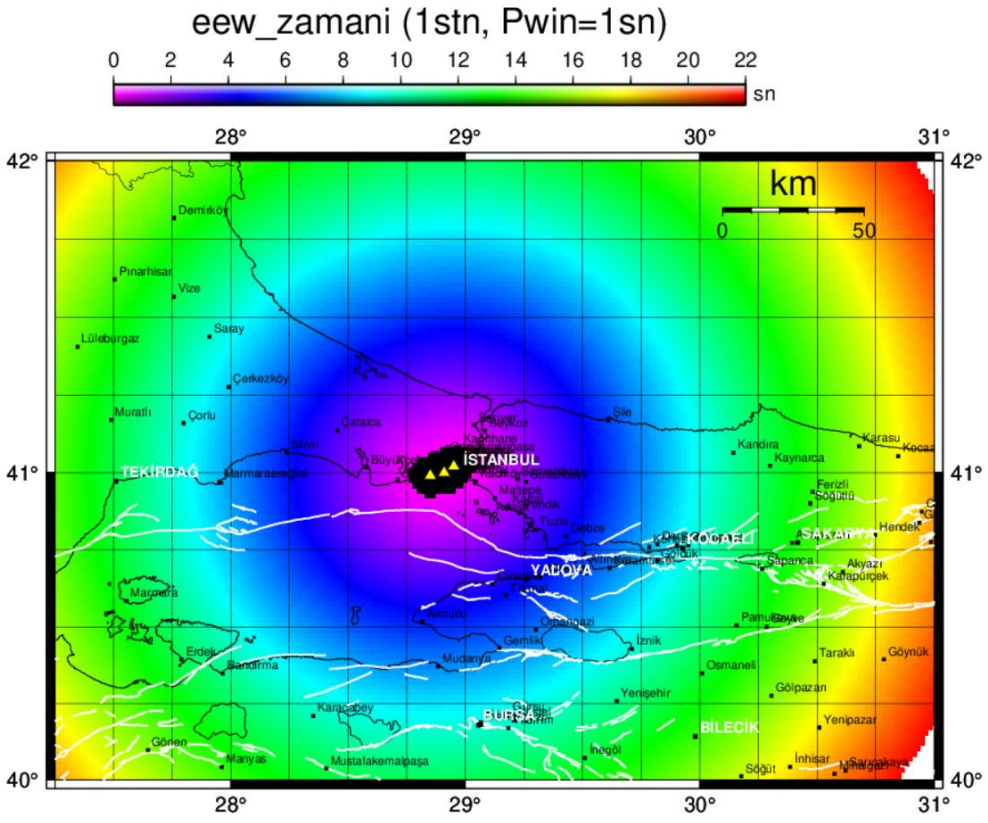

Figure 4.33. EEW Time For 1 Station and 1-second Time Window.

5. CONCLUSION

The Kocaeli (Mw 7.5) and Düzce (Mw 7.2) earthquakes that occurred in 1999 revealed the fact that they should be prepared for the possible damage that the earthquake might cause in the Marmara Region, especially in Istanbul. From this point of view, it is aimed to reduce the possible losses after a damaging earthquake and to produce Quick Loss Maps that will help the emergency response and rescue teams.

In this study, using the τ_c -Pd method (Wu and Kanamori, 2005a, 2005b) developed for early warning system in Taiwan, vertical component acceleration recordings and parameters reflecting the characteristics of the P wave of the Marmara Region were tried to be obtained. Wu and Kanamori (2005b) stated that τ_c and Pd parameters can be used independently when stations are not distributed intensely and regularly. They suggested that if the parameters τ_c and P_d are obtained from a single station or a network, the results can be evaluated in four different combinations. These; (1) Pd> 0.5 cm and τ_c > 1.0 sec; (2) Pd <0.5 cm and τ_c > 1.0 sec; (3) Pd <0.5 cm and τ_c <1.0 sec; and (4) Pd> 0.5 cm and τ_c <1.0 sec. The physical meaning of these situations is given as follows: (1) the earthquake is probably damaging for the area where the station is located and for a wider area; (2) the earthquake is not damaging to the area where the station is located, but may be damaging to remote areas; (3) the earthquake is not damaging; (4) earthquake damage is limited only by the area around the station.

According to the relationship between PGV and Pd and the correlation obtained, when the P_d parameter is taken as 0.5 cm, the corresponding PGV value is approximately 11.4 cm/sec. This value corresponds to a potentially damaging earthquake. Based on this result, it can be said that cases where the P_d parameter exceeds the 0.5 cm threshold level will be a harbinger of a damaging earthquake for the Marmara Region.

Although the relation obtained from AFAD data is based on that that are obtained from earthquakes that have taken place all over Turkey, it gives a reasonable and acceptable prediction of an earthquake magnitude and associated PGV amplitudes.

Large scattering is observed for τ_c - M_L relations whose R^2 values are in the range of 0.1-0.4 and getting less from the shortest time to longest time. On the other hand, R^2 values of P_d - PGV relations are between 0.7-0.9. Therefore, it is possible to say that P_d - PGV relations gives logical results more than Tc-ML relations. Large scattering is possible to be observed for time dependent parameters as τ_c because of the tearing rate of faults. The longer the time window length the better relations we can obtain. It could be stated that an earthquake alarm can be given from 1 second time window analysis and the alarm can be updated each second. Therefore, one may give an earlier warning with a reasonable approach. It is important to specify that data set of downholes were quite limited and records are used without any acceptance criteria.

Recently, many researchers from all over the world established earthquake parameters for early warning systems. A previous study elaborating the τ_c -Pd method for Marmara region was published by Alçık et al. (2011). Several large earthquakes have taken place in Turkey and its neighborhood since then. In this study, our aim is twofold. One is to improve the prediction models incorporating the recent earthquakes; and, the other is to elaborate the method further for İstanbul using the downhole records instead of only surface data.

Silivri earthquake and its aftershocks (September 2019) are also included in the study. After τ_c - M and PGV-Pd relations are obtained, the verification of the models has been done thorugh predicting the size of the mainshock event. Downhole array EEW relations predict accurately the magnitude and the observed PGV values. However, when τ_c and Pd parameters are determined from a surface accelerometer, the downhole prediction relations overestimate the earthquake parameters. Thus, it can be said that the obtained downhole relations are site specific and useful for utilizing the downhole data in EEW studies.

In order to issue an earthquake early warning alarm earlier, used time window duration could be decreased from 3 to 1 second. This will decrease the blind zone and increase the time left for the S wave arrivals at a target region.

Since the downholes are close to each other, there is almost no change in warning times and blind zones when number of stations being necessary to trigger are decreased from 3 to 1 assuming time window used in the analysis is constant. In 3-second time window case, there is no difference between 1-station analysis and 3-station analysis because 3 seconds corresponds to a distance of 18 km; however, the separation distance is 8 km between Ataköy and Fatih stations. However, in 1- second time window case a small difference is observed between 1-station analysis and 3-station analysis. Similarly, 1 second corresponds to about 6 km and this is less than the distance between stations. That's why no considerable change is observed in the figures.

In addition, it is stated that τ_c and P_d parameters will be useful in regions where the earthquake epicenter distance is less than 70 km (Wu and Kanamori, 2005a; 2005b). Considering that the distance of Istanbul to the main Marmara fault is between 15-25 km, the test carried out using the BOTS EEW station records of the 2019 Silivri earthquake (Mw=5.7) reveal that the Early Warning System running around Marmara Sea can generate an early warning signal in 7 seconds providing an average of 14 seconds EEW time for Istanbul Metropolitan area.

REFERENCES

Alcik, Hakan, Oguz Ozel, Nurdan Apaydin, and Mustafa Erdik. 'A Study on Warning Algorithms for Istanbul Earthquake Early Warning System'. *Geophysical Research Letters* 36, no. 5 (2009): 3–5. https://doi.org/10.1029/2008GL036659.

Alcik, Hakan, Oguz Ozel, Yih Min Wu, Nurcan M. Ozel, and Mustafa Erdik. 'An Alternative Approach for the Istanbul Earthquake Early Warning System'. *Soil Dynamics and Earthquake Engineering* 31, no. 2 (2011): 181–87. https://doi.org/10.1016/j.soildyn.2010.03.007.

Alçık, Hasan Asaf, and Can Zülfikar. 'Tau-P-Max , Tau-C ve Pd Metotları'. *Jeofizik Bülteni*, no. Allen 2011 (2012): 60–75.

Allen, R. M., P. Gasparini, O. Kamigaichi, and M. Bose. 'The Status of Earthquake Early Warning around the World: An Introductory Overview'. *Seismological Research Letters* 80, no. 5 (2009): 682–93. https://doi.org/10.1785/gssrl.80.5.682.

Allen, Richard M., and Hiroo Kanamori. 'The Potential for Earthquake Early Warning in Southern California'. *Science* 300, no. 5620 (2003): 786–89. https://doi.org/10.1126/science.1080912.

Aranda, J. M. E., A. Jimenez, G. Ibarrola, F. Alcantar, A. Aguilar, M. Inostroza, and S. Maldonado. 'Mexico City Seismic Alert System'. *Seismological Research Letters* 66, no. 6 (2011): 42–53. https://doi.org/10.1785/gssrl.66.6.42.

Ashiya, Kimitoshi. 'Earthquake Alarm Systems'. *Journal of Japan Association for Earthquake Engineering* 4, no. 3 (2004): 112–17.

Chang, Chien Hsin, Yih Min Wu, Tzay Chyn Shin, and Chien Ying Wang. 'Relocation of the 1999 Chi-Chi Earthquake in Taiwan'. *Terrestrial, Atmospheric and Oceanic Sciences* 11, no. 3 (2000): 581–90. https://doi.org/10.3319/TAO.2000.11.3.581(CCE).

Dikmen, S. U., A. Edincliler, and A. Pinar. 'Northern Aegean Earthquake (M w =6.9): Observations at Three Seismic Downhole Arrays in Istanbul'. *Soil Dynamics and Earthquake Engineering* 77 (2015): 321–36. https://doi.org/10.1016/j.soildyn.2015.06.008.

Erdik, M, M. Demircioglu, K. Sesetyan, E Durukal, and B Siyahi. 'Engineering Earthquake Hazard in Marmara Region, Turkey'. *13th World Conference on Earthquake Engineering Vancouver, B.C., Canada*, no. 270 (2004): 15.

Fahjan, Yasin M., Hakan Alcik, and Ali Sari. 'Applications of Cumulative Absolute Velocity to Urban Earthquake Early Warning Systems'. *Journal of Seismology* 15, no. 2 (2011): 355–73. https://doi.org/10.1007/s10950-011-9229-8.

Glass, Charles E. 'Seismic Wave Attenuation during the 19 September 1985 Michoacan, Mexico Earthquake'. *International Journal of Mining and Geological Engineering* 7, no. 1 (1989): 9–15. https://doi.org/10.1007/BF01552835.

Grecksch, Gunnar, and Hans Joachim Kumpel. 'Statistical Analysis of Strong-Motion Accelerograms and Its Application to Earthquake Early-Warning Systems'. *Geophysical Journal International* 129, no. 1 (1997): 113–23. https://doi.org/10.1111/j.1365-246X.1997.tb00940.x.

Gurbuz, C., M. Aktar, H. Eyidogan, A. Cisternas, H. Haessler, A. Barka, M. Ergin, et al. 'The Seismotectonics of the Marmara Region (Turkey): Results from a

Microseismic Experiment'. *Tectonophysics* 316, no. 1–2 (2000): 1–17. https://doi.org/10.1016/S0040-1951(99)00253-X.

Hauksson, E., P. Small, K. Hafner, R. Busby, R. Clayton, J. Goltz, T. Heaton, et al. 'Southern California Seismic Network: Caltech/USGS Element of TriNet 1997-2001'. *Seismological Research Letters* 72, no. 6 (2011): 690–704. https://doi.org/10.1785/gssrl.72.6.690.

Hsiao, Nai Chi, Yih Min Wu, Tzay Chyn Shin, Li Zhao, and Ta Liang Teng. 'Development of Earthquake Early Warning System in Taiwan'. *Geophysical Research Letters* 36, no. 5 (2009). https://doi.org/10.1029/2008GL036596.

Iglesias, A., S. K. Singh, M. Ordaz, M. A. Santoyo, and J. Pacheco. 'The Seismic Alert System for Mexico City: An Evaluation of Its Performance and a Strategy for Its Improvement'. *Bulletin of the Seismological Society of America* 97, no. 5 (2007): 1718–29. https://doi.org/10.1785/0120050202.

İmren, C, Emin Demirbağ, and A. M. Celal Şengör. 'Kuzey Anadolu Fayı'nın Marmara Denizi Içindeki Devamı'. *Itü Dergisi* 2, no. 212 (2003): 47–58.

KAMIGAICHI, Osamu. 'Jma Earthquake Early Warning'. *Journal of JAEEJournal of Japan Association for Earthquake Engineering* 4, no. 3 (2013): 134–37. https://doi.org/10.5610/jaee.4.3_134.

Kanamori, Hiroo. 'Earthquake Physics and Real-Time Seismology'. *Nature* 451, no. 7176 (2008): 271–73. https://doi.org/10.1038/nature06585.

Kanamori, Hiroo. 'Earthquake Prediction - An Overview'. *International Handbook of*

Earthquake and Engineering Seismology 81B (2001): 440658. https://www.sciencedirect.com/topics/earth-and-planetary-sciences/earthquake-prediction.

Kanamori, Hiroo. ‘Real-Time Seismology and Earthquake Damage Mitigation’. *Annual Review of Earth and Planetary Sciences* 33, no. 1 (2005): 195–214. https://doi.org/10.1146/annurev.earth.33.092203.122626.

LEE, S, J LEE, and D CHOI. ‘An Experimental Study on Seismic Damage Indicator Considering CAV Concept’. *Nuclear Engineering and Design*, no. August (2001). https://doi.org/10.1016/j.nucengdes.2006.01.019.

Liu, Kun Sung, Tzay Chyn Shin, and Yi Ben Tsai. ‘A Free-Field Strong Motion Network in Taiwan: TSMIP’. *Terrestrial, Atmospheric and Oceanic Sciences* 10, no. 2 (1999): 377–96. https://doi.org/10.3319/TAO.1999.10.2.377(T).

Lockman, Andrew B., and Richard M. Allen. ‘Single-Station Earthquake Characterization for Early Warning’. *Bulletin of the Seismological Society of America* 95, no. 6 (2005): 2029–39. https://doi.org/10.1785/0120040241.

M., Wu Y., Chung J. K., Shin T. C., Hsiao N. C., Tsai Y. B., Lee W. H. K., and Teng T. L. ‘Development of An Integrated Earthquake Early Warning System in Taiwan—Case for Hualien Earthquakes’. *Terr. Atmos. Ocean. Sci.*, no. September (2014): 719–36.

Nakamura, Y. ‘UrEDAS, Urgent Earthquake Detection and Alarm System, Now and Future’. *13th World Conference on Earthquake Engineering*, no. 908 (2004). https://doi.org/ISBN 4-89580-010-5.

O'Hara, T.F., and J.P. Jacobson. 'Standardization of the Comulative Absolute Velocity'. *International Nuclear Information System*, 1991.

Odaka, Toshikazu, Kimitoshi Ashiya, Shin'ya Tsukada, Shinji Sato, Kazuo Ohtake, and Daisuke Nozaka. 'A New Method of Quickly Estimating Epicentral Distance and Magnitude From A Single Seismic Record'. *Bulletin of the Seismological Society of America* 93, no. 1 (2003): 526–32. https://doi.org/10.1785/0120020008.

Okada, Yoshimitsu, Keiji Kasahara, Kazushige Obara, Shoji Sekiguchi, Hiroyuki Fujiwara, and Akira Yamamoto. 'Recent Progress of Seismic Observation Networks in Japan'. *Journal of Physics: Conference Series* 433, no. 1 (2013). https://doi.org/10.1088/1742-6596/433/1/012039.

Okay, A. I., A. Kaşlilar-Özcan, C. Imren, A. Boztepe-Güney, E. Demirbag, and I. Kuşçu. 'Active Faults and Evolving Strike-Slip Basins in the Marmara Sea, Northwest Turkey: A Multichannel Seismic Reflection Study'. *Tectonophysics* 321, no. 2 (2000): 189–218. https://doi.org/10.1016/S0040-1951(00)00046-9.

Olson, Erik L., and Richard M. Allen. 'The Deterministic Nature of Earthquake Rupture'. *Nature* 438, no. 7065 (2005): 212–15. https://doi.org/10.1038/nature04214.

Pichon, X Le, B Mercier De Lepinay, B Meyer, Rolando Armijo, N Go, R Saatc, and B Tok. 'The Active Main Marmara Fault'. *Earth and Planetary Science Letters* 192 (2001): 595–616.

Pınar, A, E Kalkan, M Çomoğlu, S Ü Dikmen, M Erdik, and E Şafak. 'GERÇEK - ZAMANLI SİSMOLOJİ İL E DEPREM ERKEN UYARI'. In *4. Uluslar Arası Deprem Mühendisliği ve Sismoloji Konferansı*, 8, 2017.

Satriano, Claudio, Yih Min Wu, Aldo Zollo, and Hiroo Kanamori. ‘Earthquake Early Warning: Concepts, Methods and Physical Grounds’. *Soil Dynamics and Earthquake Engineering* 31, no. 2 (2011): 106–18. https://doi.org/10.1016/j.soildyn.2010.07.007.

Shieh, Jang Tian, Yih Min Wu, and Richard M. Allen. ‘A Comparison of Tc and Tp Max For Magnitude Estimation in Earthquake Early Warning’. *Geophysical Research Letters* 35, no. 20 (2008): 1–5. https://doi.org/10.1029/2008GL035611.

Suarez, G., D. Novelo, and E. Mansilla. ‘Performance Evaluation of the Seismic Alert System (SAS) in Mexico City: A Seismological and a Social Perspective’. *Seismological Research Letters* 80, no. 5 (2009): 707–16. https://doi.org/10.1785/gssrl.80.5.707.

Teng, Ta Iiang, Ludan Wu, Tzay Chyn Shin, Yi Ben Tsai, and William H.K. Lee. ‘One Minute after: Strong-Motion Map, Effective Epicenter, and Effective Magnitude’. *Bulletin of the Seismological Society of America* 87, no. 5 (1997): 1209–19.

Wald, David J., Vincent Quitoriano, Thomas H. Heaton, Hiroo Kanamori, Craig W. Scrivner, and C. Bruce Worden. ‘TriNet “ShakeMaps”: Rapid Generation of Peak Ground Motion and Intensity Maps for Earthquakes in Southern California’. *Earthquake Spectra*, 1999.

Wald, David J, California Institute of Technology., California. Division of Mines and Geology., and Geological Survey (U.S.). ‘“ShakeMaps” :Instant Maps of Earthquake Shaking’. *USGS Fact Sheet*, no. 103–00 (2000). http://purl.access.gpo.gov/GPO/LPS52191.

Wu, Y.-M. ‘A Virtual Subnetwork Approach to Earthquake Early Warning’. *Bulletin*

of the Seismological Society of America 92, no. 5 (2005): 2008–18. https://doi.org/10.1785/0120010217.

Wu, Y M, T L Teng, N C Hsiao, T C Shin, W H K Lee, and Y B Tsai. 'Progress on Earthquake Rapid Reporting and Early Warning Systems in Taiwan'. *Earthquake: Hazard, Risk, and Strong Ground Motion*, no. 1 (2004): 463–86.

Wu, Yih M., and Hiroo Kanamori. 'Rapid Assessment of Damage Potential of Earthquakes in Taiwan from the Beginning of P Waves'. *Bulletin of the Seismological Society of America* 95, no. 3 (2005): 1181–85. https://doi.org/10.1785/0120040193.

Wu, Yih Min, and Hiroo Kanamori. 'Experiment on an Onsite Early Warning Method for the Taiwan Early Warning System'. *Bulletin of the Seismological Society of America* 95, no. 1 (2005): 347–53. https://doi.org/10.1785/0120040097.

Wu, Yih Min, Hiroo Kanamori, Richard M. Allen, and Egill Hauksson. 'Determination of Earthquake Early Warning Parameters, Tc and Pd, for Southern California'. *Geophysical Journal International* 170, no. 2 (2007): 711–17. https://doi.org/10.1111/j.1365-246X.2007.03430.x.

Wu, Yih Min, Hsin Yi Yen, Li Zhao, Bor Shouh Huang, and Wen Tzong Liang. 'Magnitude Determination Using Initial P Waves: A Single-Station Approach'. *Geophysical Research Letters* 33, no. 5 (2006): 1–5. https://doi.org/10.1029/2005GL025395.

Wurman, Gilead, Richard M. Allen, and Peter Lombard. 'Toward Earthquake Early Warning in Northern California'. *Journal of Geophysical Research: Solid Earth* 112, no. 8 (2007): 1–19. https://doi.org/10.1029/2006JB004830.

APPENDIX

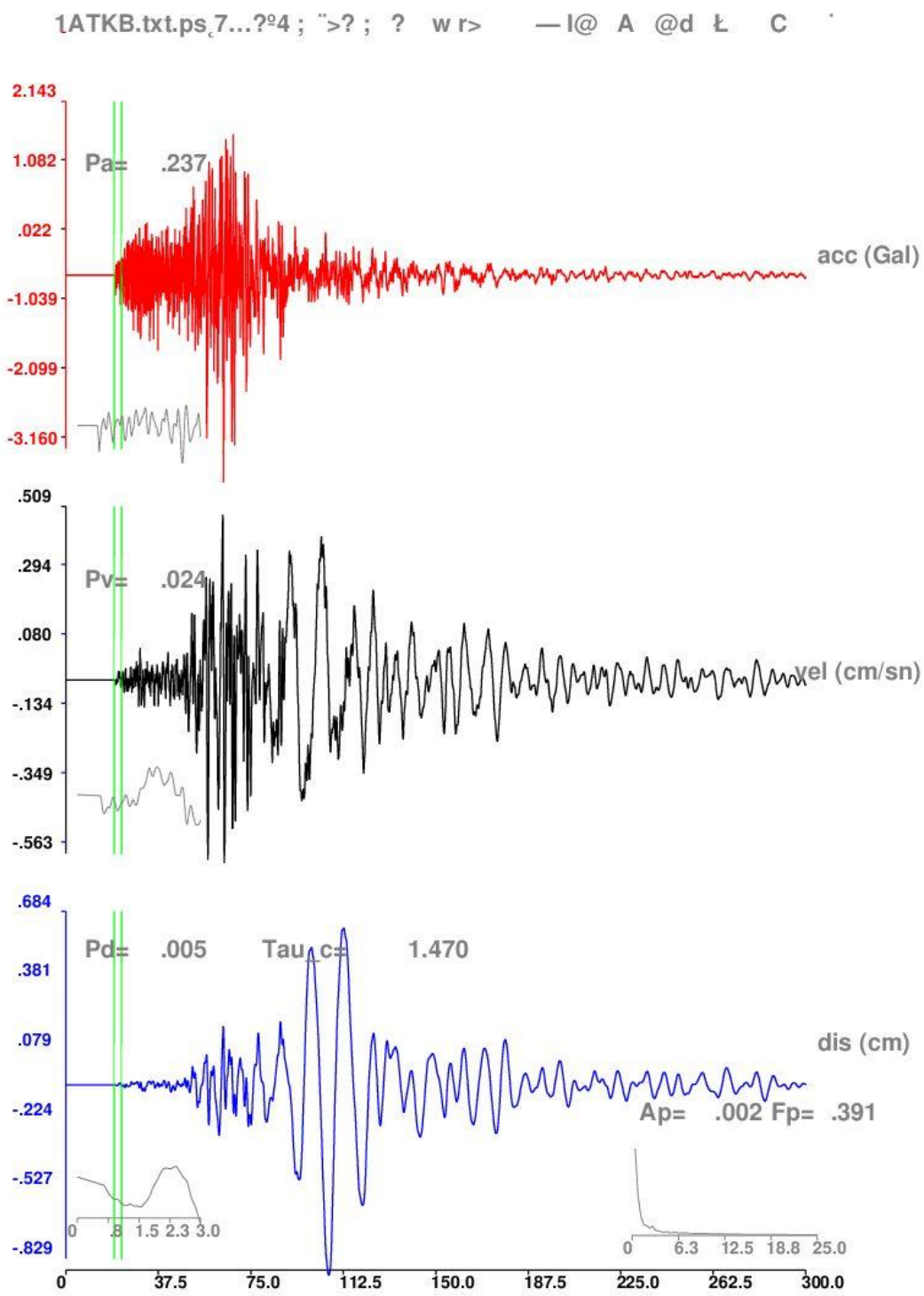

Figure A.1. Gökçeada Earthquake Downhole Record.

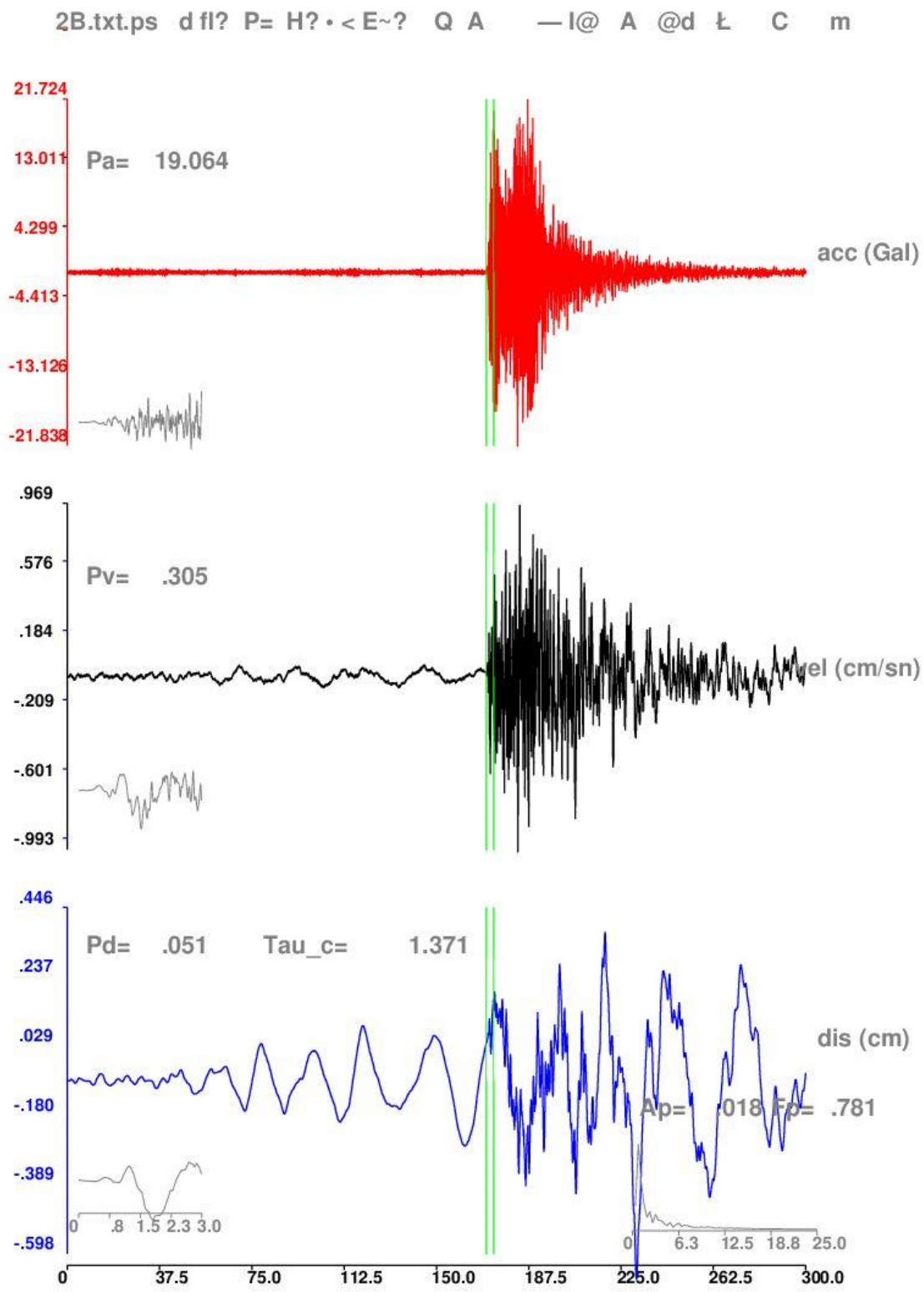

Figure A.2. Marmara Sea (Tekirdağ) Earthquake Downhole Record.

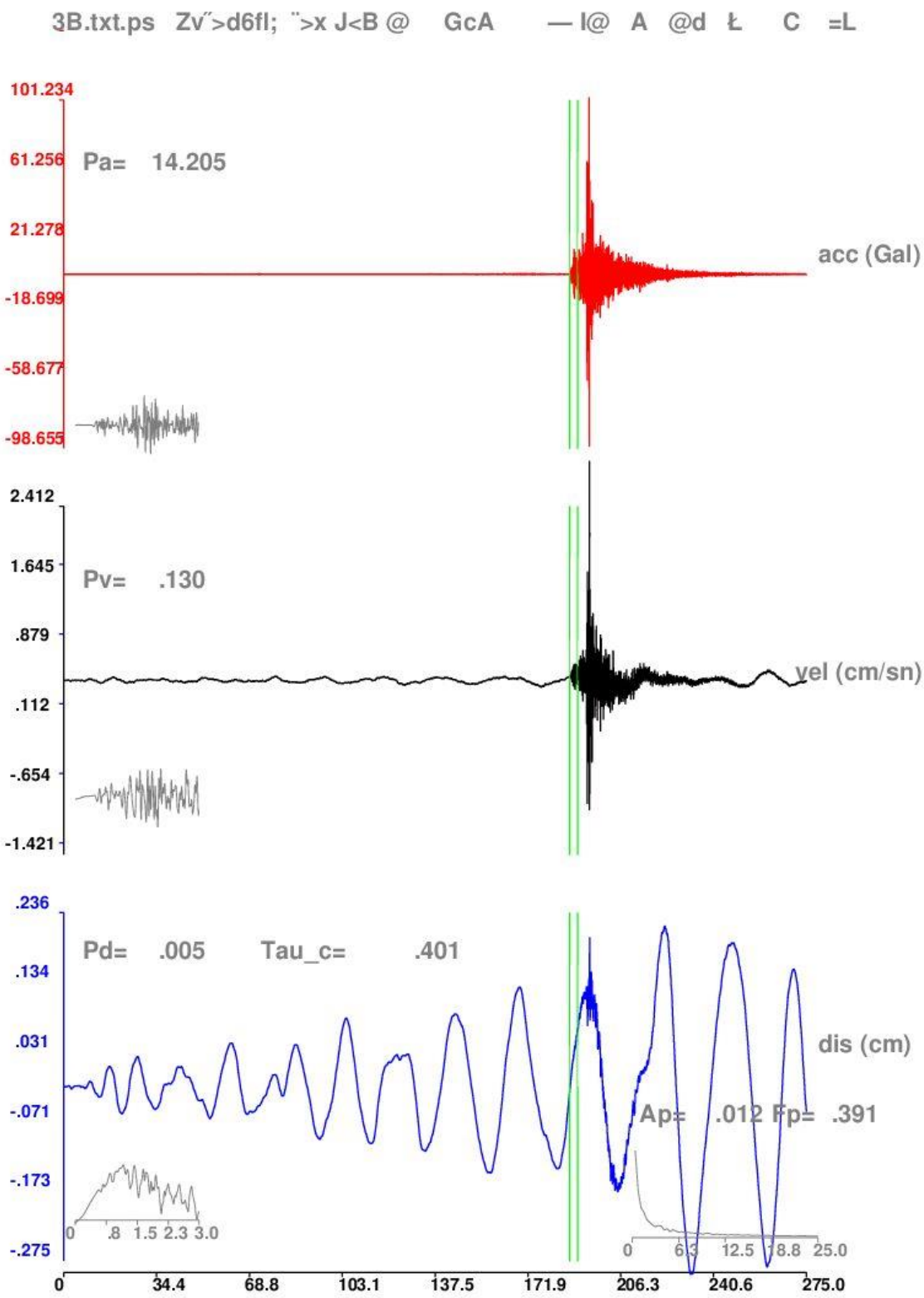

Figure A.3. Blacksea (İstanbul) Earthquake Downhole Record.

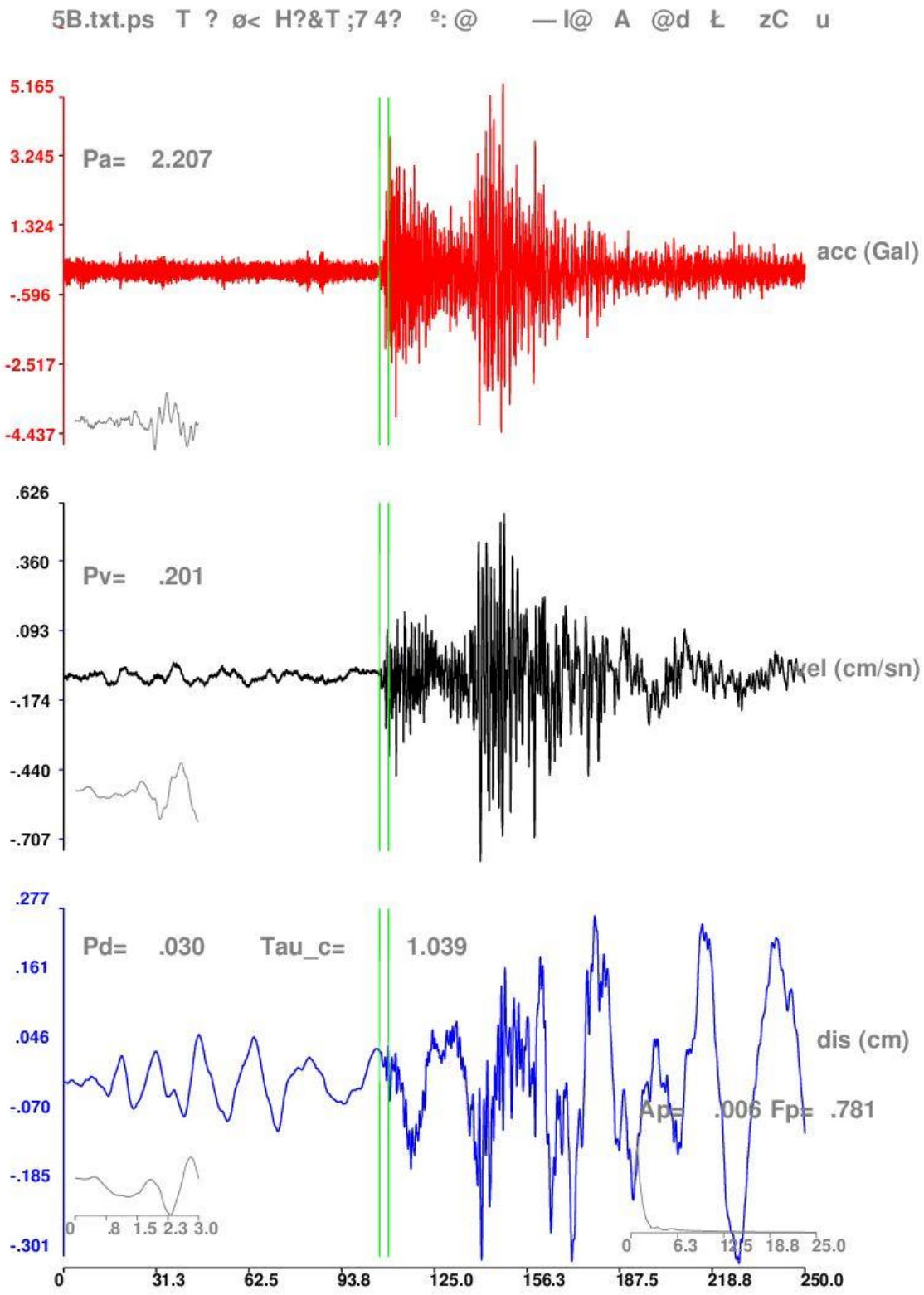

Figure A.4. Bolu Earthquake Downhole Record.

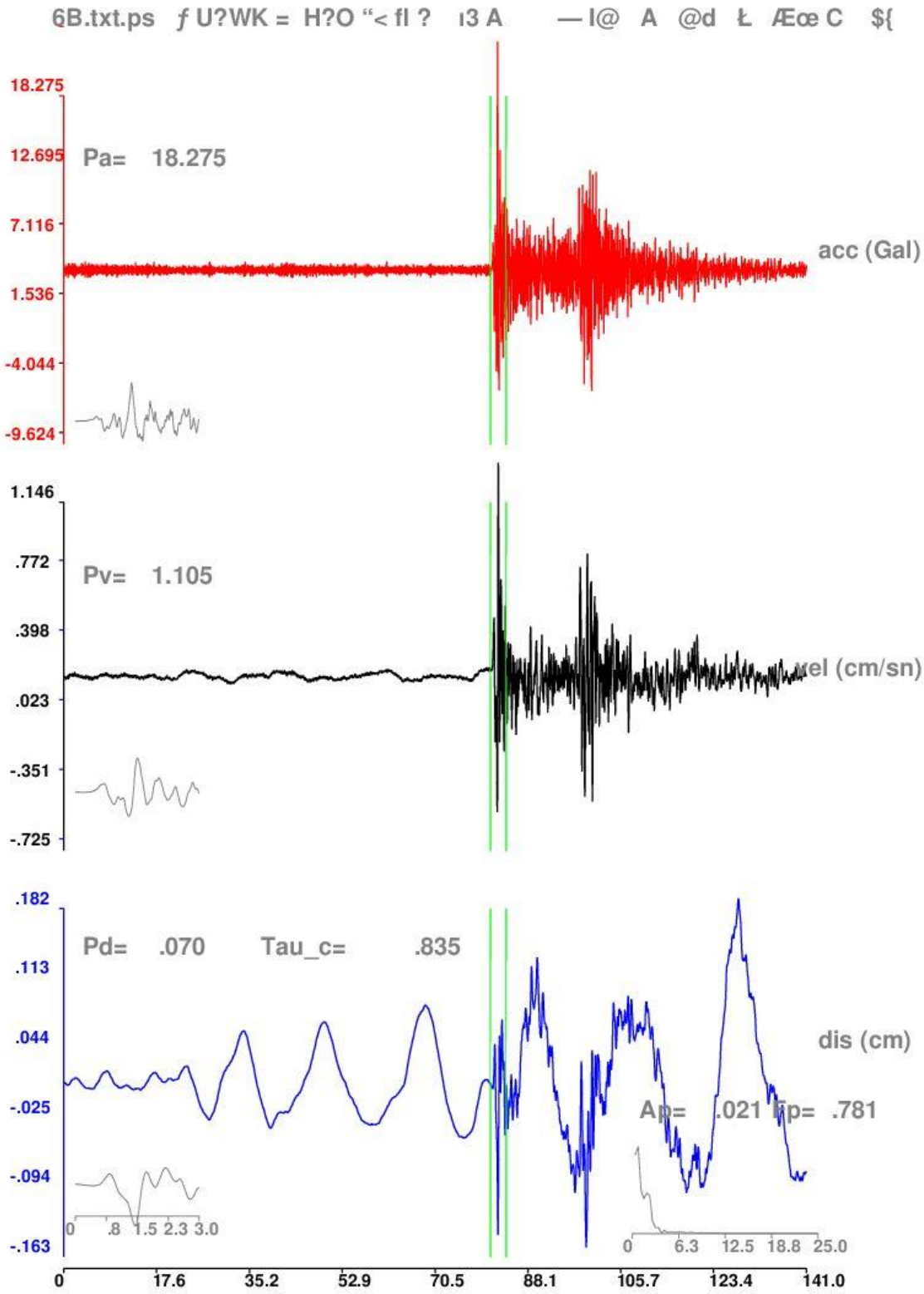

Figure A.5. Bird Lake Earthquake Downhole Record.

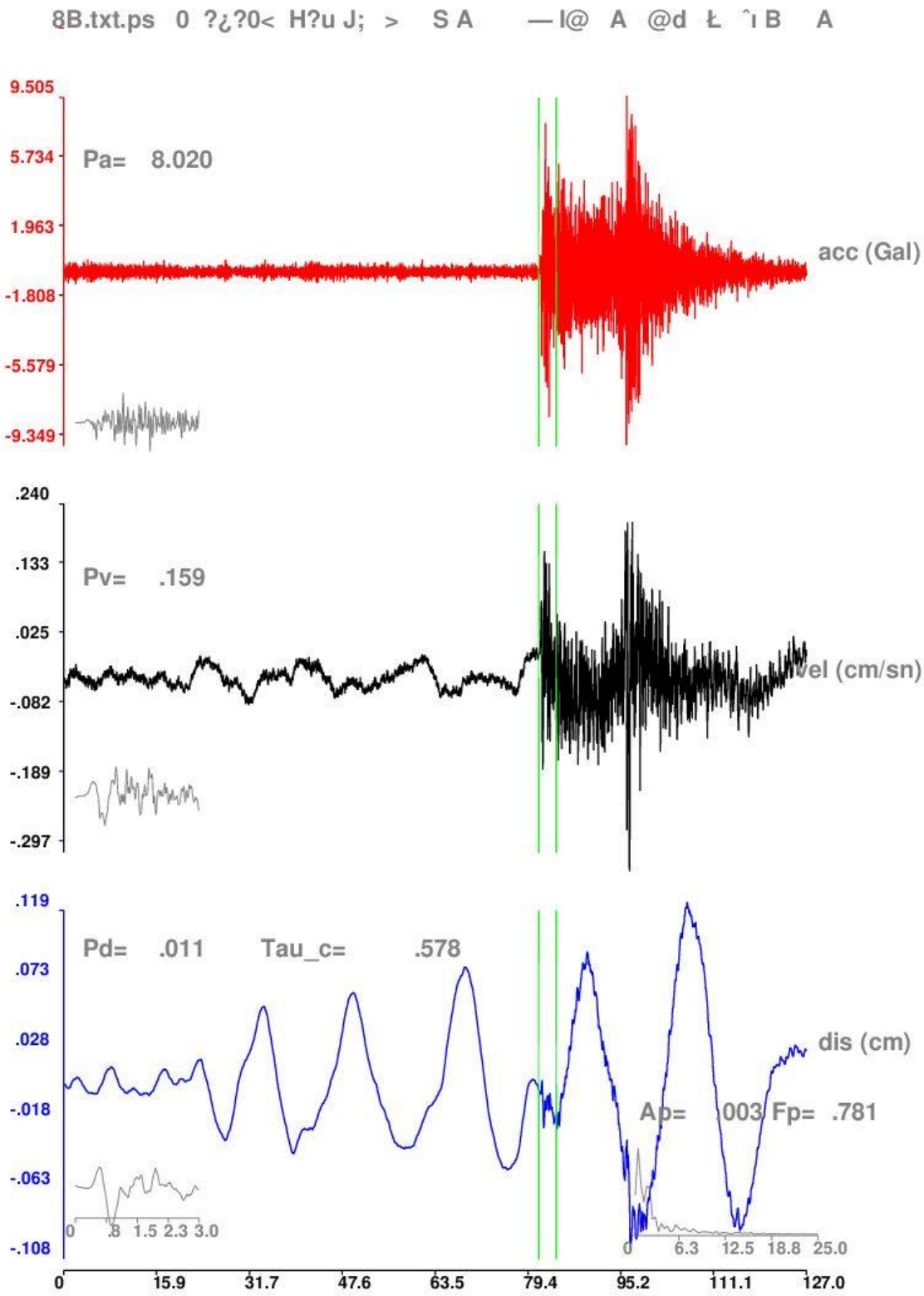

Figure A.6. Blacksea Earthquake Downhole Record.

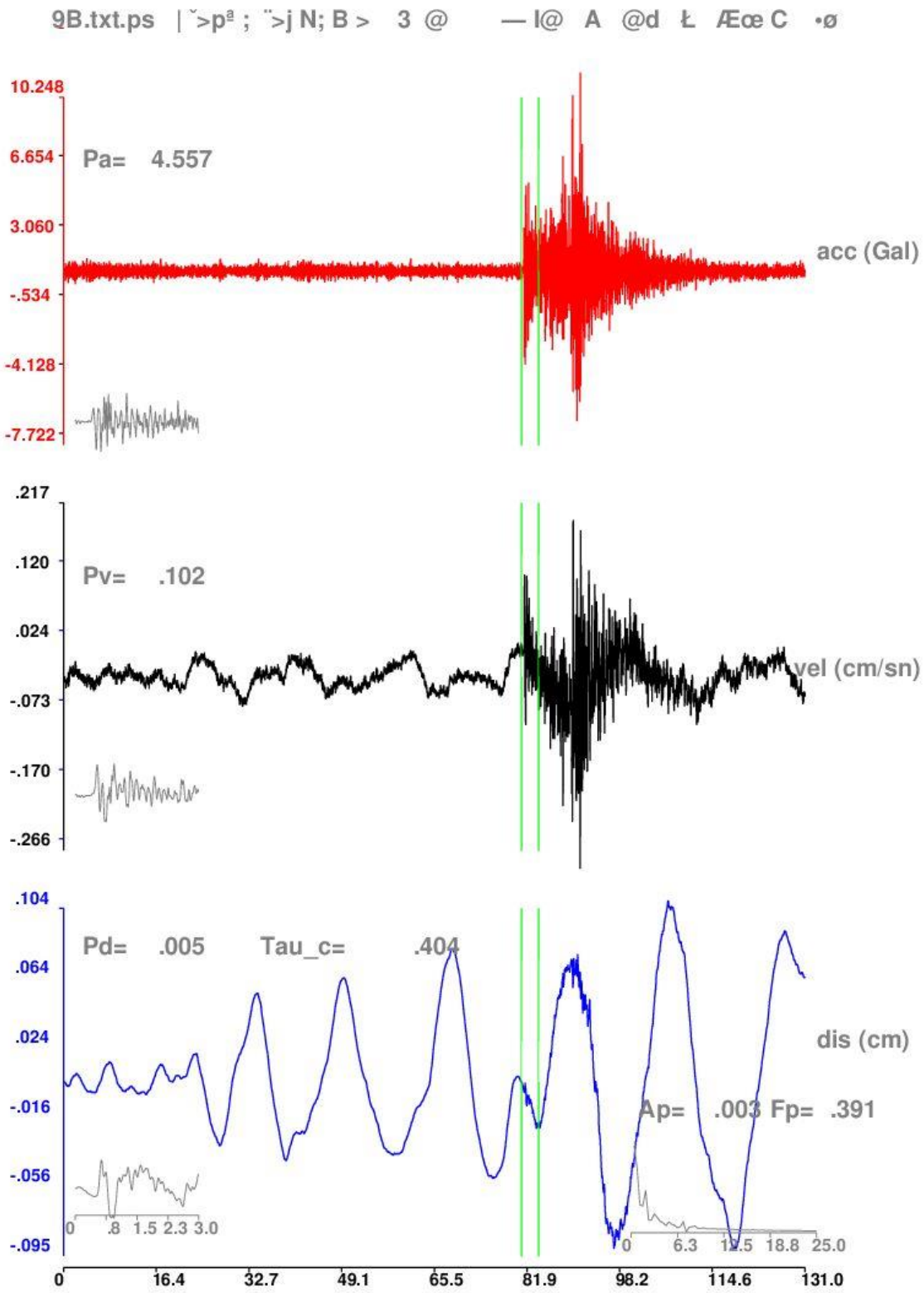

Figure A.7. Gemlik Earthquake Downhole Record.

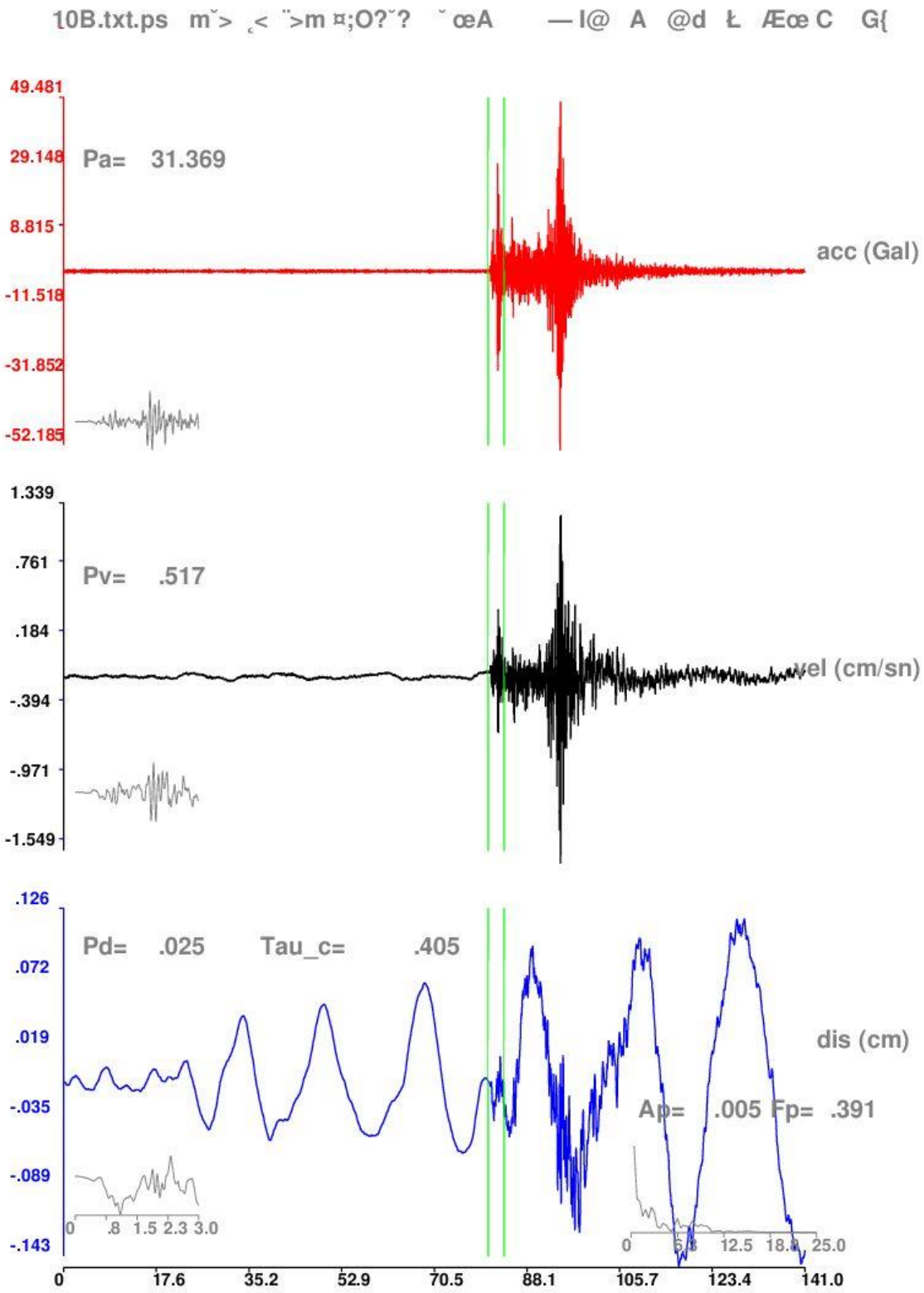

Figure A.8. Gürsu Earthquake Downhole Record.

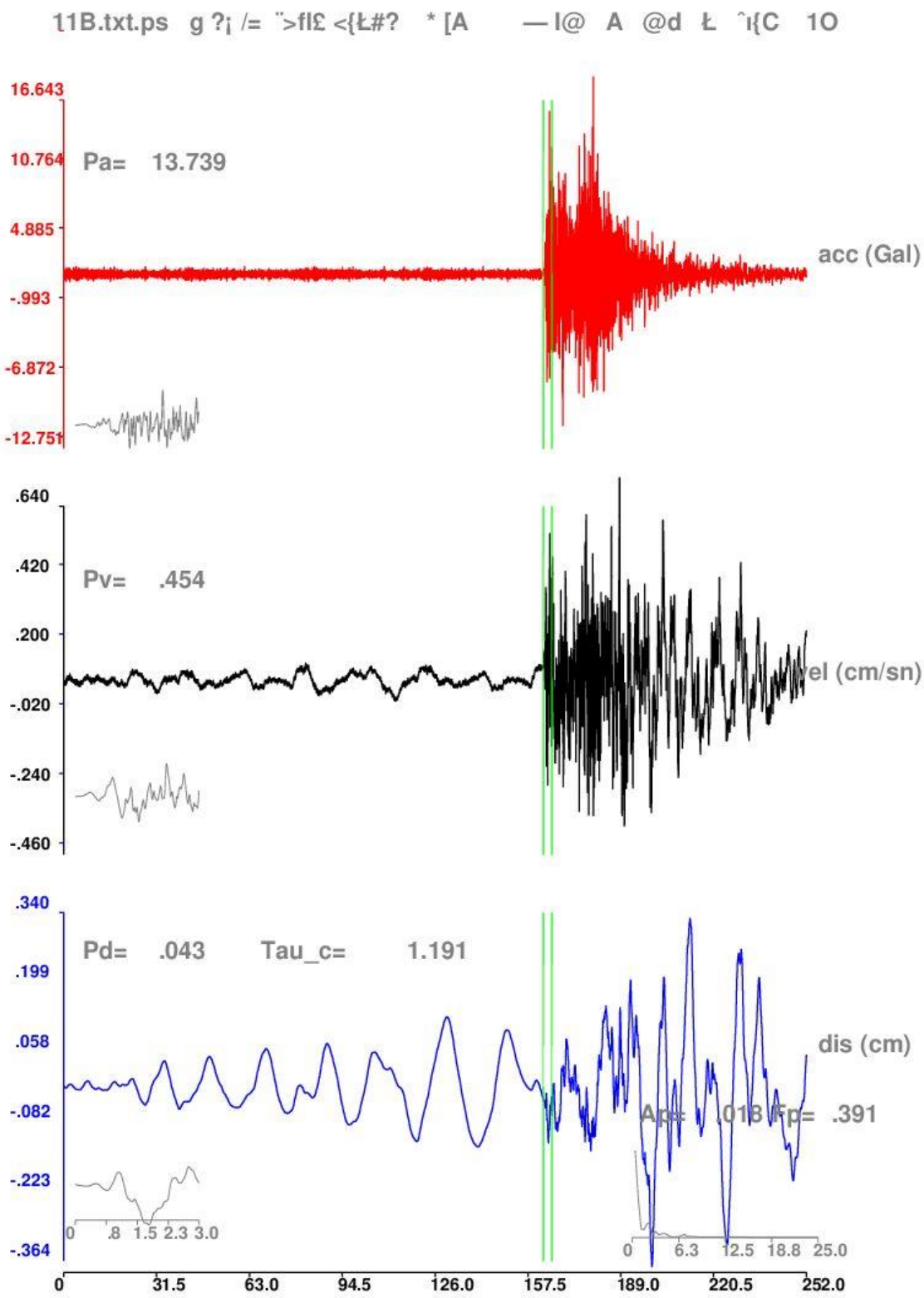

Figure A.9. Marmara Sea (Yalova) Earthquake Downhole Record.

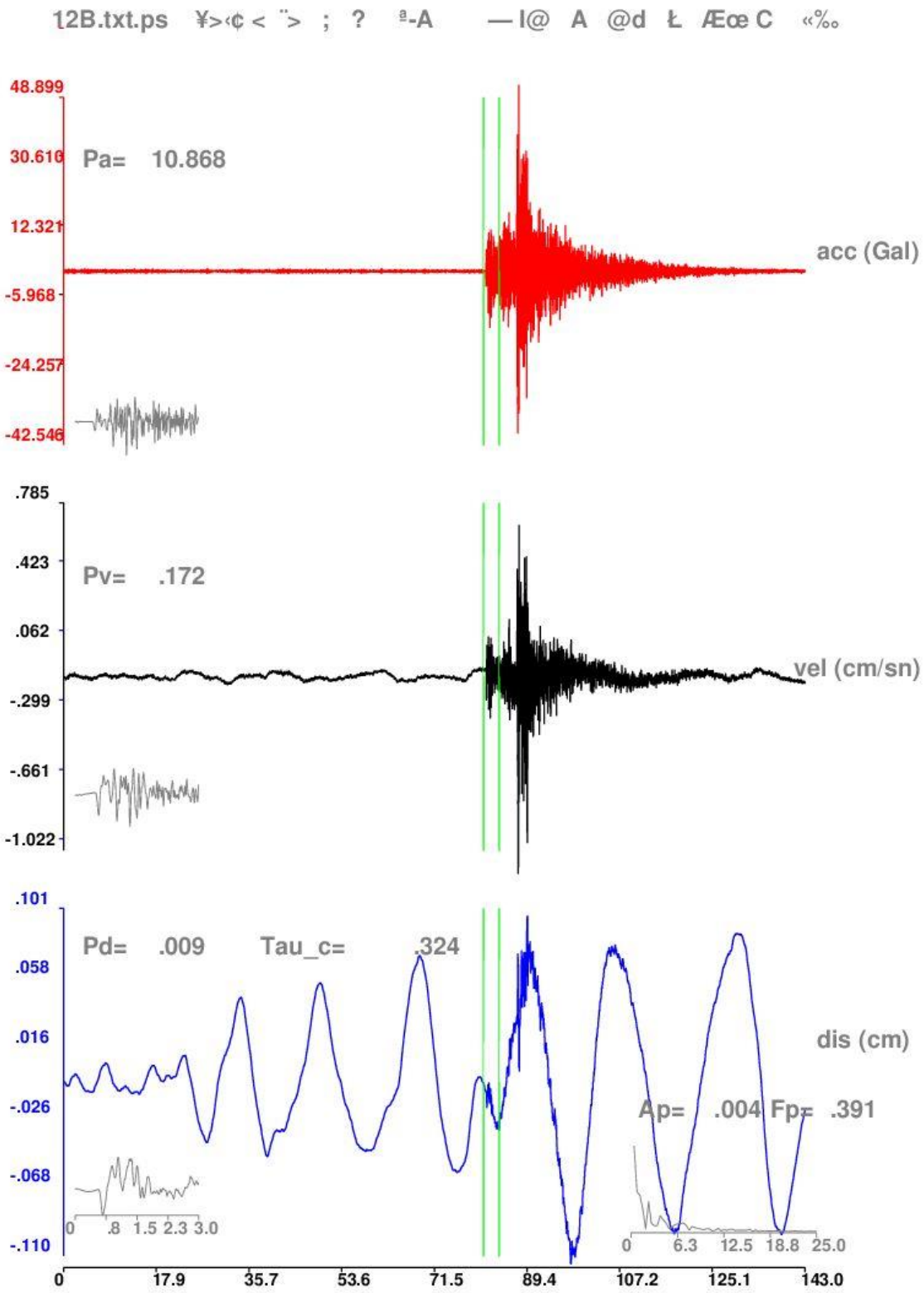

Figure A.10. Marmara Sea Earthquake Downhole Record.

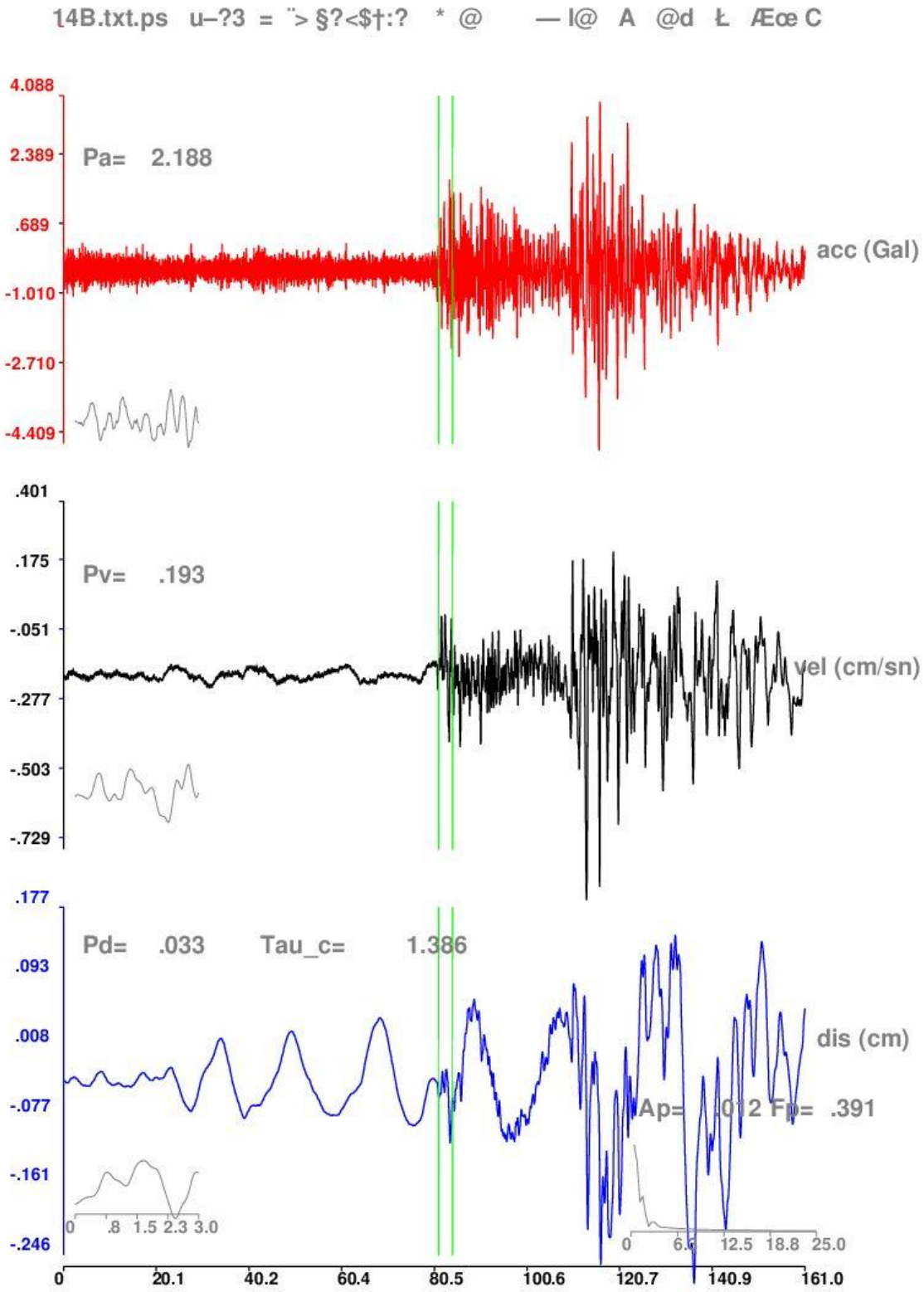

Figure A.11. Marmara Sea Earthquake Downhole Record.

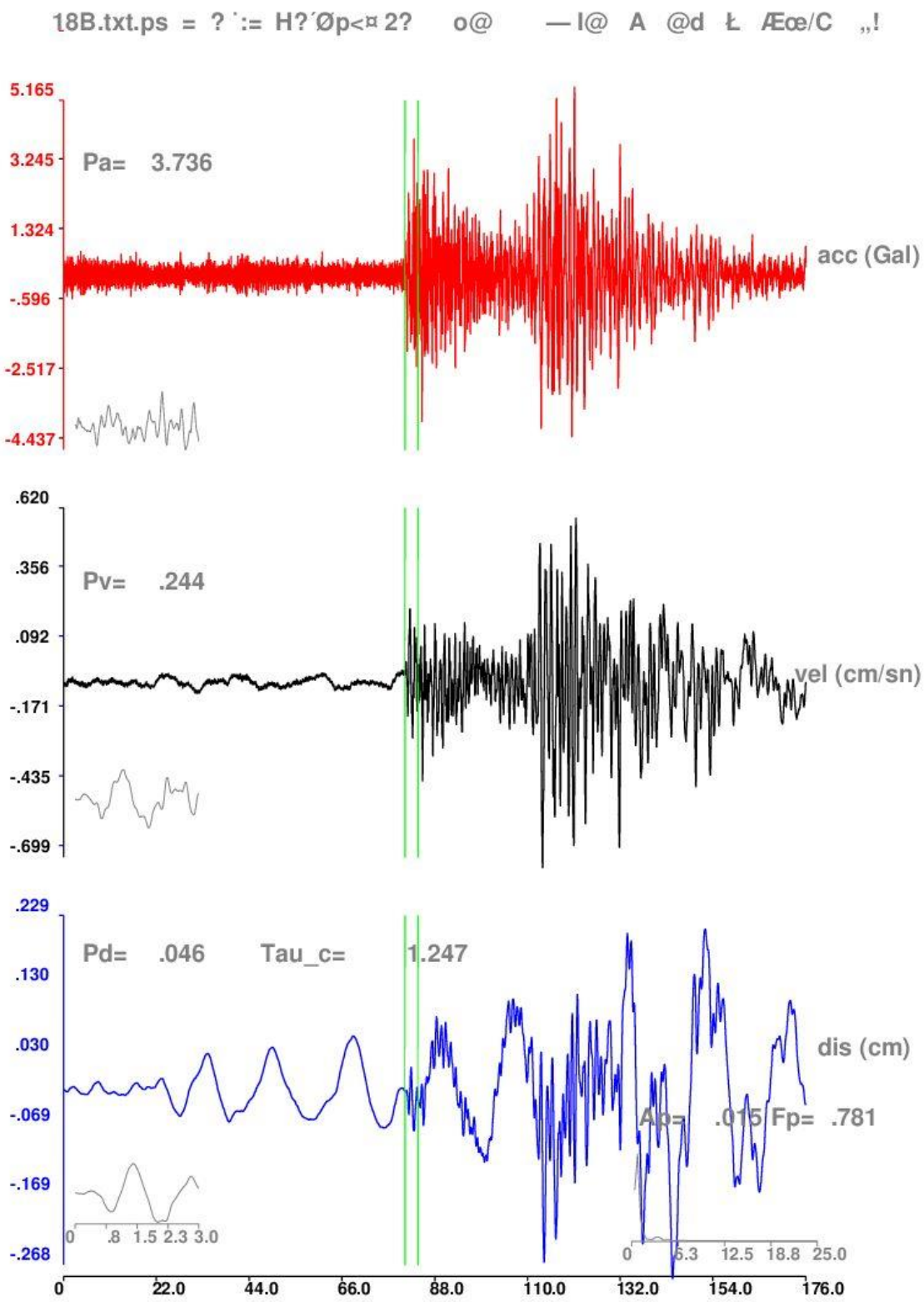

Figure A.12. Blacksea Earthquake Downhole Record.

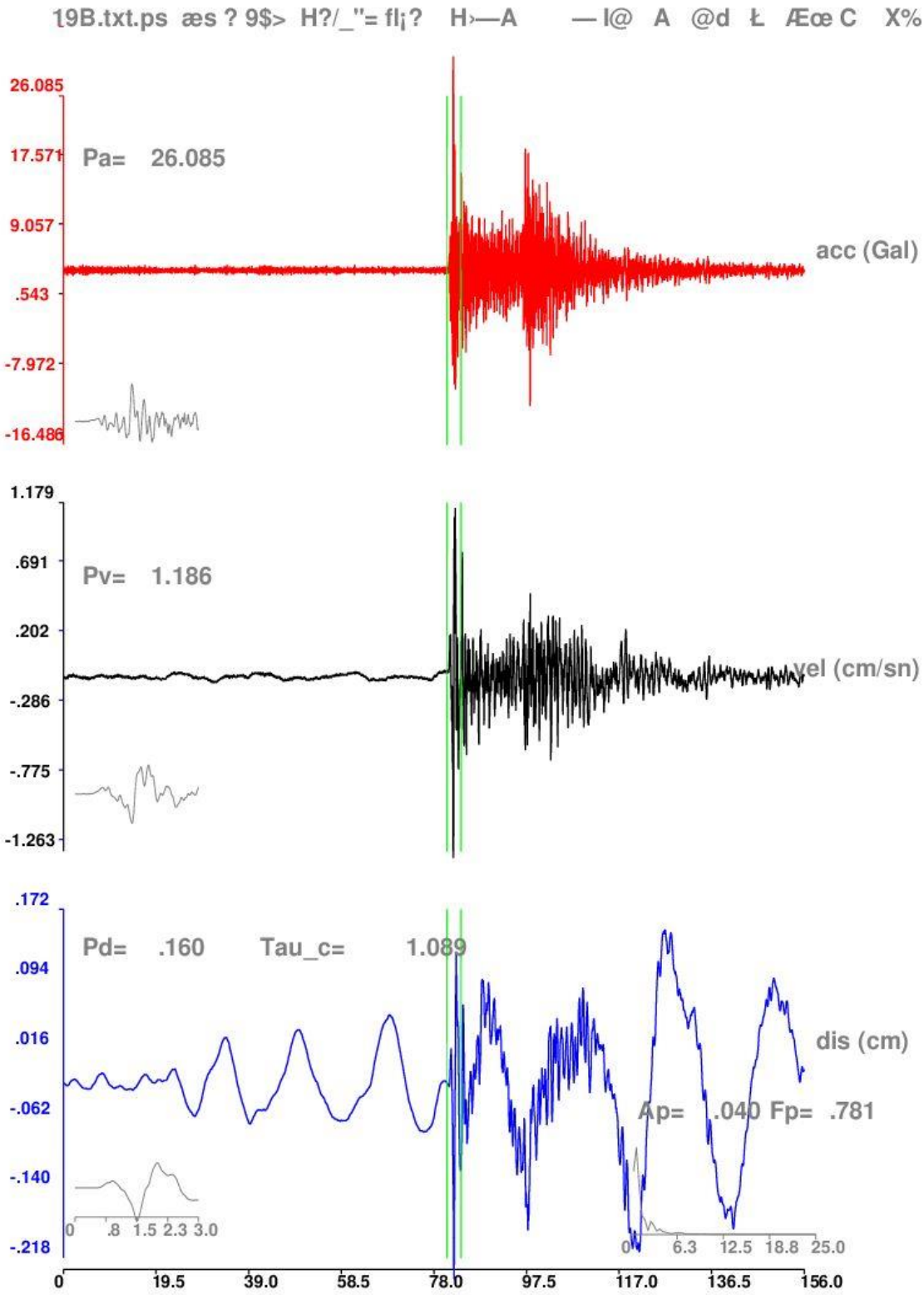

Figure A.13. Marmara Sea (Avcılar) Earthquake Downhole Record.

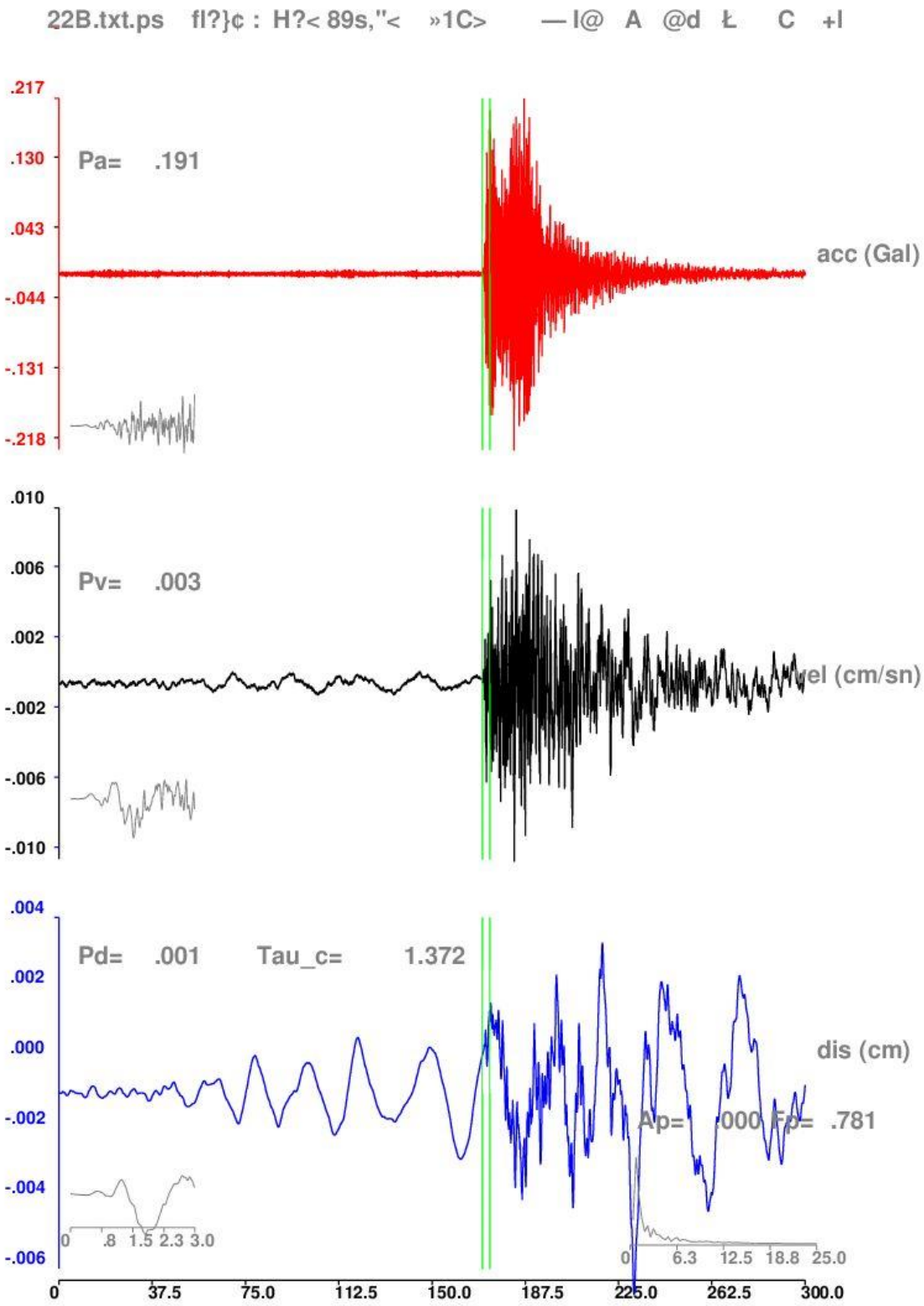

Figure A.14. Marmara Sea Earthquake Downhole Record.

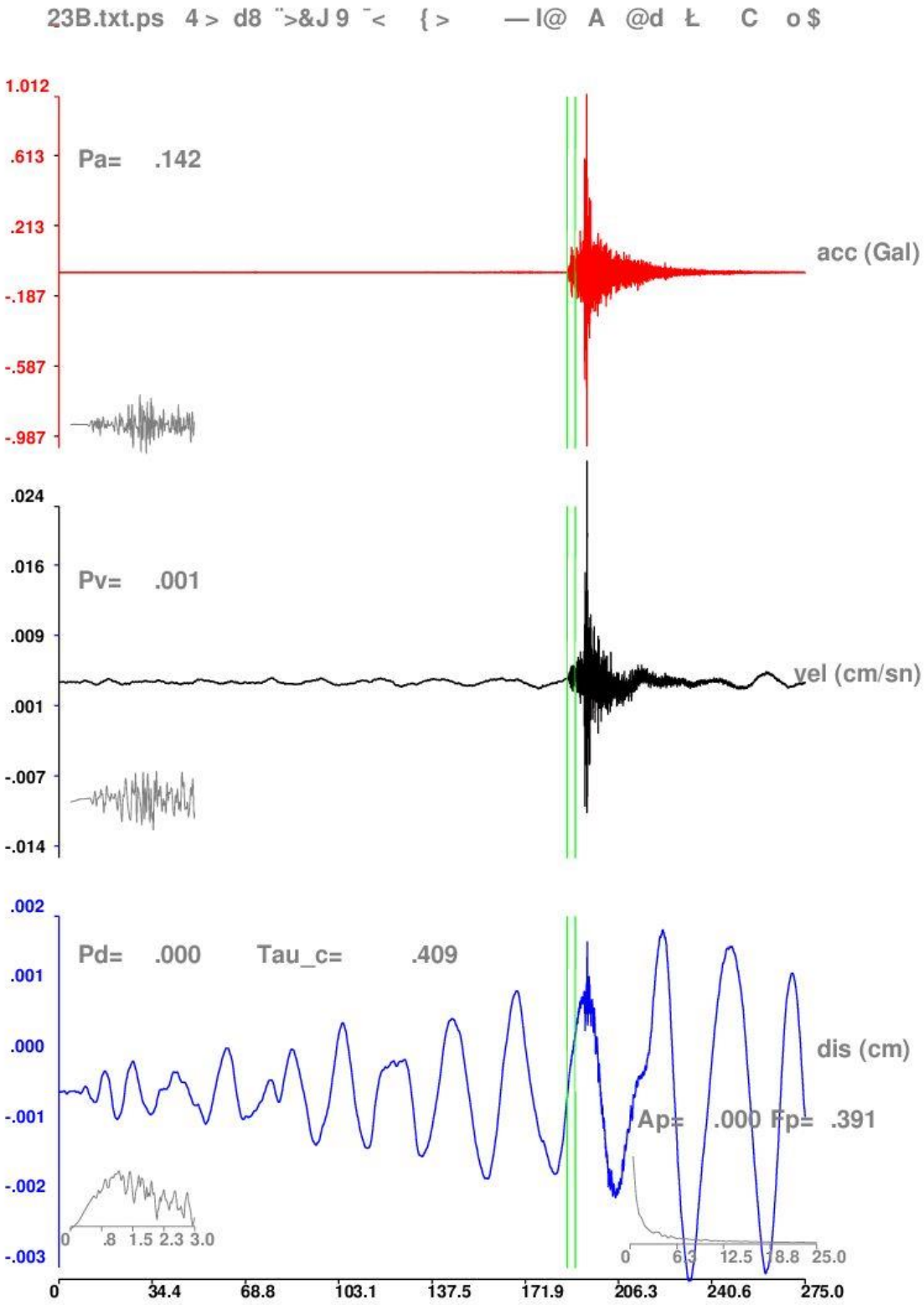

Figure A.15. Gemlik Earthquake Downhole Record.

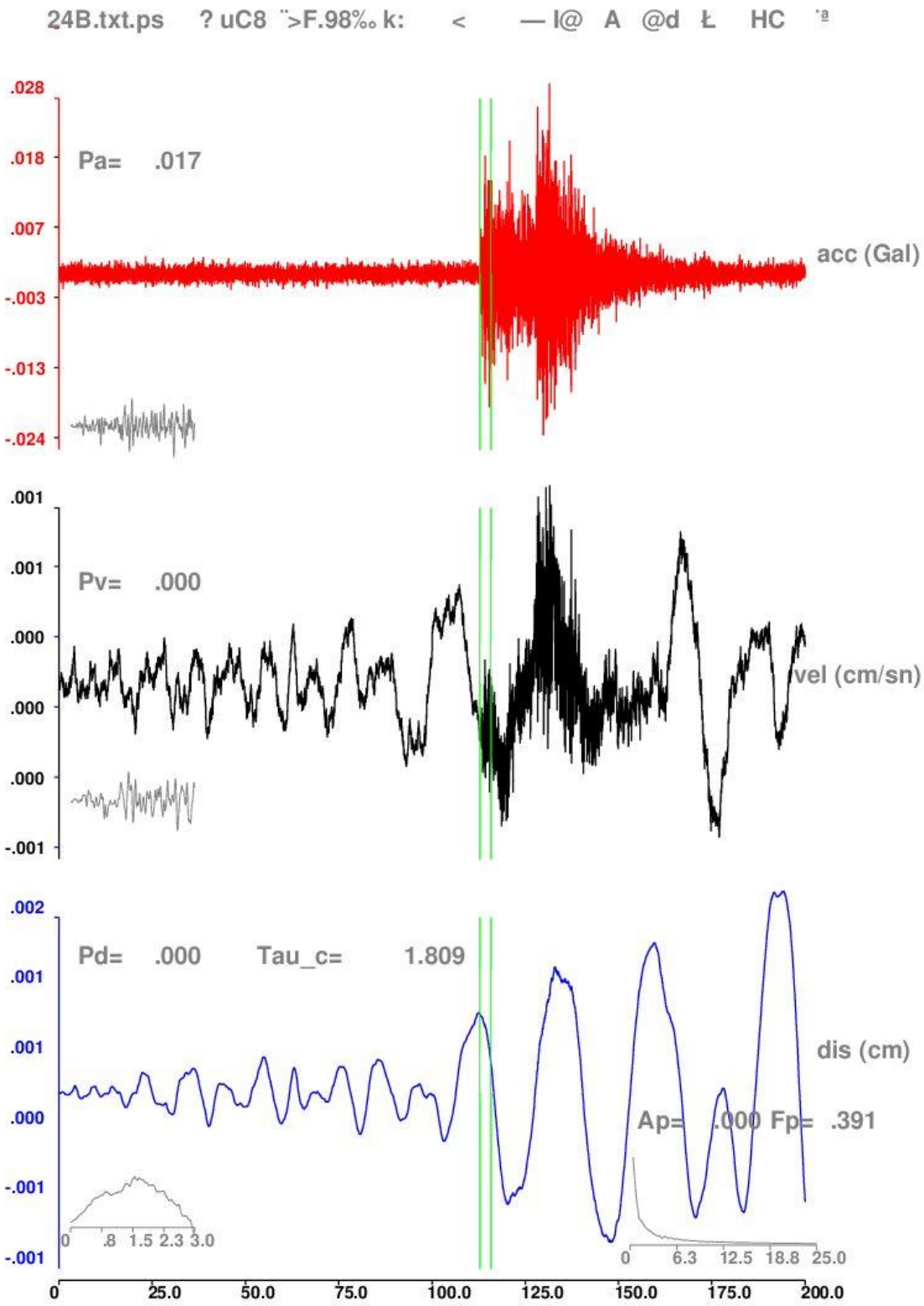

Figure A.16. Marmara Sea Earthquake Downhole Record.

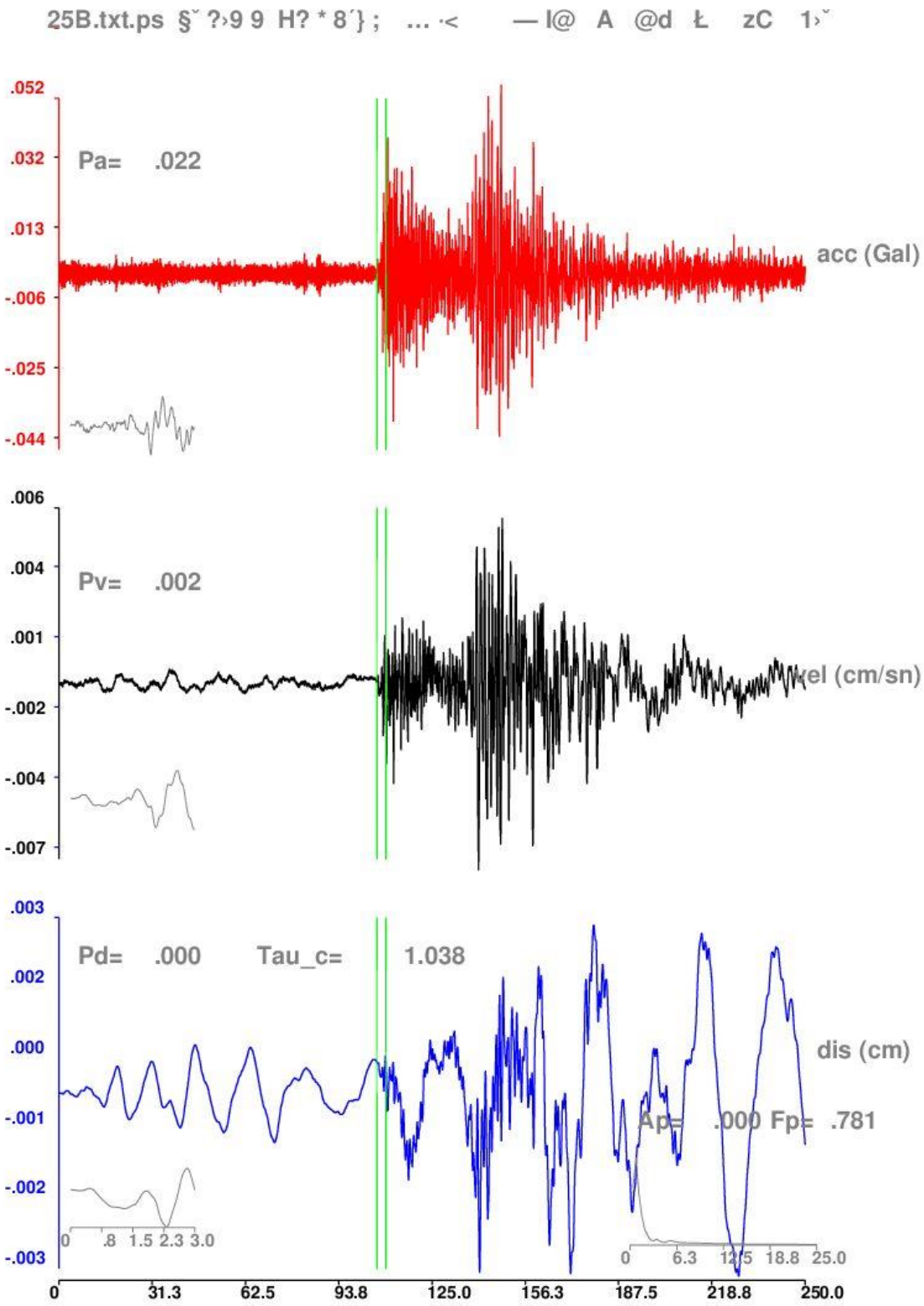

Figure A.17. Marmara Sea Earthquake Downhole Record.

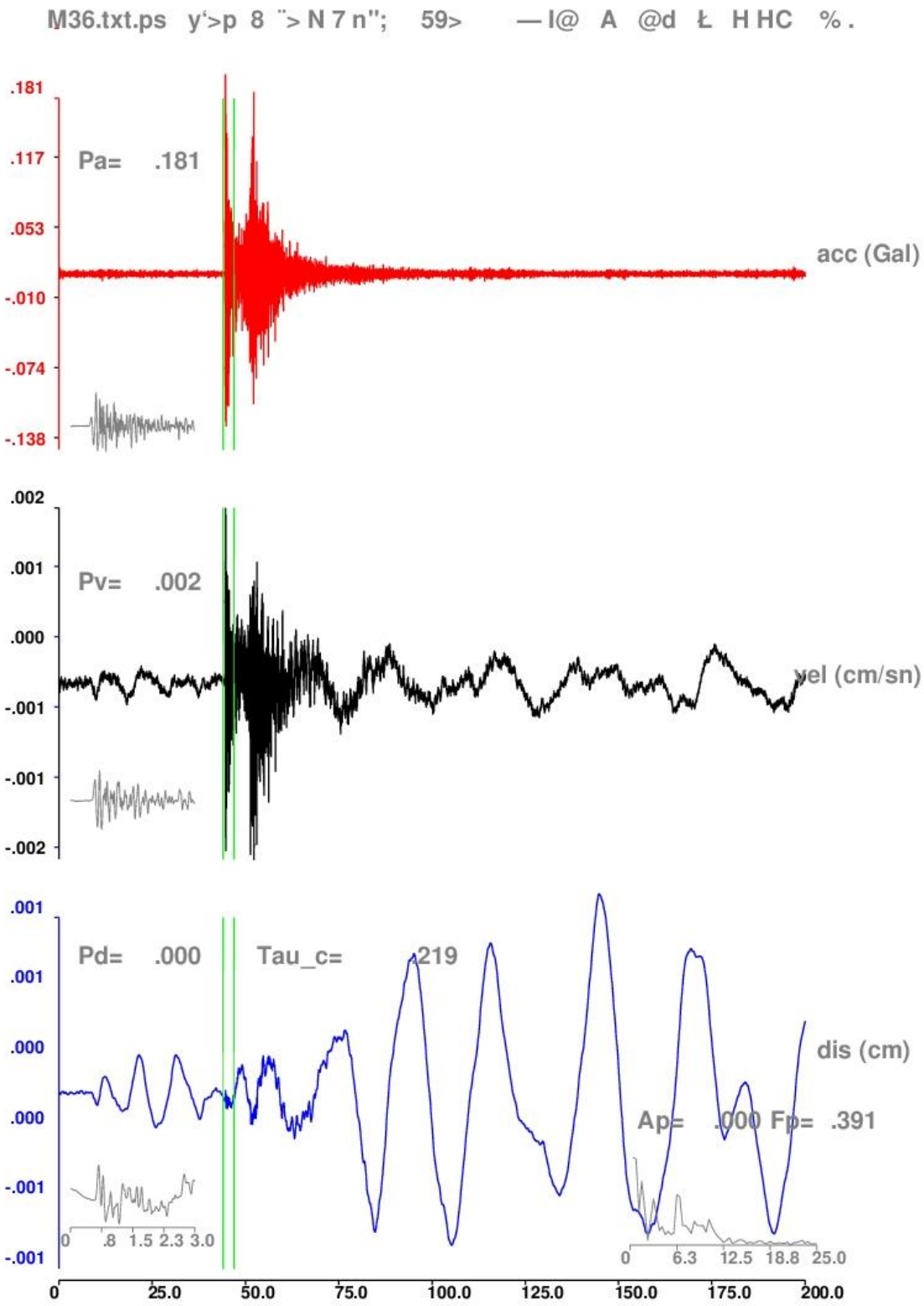

Figure A.18. Silivri Earthquake One of Aftershock Downhole Record.

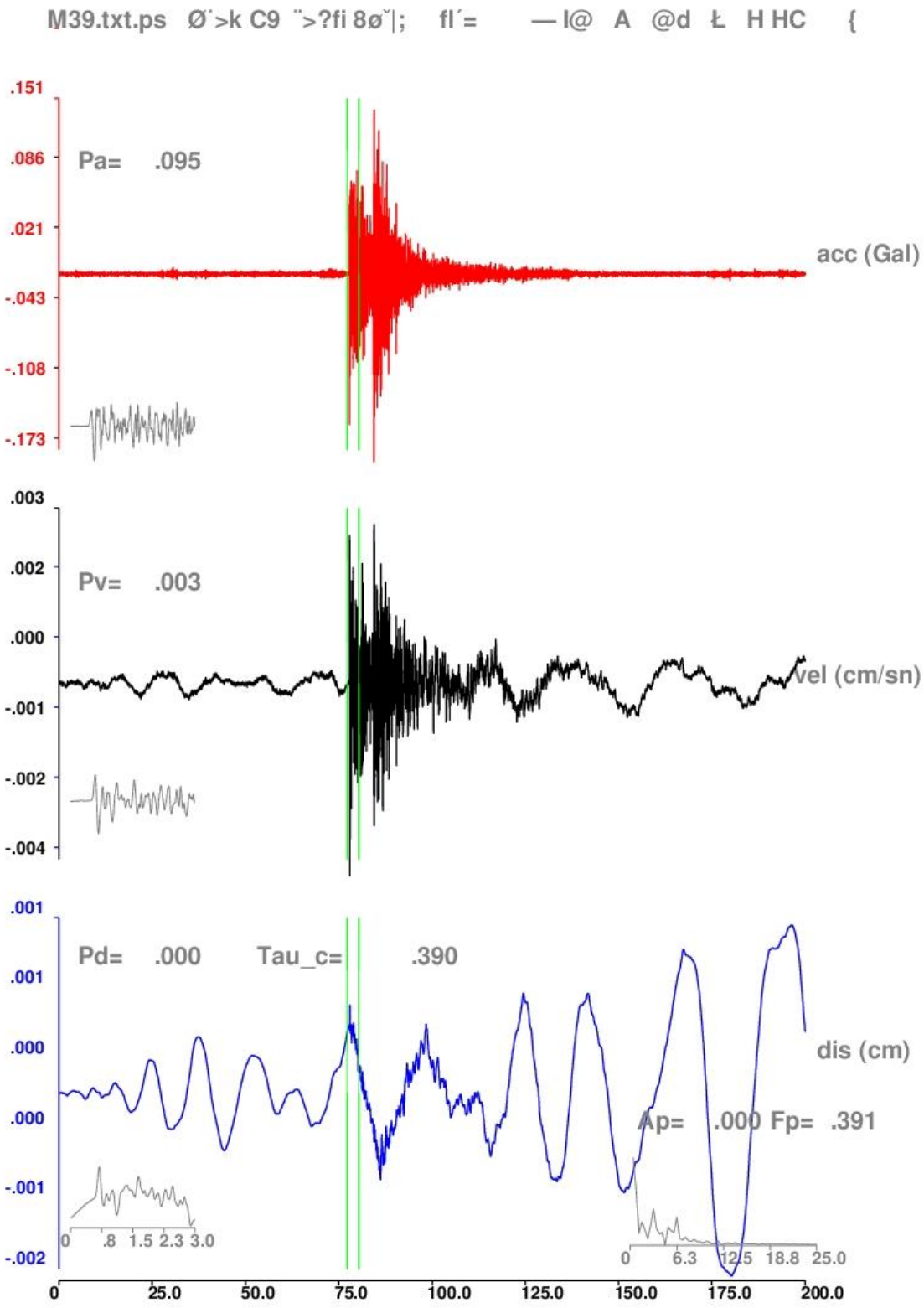

Figure A.19. Silivri Earthquake One of Aftershock Downhole Record.

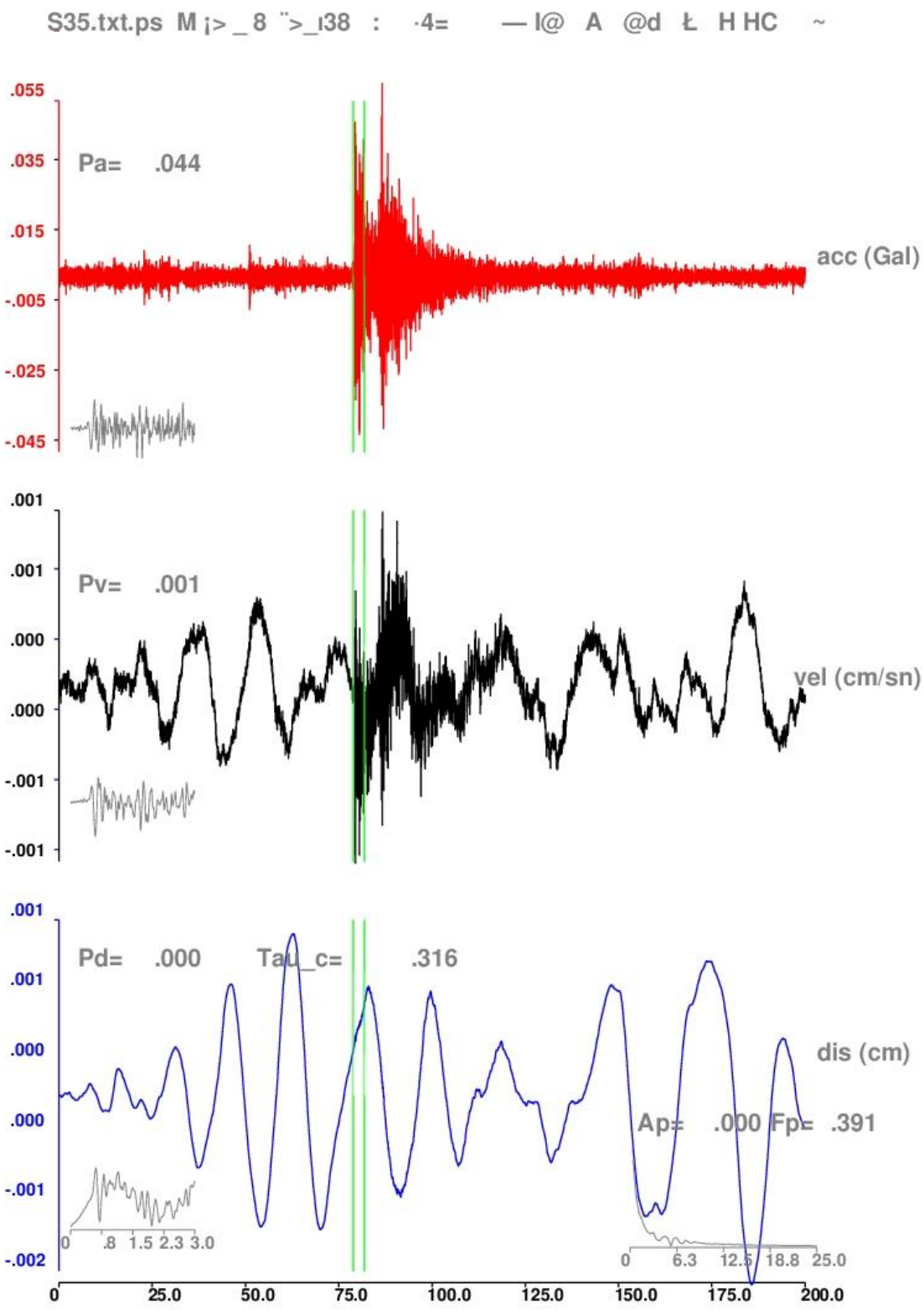

Figure A.20. Silivri Earthquake One of Aftershock Downhole Record.

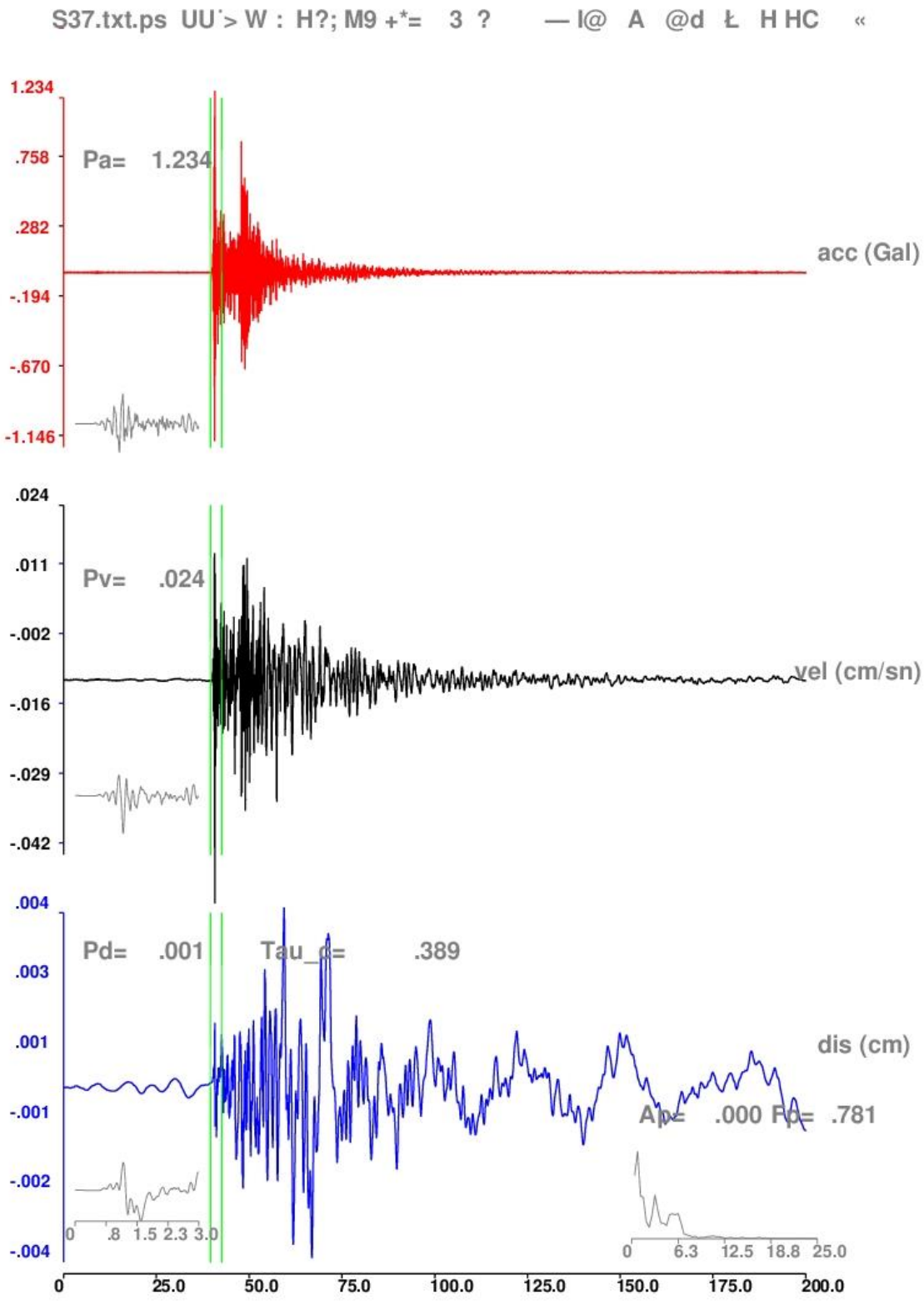

Figure A.21. Silivri Earthquake One of Aftershock Downhole Record.

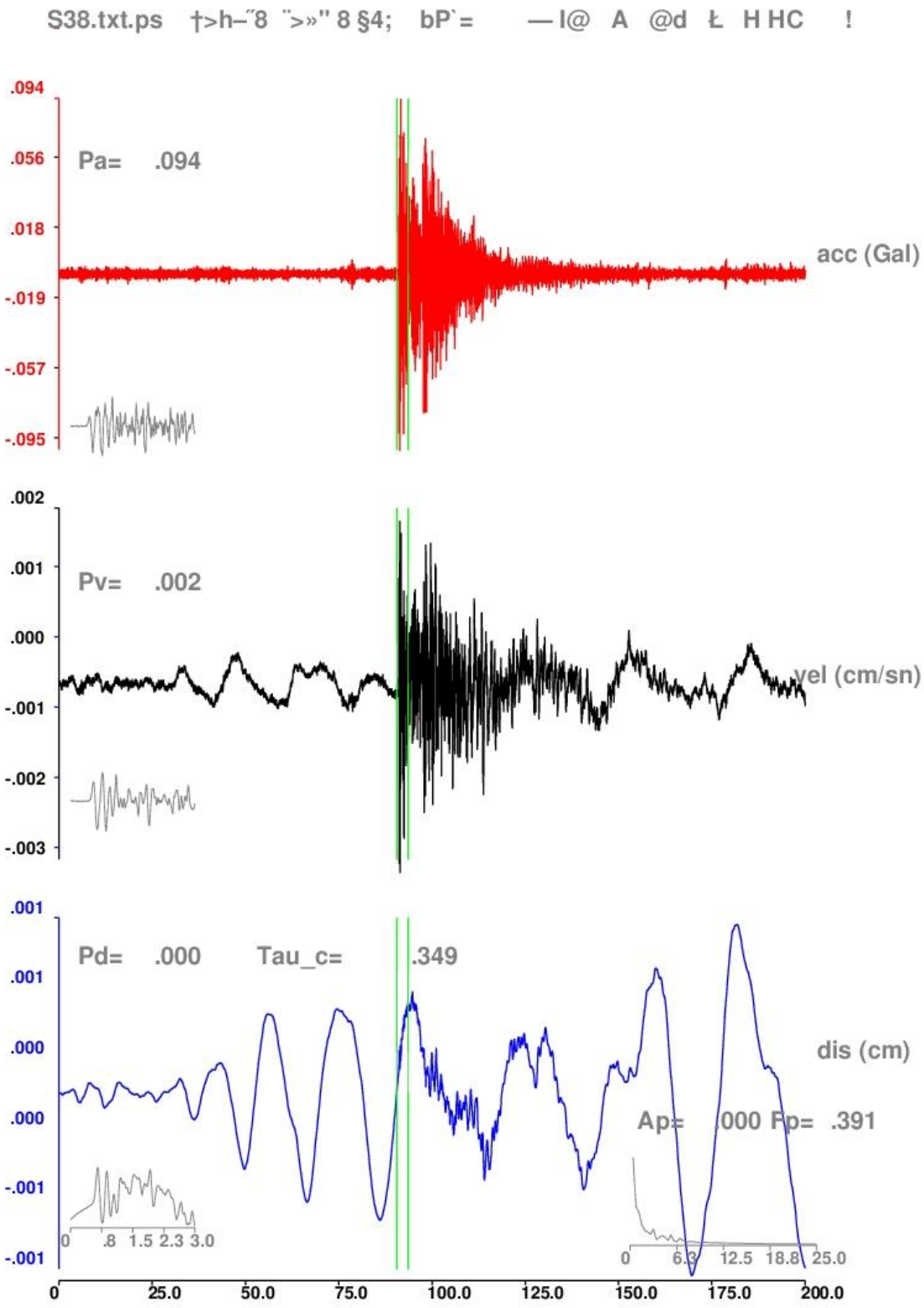

Figure A.22. Silivri Earthquake One of Aftershock Downhole Record.

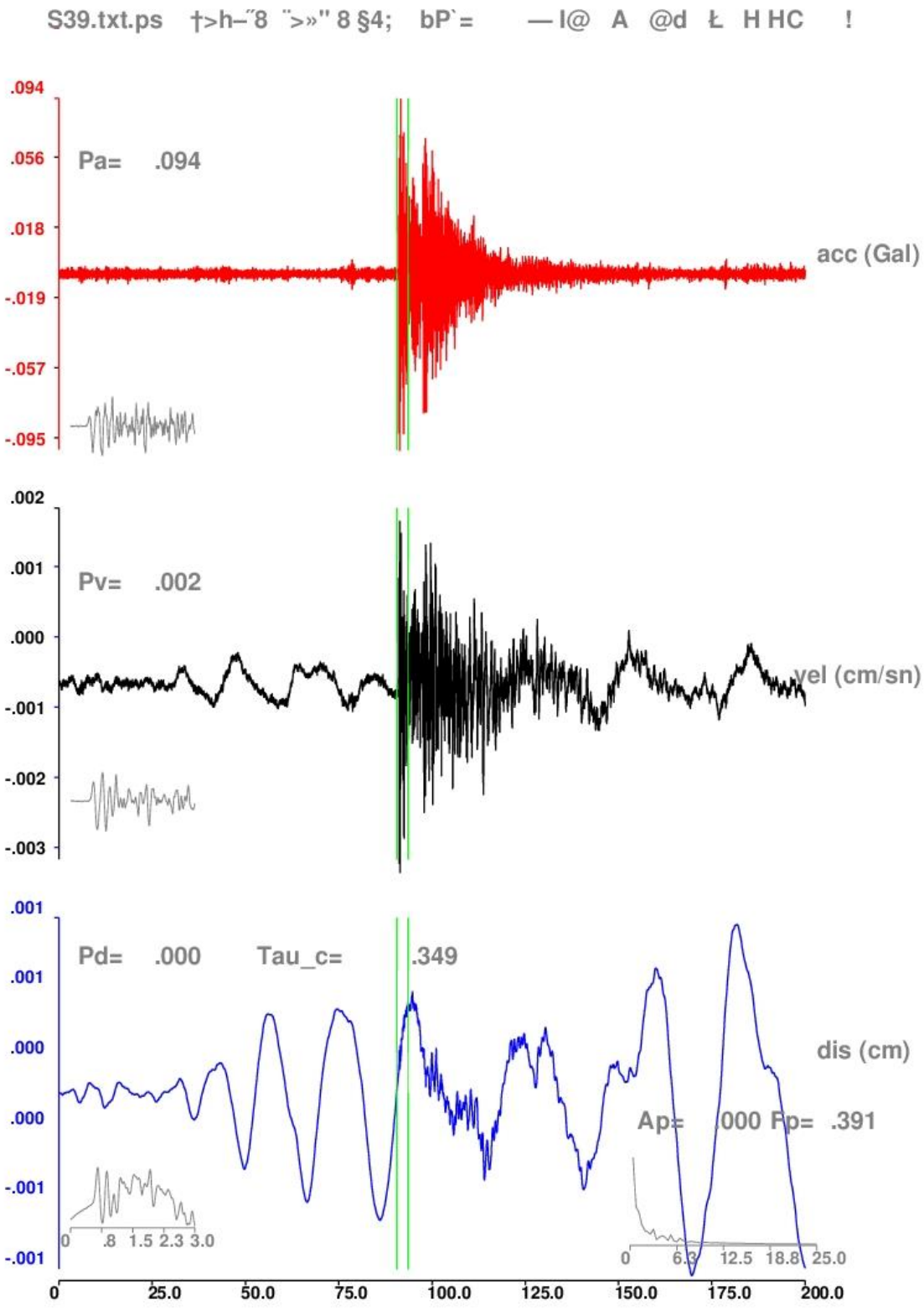

Figure A.23. Silivri Earthquake One of Aftershock Downhole Record.

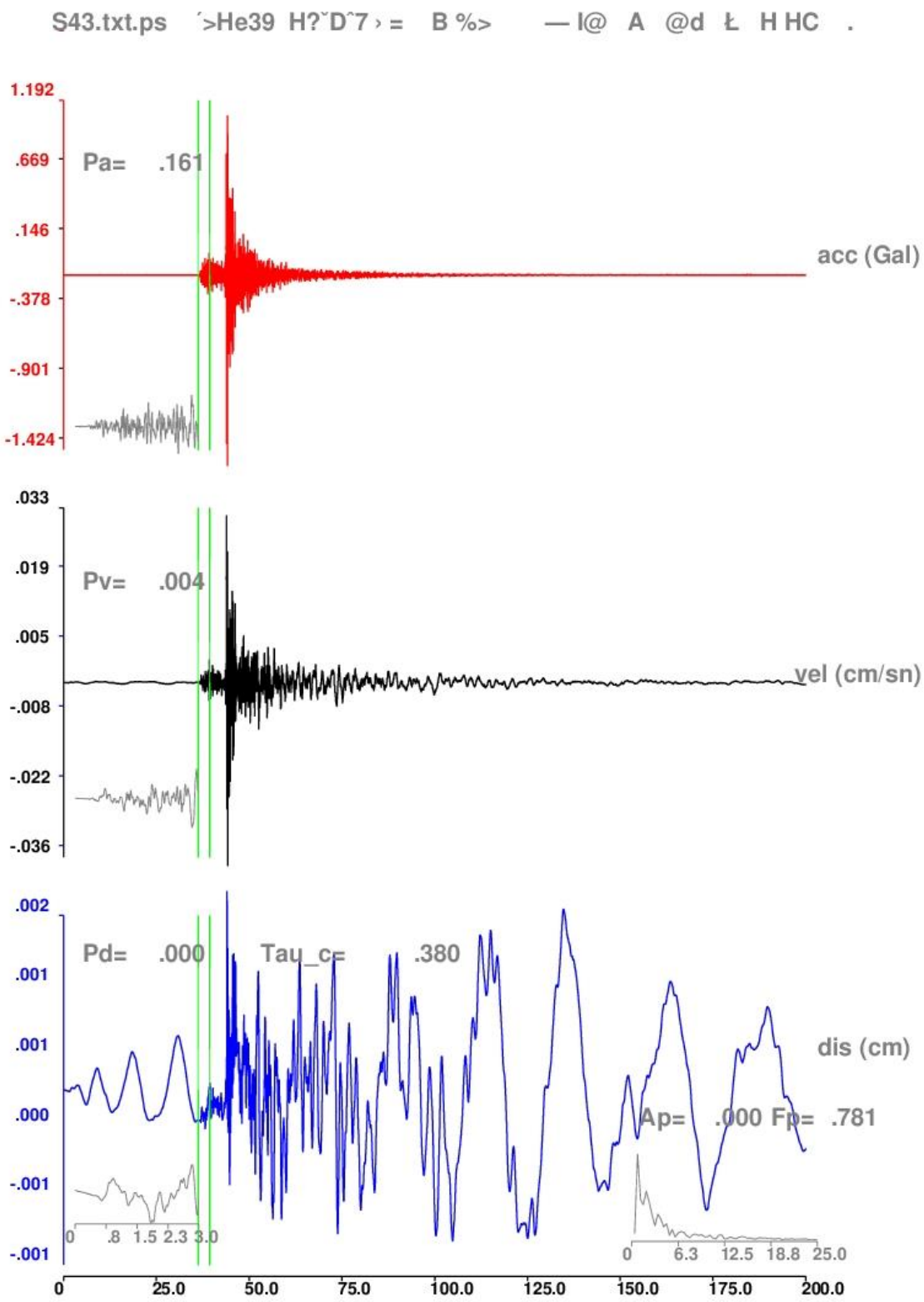

Figure A.24. Silivri Earthquake One of Aftershock Downhole Record.

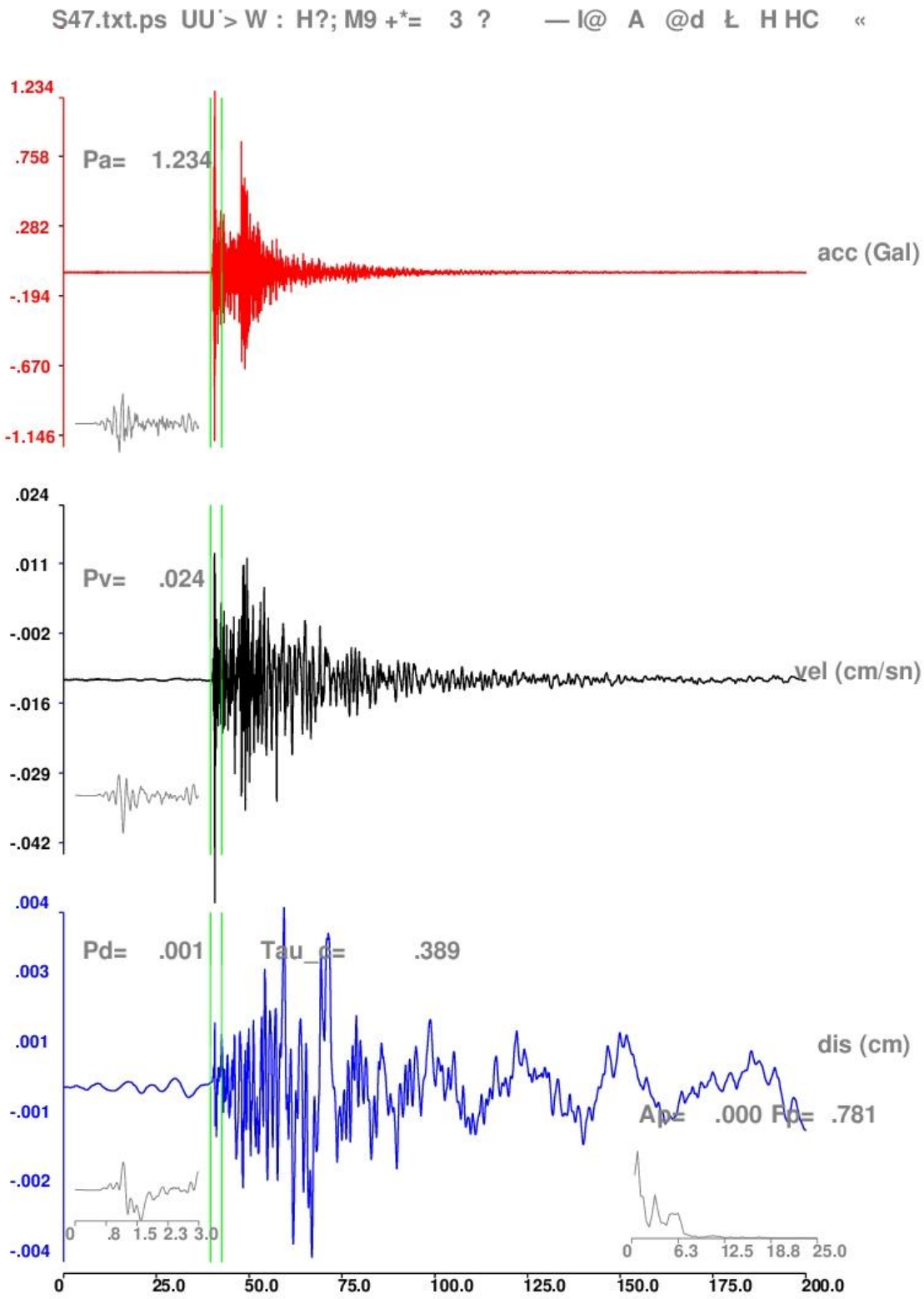

Figure A.25. Silivri Earthquake One of Aftershock Downhole Record.

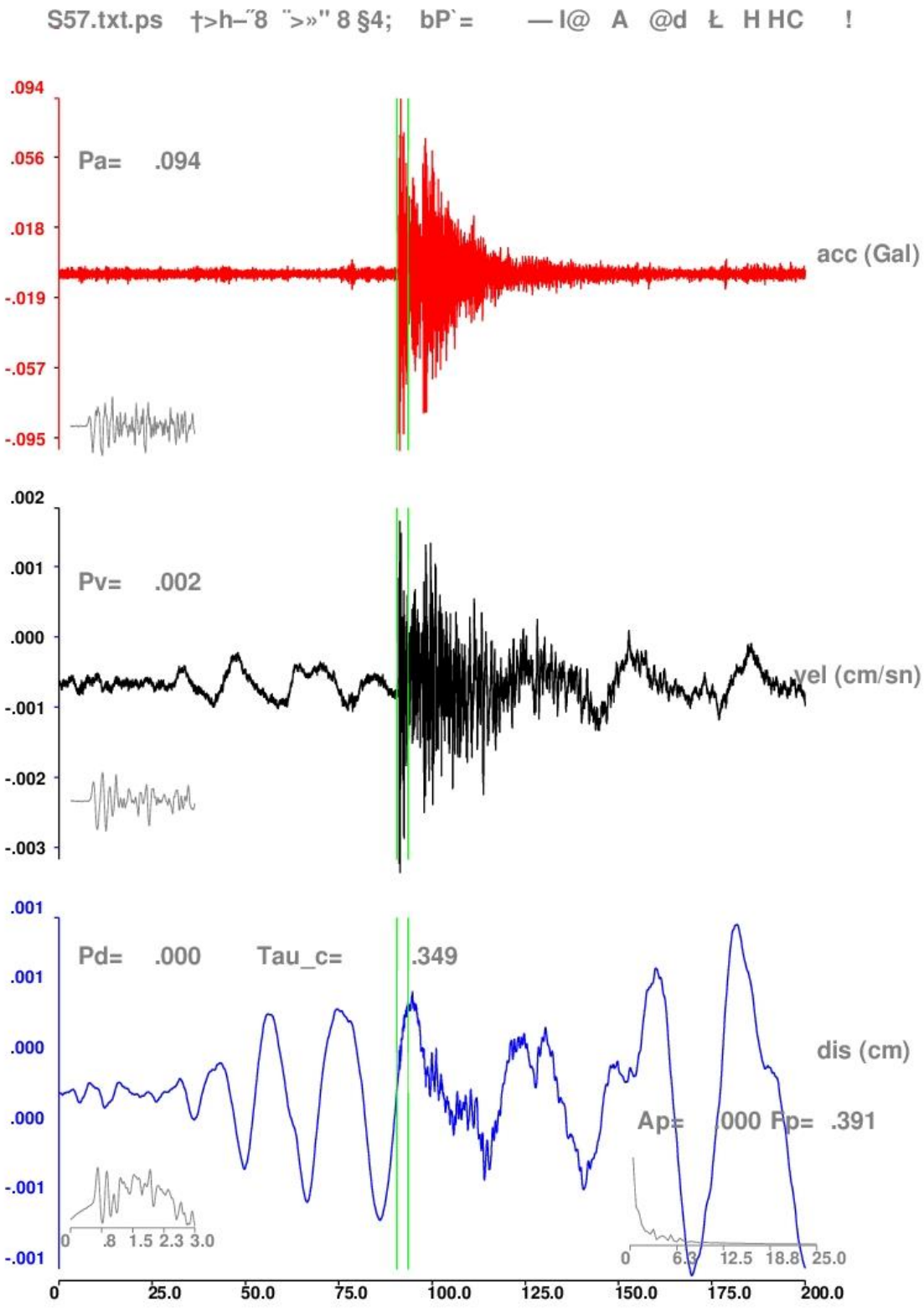

Figure A.26. Silivri Earthquake One of Aftershock Downhole Record.

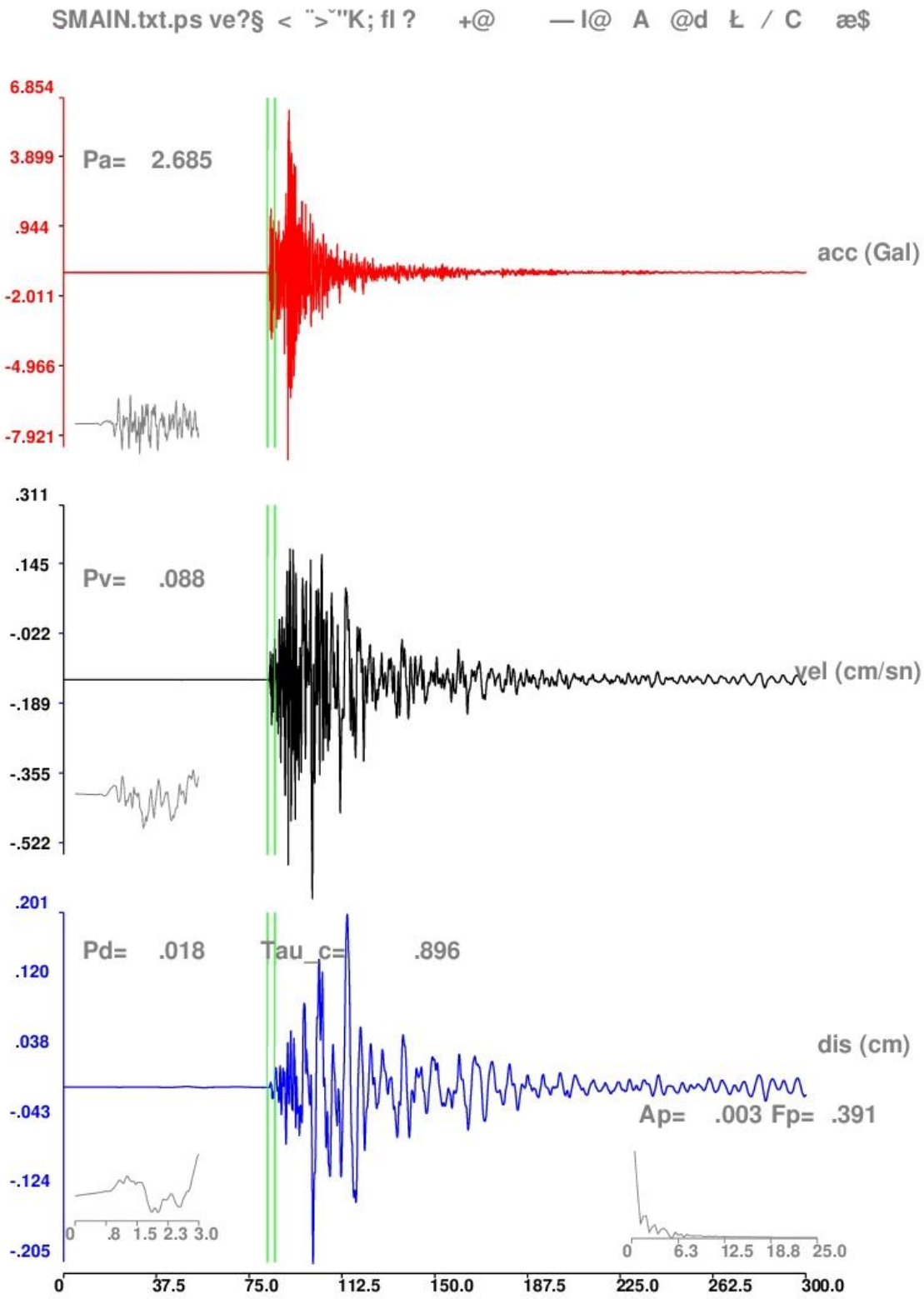

Figure A.27. Silivri Main Earthquake Downhole Record.